JOURNAL ON
COMMUNICATIONS
VOLUME XLII SEPTEMBER 1991

MICROWAVE INTEGRATED CIRCUITS

JOURNAL ON COMMUNICATIONS

A PUBLICATION OF THE SCIENTIFIC SOCIETY FOR TELECOMMUNICATIONS, HUNGARY

SPONSORED BY

Editorial office
Gábor Áron u. 65.
Budapest, O.O.Box 15.
Hungary, H—1525

phone (361) 135-1097
(361) 115-2247
fax (361) 135-5560

Subscription rates
Hungarian subscribers
1 year, 12 issues 2900 HUF, single copies 360 HUF
Individual members of Sci. Soc. for Telecomm.
1 year, 12 issues 480 HUF, single copies 60 HUF
Foreign subscribers
12 issues 90 USD, 6 English issues 60 USD, single copies 15 USD
Transfer should be made to the Hungarian Foreign Trade Bank, Budapest, H—1821, A/C No. MKKB 203-21411

JOURNAL ON COMMUNICATIONS is published monthly, alternately in English and Hungarian by TYPOTEX Ltd. H—1015 Bp. Batthyány u. 14., phone: (361) 201-3317, fax: (361) 162-1804. Publisher: Zsuzsa Votisky. Type-setting by DIAMANT Ltd. Printed by HUNGAPRINT, Budapest, Hungary
HUISSN 0866-5583

EDITORIAL

Eight years after Kilby's patent about silicon integrated circuits, the new idea of the gallium arsenide Schottky—gate field effect transistor (GaAs MESFET) was discovered in 1986 by C.A. Mead. Due to the better electron transport properties of GaAs and the drastically decreased gate length, GaAs MESFETs became in few years the most promising microwave active devices.

Though the technological properties of GaAs are quite different from those of Si, new technological methods have been discovered, thus leading to a widespread application of GaAs MESFETs in the early 70's. Hybrid microwave integrated circuits (HMICs) apply MESFETs in form of chips, and the interconnections are realized by properly designed transmission lines deposited on a low—loss microwave dielectric. Active devices requiring quite different technologies can thus also be integrated without greater problems. On the other hand, the possibility of making GaAs semi-insultating layers offers the opportunity of integrating different devices (passive and active) on the same substrate. Thus a considerable progress of monolithic integration on semi-insulating GaAs (MMIC) has started, and the first GaAs digital device was built by Hewlett-Packard in 1974. It demonstrated the high-speed switching characteristics of a buffered FET logic gate.

A revolutionary progress began in the field of high quality semiconductor layer structures, and nowadays heteroepitaxial growth of two, three or even four component compound materials is a common practice in advanced laboratories.

The aim of constructing such complicated layer sequences containing often superlattices (SL) of more than ten periods is always to produce better and better transport properties—even at high carrier concentration—not sensitive to the actual layer temperature or the incident light. This progress has been leading to other FET type active devices, with gate lengths in the range of 100 nm and maximum oscillation frequencies often above 100 GHz. At such high frequencies, the wavelength is in the mm-range where hybrid integration fails, and monolithic integration becomes more and more attractive.

On the other hand, large-scale monolithic integration on compound semiconductor materials suffers from the crystal defects, and the defect-concentration is much higher than for silicon. However, by advanced crystal growth techniques characterized by full digital control and multizone systems, single crystal quality of high perfection can be achieved. These methods can be combined by the space-growth technique eliminating the disturbing effect of gravitation. Substrate materials governing the growth of epitaxial layers can thus be produced with perfection.

The growth of epitaxial layers with ultra-low defect density has also been achieved by using molecular beam epitaxy (MBE) or metal-organic vapor phase epitaxy (MOVPE). The defect density of such layers can be better than 10 cm^{-2}. Note that defect densities under 1 cm^{-2} were often achieved by using AIXTRON (Aachen, Germany) MOVPE reactors. Thus large scale integration is more and more possible, and low power, low cost devices are beginning to be used in volume by mainstream computer manufacturers.

Another problem which becomes more and more important at extreme operation speeds is the growing importance of circuit discontinuities. As geometrical dimensions decrease, the electromagnetic field distribution inside the integrated circuit will have more and more a two or even three dimensional character. On the other hand, decreasing dimensions result in extreme high field strength, leading to the necessity of nonlinear treatment in the computations. These are the basic arguments for the application of advanced CAD methods even at smaller integration scale, and this is the reason for presenting a review about the CAD techniques for integrated microwave oscillators and about the discontinuity problems in this issue.

The woldwide interest in the rapid progress in the field of MMICs is also reviewed. In addition to the two leading countries, USA and Japan, where well organized scientific programs show the particular attention for this subject, national programs and broad international cooperation are characterizing the answer of European countries to the MMIC challenge. The review paper presented in this issue focuses on the European trends and activities. In Hungary, considerable progress has alerady been made in the field of GaAs technology, together with the first steps in MIC an MMIC research. The research work started with the development of discrete GaAs devices which are mostly applied in hybrid microwave circuits in mediumsclae microwave modules. Special problems of the technology as e.g. the ohmic contact formation on compound semiconductors were studied in great detail.

In recent years, special attention was given for the light sensitivity of GaAs devices, and a picosecond optical switch (POS) prepared by MESFET technology was developed. Such switching device will form later on an important part of an integrated sampling unit which is now under development.

The Hungarian research work has been closely connected since many years, among others, with the research activities of German Universities (RWTH Aachen, University of Duisburg, Technical University of Darmstadt). By further intensification of present cooperations and extension of scientific connections to other European countries, we envisage an acceleration and broadening of our activities in this important field.

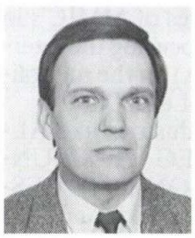

Péter Gottwald was born in Hungary in 1943. He graduated and took a Ph. D. in electrical engineering from the Technical University of Budapest in 1966 and 1978.

He joined the Department of Electronic Devices of Budapest Technical University, and was a visiting scientist at the Technical University of Aachen (RWTH-Halbleitertechnik) and the Technical University of Duisburg (Halbleitertechnik) in 1978, 1986 and 1990. He has acted for many years as a consultant to the Research Institute for Technical Physics of the Hungarian Academy of Sciences. He teaches solid-state electronics, and his research interests are in the field of microwave solid-state devices, III-V semiconductor technology, theory of microwave and optical interaction in solid-state microwave devices and noise problems of III—V semiconductor materials.

MMIC ACTIVITIES AND TRENDS IN EUROPE

F. GIANNINI

UNIVERSITY OF ROMA "TOR VERGATA"
DPT. OF ELECTRONIC ENGINEERING
VIA ORAZIO RAIMONDO – 00173 ROMA, ITALY

The continuous growth in the MMIC field is shown by industrial and academic initiatives, programs at national level and the research trends and challenges. Aim of this contribution is to highlight the above features at European level and, thus, to forecast the near and medium term involvements in MMIC activities.

1. INTRODUCTION

The last five years have seen a world-wide growing of interest and activities in the field of microwave and millimeter wave monolithic integrated circuits (MMICs).

The establishment of an affordable technology, in particular, seems to be the best way to acquire the performance requirements in terms of quality and reproducibility. Furthermore, the assessment of powerful hardware and software tools for computer-aided engineering can allow the achievement of an actual yield-driven optimization in the design of the MMIC under development.

These tools have been the challenging issues which have driven many national and international efforts in the GaAs MMIC arena.

The seven-years Microwave and Millimeter Wave Monolithic Integrated Circuits (MIMIC) Program of the Department of Defense (DoD) of the United States [1], for instance, as well as the Japanese Scientific Computer Systems Program and the Future Electronic Devices Program of the Ministry of International Trade and Industry (MITI) [2], represent a remarkable demonstration of the particular attention paid for this subject by the two leading countries in the field of advanced semiconductor production.

Similar initiatives have been taking place in many European Countries where industries, universities and research centers have begun working and collaborating in the development of advanced skills and know-how in the field of MMIC design and fabrication.

National programs, like the MADESS finalized projects of CNR in Italy, or international ones like the GIANTS, AIMS, OLIVERS, COSMIC Programs of the ESPRIT II Project of CEE [3] and the NOGAP (North European Gallium Arsenide Program) of the Scandinavian Countries have been driving some coordinate efforts in the achievement of the previously mentioned goals.

Furthermore, some interesting features of MMIC's in terms of weight, size and reliability, are focusing the interest of the European Space Agency (ESA) on the monolithic solution, at a "Space Qualification Level" [4].

At the same time many European industries like ALCATEL, SELENIA, TELETTRA, AEG TELEFUNKEN, SIEMENS, PHILIPS, THOMSON and PLESSEY, are establishing their own fabrication and/or design capabilities in order to guarantee the requested level of affordability and reproducibility.

The paper reviews the European status on MMIC activities, long-term programs, state-of-the-art achievements from both process-related and CAD-oriented points of view. In particular, highlights on the major efforts played at national level and at company level are presented to derive an overall picture and a dependable forecast on the MMIC field trends.

2. THE EUROPEAN EFFORTS IN MMIC ACTIVITIES

Most of the studies presently performed by European teams in the field of monolithic microwave integrated circuits are generally related to different aspects of the design, manufacturing and testing procedures involved in the development of modules specially devoted to civil applications. In fact, satellites (DBS, DRS, GPS), communications (mobile telephone) and transport and domestic applications (automatic payment, identification badges, car anticollision radar, etc.) [5] will require large quantities of monolithic microwave chips so these new civil markets can represent unique opportunity for the European Industries in the Nineties.

Therefore, the establishment of advanced design tools, characterization methods and realization techniques for monolithic integrated modules appear to be the final goal of cooperative activities of the various partners.

The research and development activities of the various operating groups are shared by the following five fields:

1. Material characterization and fabrication techniques [6]—[9]
2. Design techniques [10]—[15]
3. Measurement strategies and techniques [16]—[17]
4. Advanced modelling [18]—[24]
5. Packaging techniques [25]

It is worthwile noting that each of the above operating fields requires a continuous effort to be developed further, and every new achievement can normally represent an additional goal in the main project.

The practical implementation of monolithic integrated circuits, in fact, is rapidly changing all the perspectives of the microwave and millimeter wave electronics field.

The system engineer is becoming more condifent with the use of GaAs MMICs in system design, so taking full advantage of the appealing features of monolithic approach.

It ensues that present principal trends in the MMIC scenario can be linked to the two following aspects:

- A gradual substitution of hybrid subsystems and entire systems with the corresponding monolithic units. The improvement in MMIC technology, the increased single wafer dimensions, the establishing of the crucial process steps (so reducing the windows of performance, without a corresponding severe cutting of the final yield), represent favourable conditions for pushing the development of many system building blocks in a monolithic form.
- A development of monolithic units and subsystems of totally new concept and with a high level of functional integration. In a similar way as it happened with low frequency silicon integrated circuits, the suitability to use a great number of space-saving elements in MMIC technology is highly encouraging for modules like phase shifters

[26], phase detectors [27], transimpedance amplifiers [28]. These are based on concepts and topological solutions that are not any longer a straightforward extension or a copy of a well-established hybrid MIC solution.

3. EUROPEAN COUNTRIES AND MMIC PROGRAMS

An excellent opportunity of the cooperation at European level consists of the 7 programs of Esprit II Projects by CEE, related to the three-five components area, including the MMICs activities [3]. In Table 1. the above programs are summarized.

Following the positive experience of the 10 programs of the Esprit I Project, the European Community gathered 7 large international teams of universities, industries and research Labs deeply involved in a coordinate effort, to establish the proper level of knowledge to push ahead GaAs microwave and millimeterwave technology.

As it is easy to see, a large part of Western Countries are giving their contribution to different aspects of the MMICs activities.

The European Space Agency (ESA) activities in the MMIC area appear to be meaningful as well. These can be divided into the following main areas [29]:

- qualification for space application of European MMIC manufacturers (the so-called "capability approval");
- realization of specific MMIC devices for future space applications (FSS, SAR 2000, DRS, ABFN, etc.) through contracts awarded to European industries;
- in-house activities for training and research.

The last one represents a significant contribution to the development of the "monolithic culture" in Europe. ESA, in fact, is carrying out an internal training exercise aimed at training ESTEC engineers and young graduated engineers coming from all ESA member countries on design and test of MMIC devices.

Additionally, further remarkable activities in the MMIC field have been carried out at national level as described in the following.

3.1. Belgium

The MMIC activity is well represented by the program at IMEC (Leuven), presently based on submicron (0.5 to 0.25 μm) gate MESFET technology for low power applications. It is carried out in cooperation with the Belgian industry. Present realizations include LNAs operating around 15 GHz as well as mixer elements.

Efforts are also devoted to design techniques and modelling of microwave components. At the same time, an activity is being performed on the optimization of HEMT devices for MMIC applications. HEMT devices down to 0.1 μm gate lengths have been fabricated and characterized.

In the second stage of this project (1991), the above HEMT technology will be integrated into a complete MMIC process.

3.2. France

Several industries, organization and uniersities are involved in MMIC activities such as Alcatel Espace, CNES, CNET, Electronique Serge Dassault (ESD), Philips-LEP, Thomson and the University of Lille.

Philips-LEP and the Centre Hyperfréquences et Semiconducteurs (University of Lille) represent the two largest laboratories working in MMICs. The latter, in particular, has worked on different aspects of III—V components, such as material epitaxy by molecular beam, 1D or 2D modelling of any kind of III—V microwave components, microwave measurements, etc.

Other laboratories, like the Institut de Recherche en Communications Optiques et Microondes, Limoges University, Ecole National Superieure de l'Electronique et de ses Applications, CERCY-POINTOISE, work on CAD and models for MMICs.

A common aspect in the various MMIC activities is an advanced technological capability and a continuous improvement of process toward higher frequencies and more complex circuit functions.

A CNES contract (1989—1992) has been awarded to Alcatel Espace and ESD, aiming the development and integration of MMIC T/R modules for an SAR antenna.

3.3. Germany

The country is deeply involved in MMIC activities. The Ministry of Defence (MOD) and the Ministry of Research are promoting and funding specific supercomponents design and fabrication in the frame of a National GaAs Program.

A strong cooperation has been settled between industries and research centers such as the Universities of Duisburg, Darmstadt and Munich, the Fraunhofer Institute, the Daimler Benz Research Institute and the SEL Research Institute.

The development of improved technological steps and the design and fabrication of both digital and analog monolithic subsystems represent the major aim of the joint efforts.

A further activity in MMIC is ongoing in the Academy of Sciences in Berlin. In particular, technological (E-beam, epitaxy, ion implantation) and device development (up to 0.3 μm gate length MESFET, HEMT, JBT) are focused for low noise and power applications.

3.4. Greece

The MMIC activity is mostly represented by the technological efforts provided by F.O.R.T.H. (Foundation for Research and Technology Hellas, Heraklion-Crete). In particular, major developments are concentrated on material and devices.

F.O.R.T.H. is well inserted in many ESPRIT programs, and is now pushing on its in-house capabilities in the field of monolithic design and test procedures.

3.5. Italy

An example of the importance of a coordinate activity in the field of monolithic integrated circuits is provided by the Italian program funded by the Consiglio Nazionale delle Ricerche in the frame of the MADESS finalized project (started in 1986).

The program has gathered many industrial and academic efforts, in particular represented by Selenia and Telettra, the CRES Research Laboratory, the Universities of Bologna, Padova, Palermo, Pavia, Roma "Tor Vergata" and the Polytechnic of Torino.

All participants have been collaborating for four years in the establishment of capabilities in modelling, design test and fabrication of monolithic integrated subsystems in the 20—30 GHz frequency range.

More precisely, the studies are related to different aspects of the design, manufacturing and testing procedures

involved in the development of two particular demonstrators: a 21—25 GHz monolithic 18 dBm power amplifier (Gain: 12 dB; power added efficiency 20%) and 4 to 26.5 GHz (—6 dB) distributed amplifier.

3.6. Scandinavian countries

A coordinate activity in MMICs has been carried out in the frame of NOGAP, a three-year program started in 1986. The program consists of a joint effort among industrial companies and research institutes located in Finland, Sweden and Norway.

The major tasks of modelling, design and evaluation of MMICs have been shared among the three countries, with the main aim of increasing the availability of GaAs technology to industry in the Nordic countries. USA foundries are utilized as suppliers of the required technologies.

The results obtained through the program, which probably represents the first multinational trial of its kind in Europe, and the synergic cooperation between the Nordic Countries on advanced technology are stimulating all the partners in starting up a similar initiative, renewing the efforts and the aims of the first one. Denmark, perhaps, would be also included in the new program.

3.7. Spain

A national initiative utilizes the governmental funding of the Commission International de Ciencia y Tecnologia. The SSR Department of the Polytechnic of Madrid and the Electronic Department of the University of Cantabria participate in the program. The principal aim is the development and dissemination of know-how in the design and characterization of MMIC s, including the training of two University groups specialized in "Foundry Services" monolithic design.

The definition of MMIC subsystems and circuits of major interest for the Spanish industry, together with their design, fabrication and testing are some of the specific items under present consideration.

3.8. United Kingdom

MMIC activities are widespread and many industries as well as universities are involved. Plessey, STC, Universities of Cambridge and Glasgow and the University College of London are some of these.

The main efforts are focused to the design and development of circuits and subsystems in the microwave and millimetre-wave frequency ranges.

A continuous and noticeable improvement has been achieved in device, circuit and sub-system technology.

4. THE ROLE OF EUROPEAN INDUSTRIES IN MMIC ACTIVITIES

Many European industries have been involved in MMIC activities either in process and fabrication or in CAD tools. Among others, the following appear to be particularly active: Alcatel-Espace and Telettra, Plessey, Philips, LEP, Selenia, Siemens, Telefunken and Thomson.

4.1. Alcatel-Espace

Alcatel Espace (AES) has been present in the MMIC market since 1986. The activities started with a complete survey of GaAs foundries in Europe, USA and Japan, soon followed by pratical realization of AES own designs by various manufactures [30], [31].

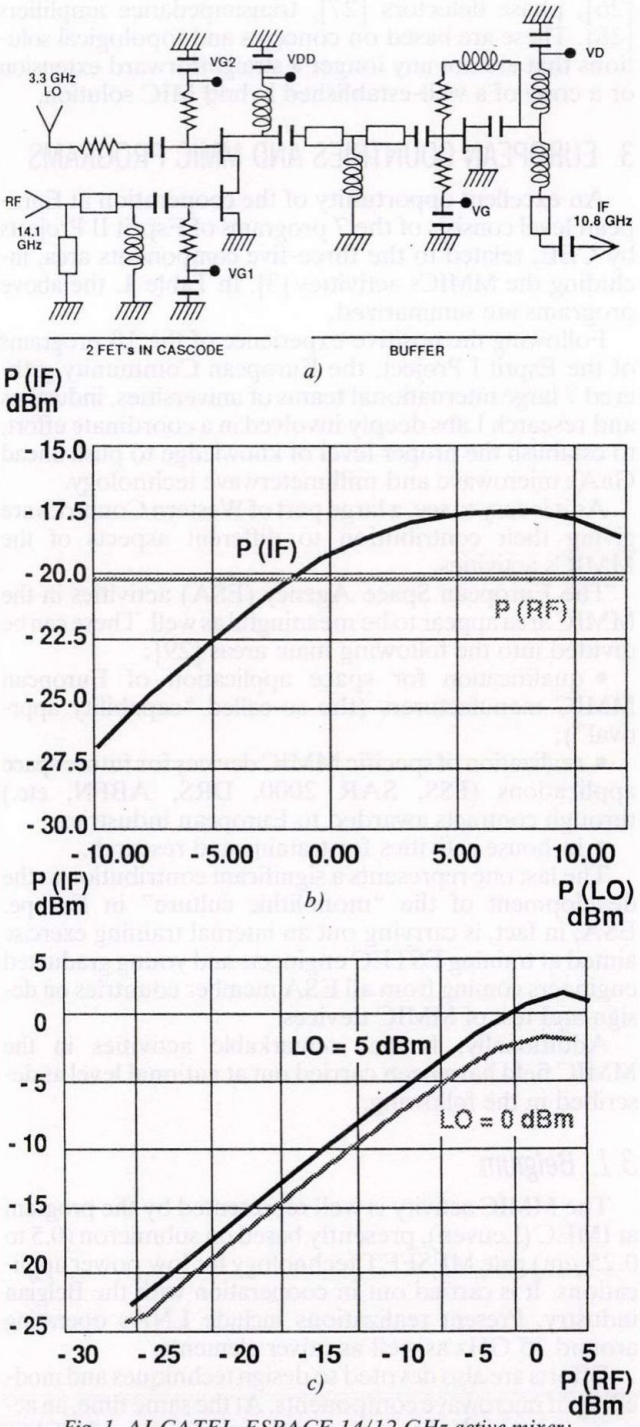

Fig. 1. ALCATEL-ESPACE 14/12 GHz active mixer: a) schematic; b), c) conversion performance

Low consumption, simple commands, large production (for phased array) as well as small size are of major concern. As a consequence, large efforts have been directed to design quality [14] or sophisticated yield prediction [32]. Furthermore, one of the AES' major involvements concerns the establishment of future space qualification procedures [33], [34].

Presently, AES is developing new versions of MMICs to be included in the following programs [35], [36]: C-band ESA'S SAR 2000; X-band CNES' RADAR 2000 France Telecom's Ku-band active antenna. The latter project involves several designs already developed and tested [36], such as a 14 GHz low noise amplifier, a 14/12 GHz active mixer (Fig. 1), a variable attenuator (PI-type) and its possible alternative, a frequency-scaled version of

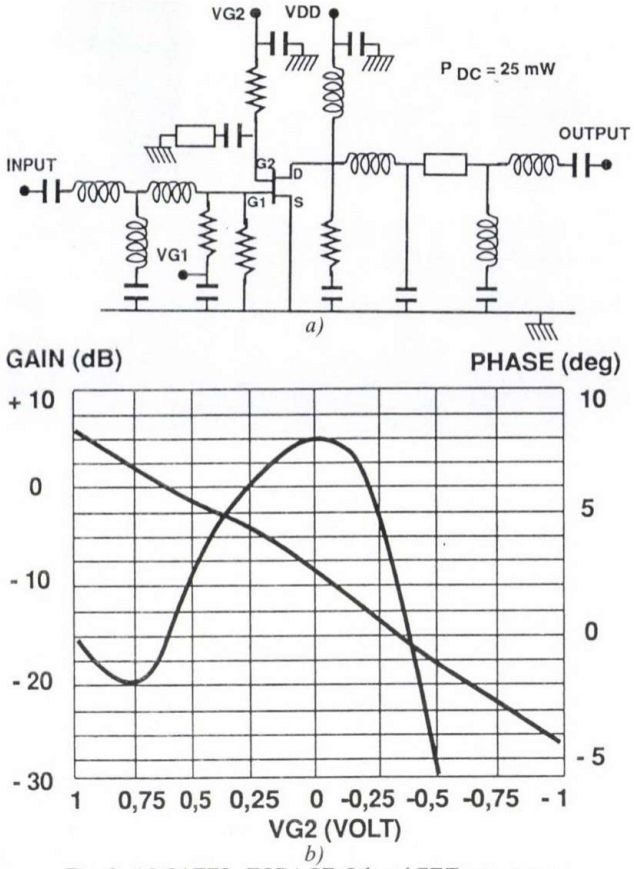

Fig. 2. ALCATEL-ESPACE C-band FET attenuator: a) schematic; b) gain and phase performance

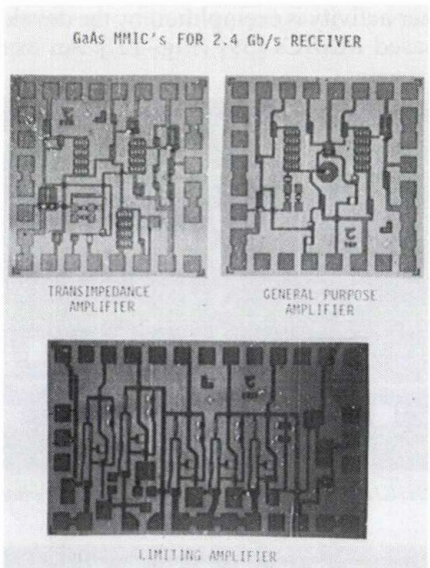

Fig. 3. TELETTRA chips for 2.4 Gbit/s fiber optic link

a dual-gate-FET C-band attenuator (Fig. 2); a 12 GHz medium level amplifier; a 2/MSB digital phase-shifter (180°, 90°), a 0° to 90° analog phase shifter; an X-band mixed digital/analog full 360° phase-shifter; a 4 LSB phase-shifter (45, 22.5, 11.5, 5.6 degs).

Encouraging results are claimed for the first-design developments, and improved versions of the present design are already in fabrication.

Other on-going projects at AES concern telecommunication applications at S, C and Ku-bands. Finally, AES is also involved in two ESPRIT projects covering the millimetre-wave area.

4.2. Telettra

Recently included in the Alcatel organization, Telettra has been a pioneer company in Italian MMIC activities. The main activity initially covered discrete MESFET power microwave transistors of which the Company uses several ten-thousand pieces per year for its own production of microwave Radio Links. The most representative devices in this sector are, at present, a 4W C-band MESFET, and a 100 mW K-band MESFET.

More recently (1987) the design and fabrication of MMICs was started, with the objective to use them in various telecommunication applications, thus improving performance, cost and reliability of systems. The main applications are again in Radio Links, but also in fiber optics circuits.

In Fig. 3., for example, a set of MMICs designed and developed for use at the receiving side of a fiber optic link (2.4 Gbit/s) is shown.

The three circuits are, respectively, a transimpedance amplifier, the function of which is to amplify the output signal of a photodetector, a general purpose amplifier, to further amplify the output signal of the transimpedance amplifier, and a limiter device to prevent circuit saturation.

Further monolithic chips developed at Telettra are depicted in Figs. 4 to 6.: a 4—8 GHz general purpose amplifier, a distributed amplifier and a transimpedance amplifier.

4.3. Plessey

Plessey Research and Technology is presently tasked with the development of advanced technologies, circuits and CAD tools. The aim of the company is to remain at the forefront of microwave applications, increasing the wide range of experience accrued in the last 15 years.

Following the realization of 1976 of the World's first GaAs MMIC, an X-band amplifier (6—12 GHz), Plessey has been assessing and developing new technologies and has been spending a considerable effort in research programs, as it is demonstrated by a total of over 500 scientist-years of GaAs research in the last 7 years.

Among the many different MMICs developed until now, achievements in following research topics appear to be particularly interesting.

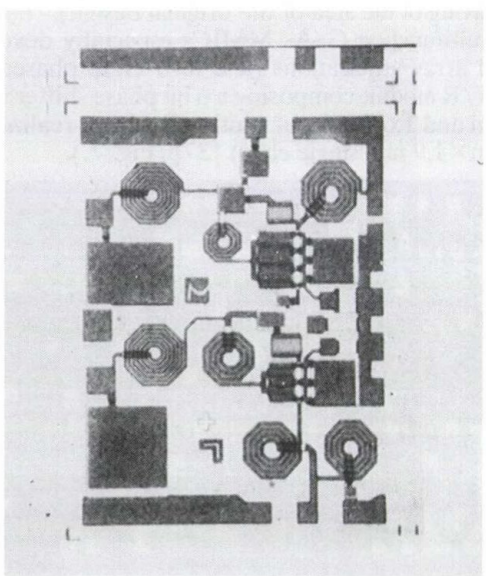

Fig. 4. TELETTRA 4—8 GHz general purpose amplifier

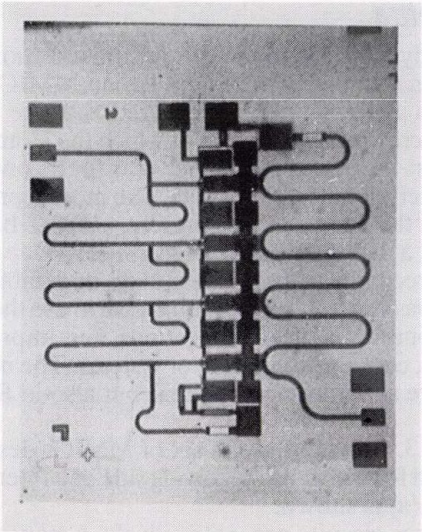

Fig. 5. TELETTRA distributed amplifier

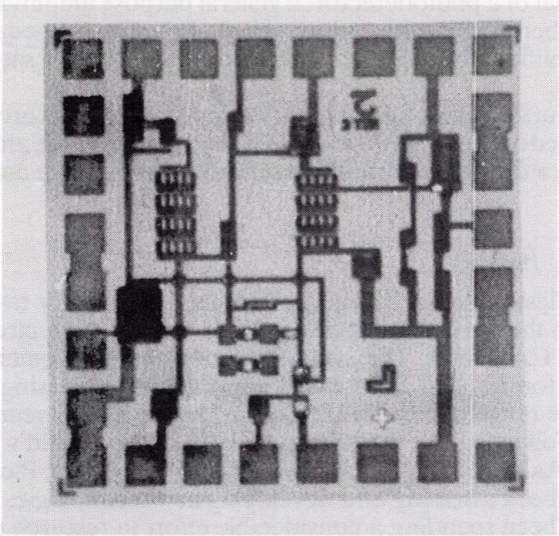

Fig. 6. TELETTRA transimpedance amplifier

• High-packing density conventional and novel circuits (a standard feedback amplifier currently offered by Plessey was redesigned and realized with the use of stacked inductors and input and output lumped matching network with a 70% saving of the area of the original design).

• Multifunction GaAs MMICs especially devoted to phased array applications (a 2 to 6 GHz phased array radar T/R module composing a 6 bit phase shifter with 20 dB gain and Tx/Rx signal routing has been realized on a 5.8 mm×1.9 mm single chip) [37] (Fig. 7.).

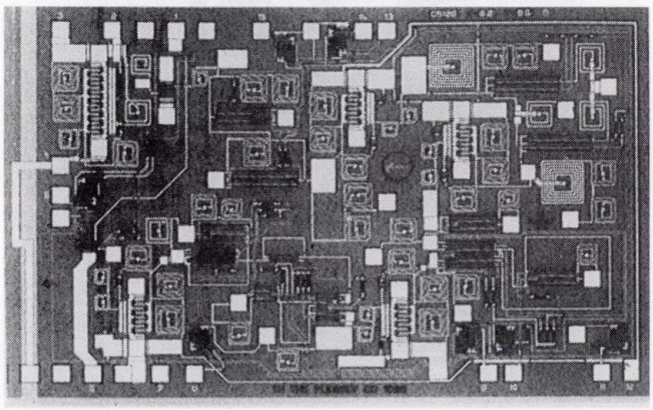

Fig. 7. PLESSEY 2—6 GHz phased array radar T/R module

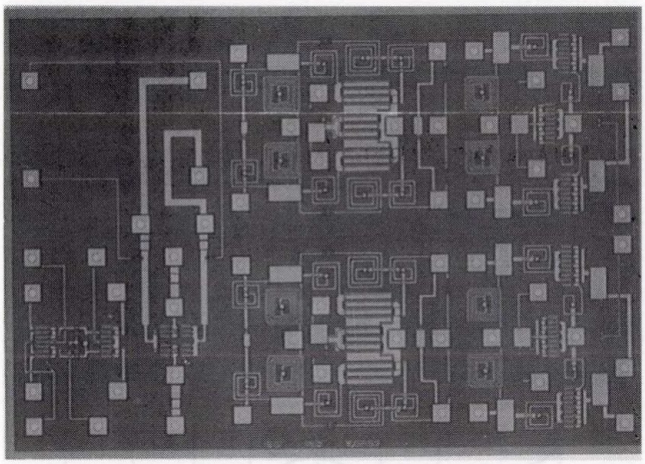

Fig. 8. PLESSEY S and C band receiver

• Flip-chip solder bondable MMICs (the ability to modify both the functionality and the frequency response of a GaAs MMIC by a flip-chip single solder bonding operation to a specific ceramic substrate has been demonstrated, through the realization of a 4.0×2.7 mm^2 uncommitted receiver chip to operate in S- and C-bands, with a total of 54 solder bonds) (Fig. 8.).

4.4. Philips-LEP

MMIC activities at LEP are mostly focused in the direction of developing fairly complex functions [38]. Example of the achieved capabilities are both a 0.1—4.5 GHz quadrature phase-shifter (Fig. 9.) and an S-band QPSK modulator (Fig. 10.).

A further activity is exemplified by the development of HEMT-based MMICs [39] (Fig. 11.). An example is a

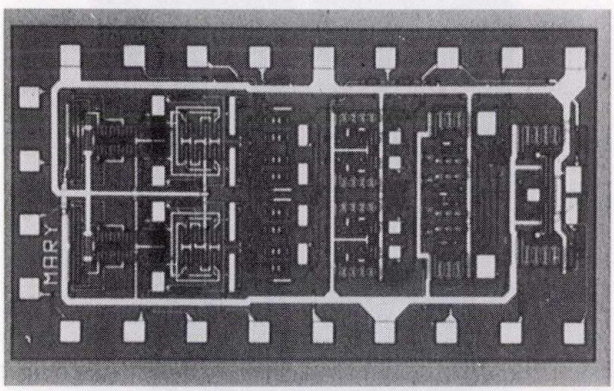

Fig. 9. PHILIPS-LEP 0.1 to 4.5 GHz quadrature phase shifter

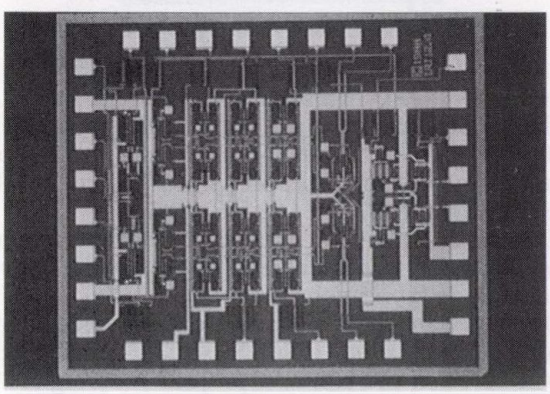

Fig. 10. PHILIPS-LEP S-band QPSKmodulator

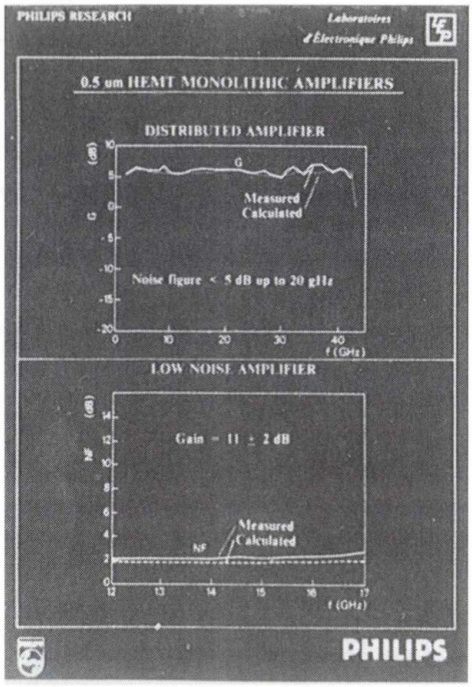

Fig. 11. PHILIPS-LEP Performance of HEMT-based distributed amplifier

cascode distributed amplifier in the 2 to 42 GHz frequency band, providing 6 dB gain. A further example is a two-stage reactive matched amplifier which provides 2.3 dB noise figure with 12 dB of associated gain at 15 GHz.

4.5. Selenia

Selenia's MMIC fabrication facility utilises both selective ion implantation and heterostructure growth by MBE for active layer formation. With these basic technologies, a wide range of MESFET and HEMT MMICs has been fabricated. Amongst the more conventional circuits such as oscillators and control devices, fabricated in Selenia, the family of MMIC amplifiers is of interest, in particular the X-band low-noise amplifiers (N.F.=2.8 dB, Gass=22 dB, and N.F.=2.0 dB and Gass=28 dB at 12 GHz), fabricated with MESFET and HEMT technology; the wide band travelling wave amplifier with approximately 6 dB gain in the 2 to 18 GHz frequency range (Fig. 12.); the cascadable wideband feedback amplifiers with either 10 or 20 dB gain in the 2 to 6 GHz frequency range (Fig. 13.); and finally the 1 Watt X-band power amplifier with 6 dB gain and minimum power added efficiency of 30% (Fig. 14.).

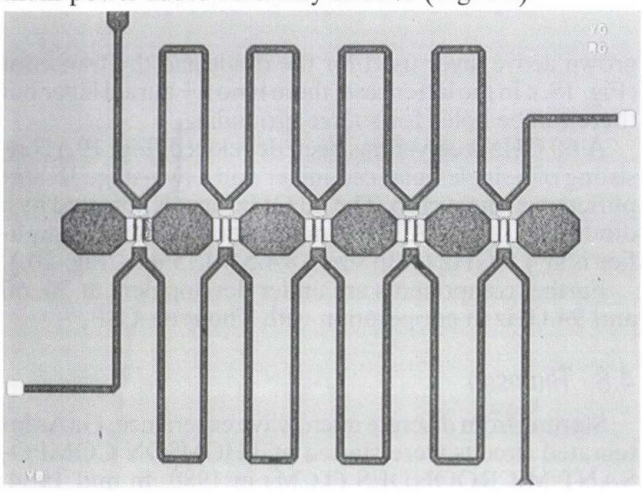

Fig. 12. SELENIA 2 to 18 GHz travelling wave amplifier

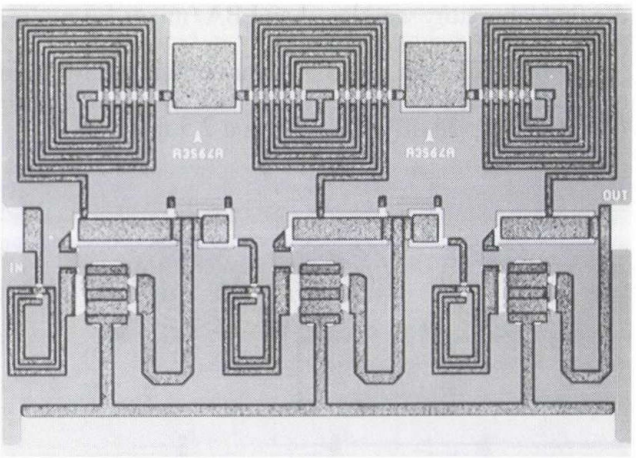

Fig. 13. SELENIA 2 to 6 GHz feedback amplifier

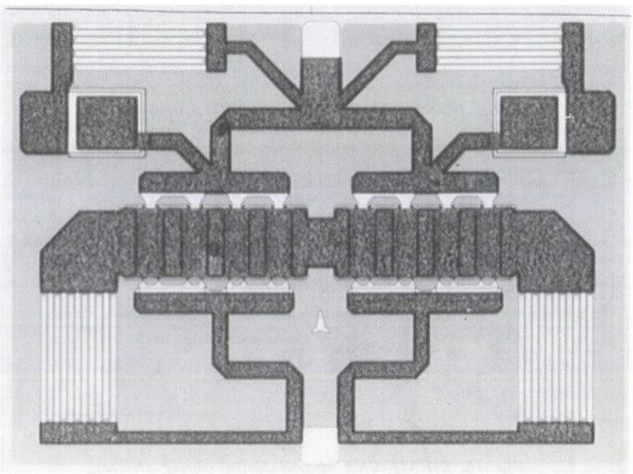

Fig. 14. SELENIA X-band power amplifier

4.6. Siemens

Beside NEC, Mitsubishi and Avantek, Siemens is one of the largest producers of GaAs microwave devices. Presently, about 4 million MESFETs and 100.000 MMICs are fabricated per year.

An important technological aspect is the wafer production, and development through realization on a modern 3″-wafer line using cassette-to-cassette equipment, I-line wafer stepper lithography and a special gate technology (the so-called DIOM process).

The work is focused on microwave applications especially in the 1—20 GHz frequency range. An example is a broadband IF amplifier (CGY50) (Fig. 15.). It is a one-stage amplifier with a 0.1—24 GHz bandwidth, providing a low noise figure ($\simeq$ 3 dB) and a very good linearity (IP3=31 dBm). This device is claimed to be the first MMIC commercially available (since 1981) produced in high quantities.

Concerning the development project, special emphasis is directed to MMICs for mobile communications (0.9—2.5 GHz), C-band T/R radar modules and landing systems, DBS receiver chips and T/R radar modules in X-band. In C-band, a complete set of MMICs (LNA, VGA, phase-shifter, MPA, HPA) is available as laboratory samples. Examples are a 6-bit digital phase-shifter with 10 dB insertion loss (Fig. 16.); a 2 stage MPA (realized in DIOM technique), showing 16 dB gain and 3.6 W output power (at 1 dB gain compression) with 26% efficiency (Fig. 17.). Finally, very good results are claimed for

the first laboratory samples of an LBA/mixer for mobile (handhold) communications.

About 13 dB gain and 5.5 dB noise figure have been measured with good linearity (IP3=10 dBm) and isolation (LO/RF: 30 dB) at 0 dBm and 2.5 mA/3.8 V.

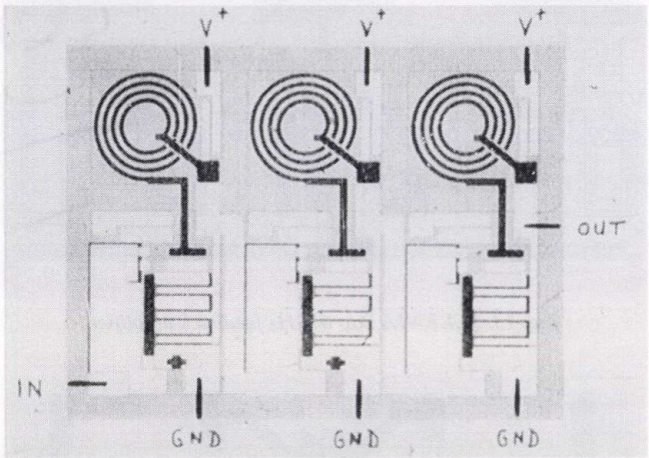

Fig. 15. SIEMENS broadband IF amplifier

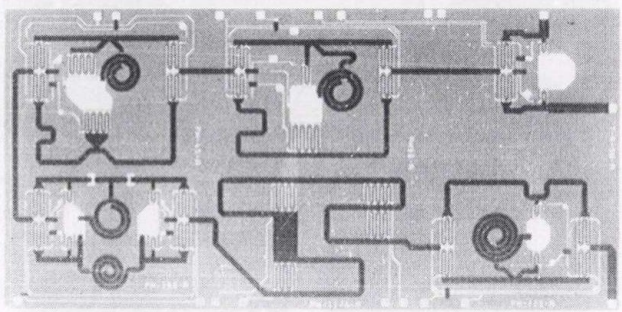

Fig. 16. SIEMENS C-band digital phase-shifter

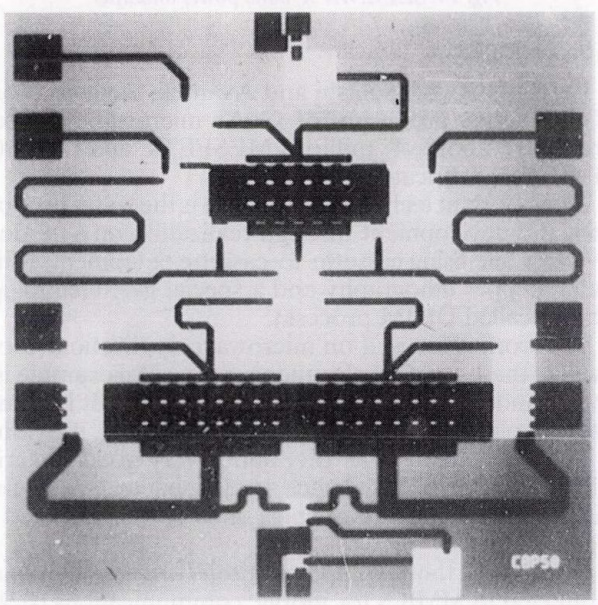

Fig. 17. SIEMENS C-band power amplifier

4.7. Telefunken

The company has acquired a wide experience in mm-wave sub-assemblies. The major technological highlight is a single process sequence for Schottky diodes and MESFET's, capable to integrate both diode mixers and MESFET amplifiers on a single chip. The technique makes use of deep implanted n+ wells underneath an epi MBE grown active layer used for the diode and the transistor (Fig. 18.). In the latter case, there is no n+ buried layer but there can be holes for source grounding.

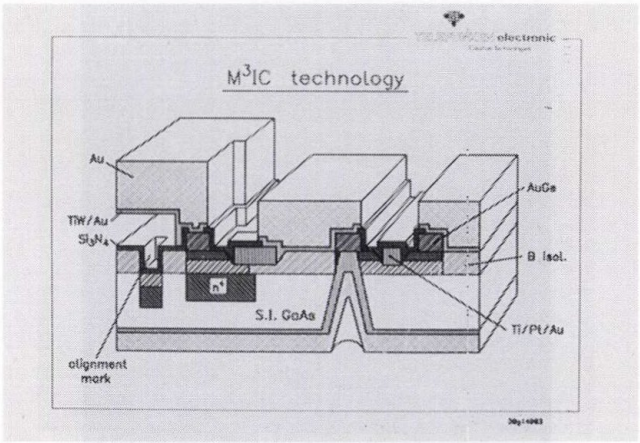

Fig. 18. TELEFUNKEN technology for diode and MESFET single process sequence

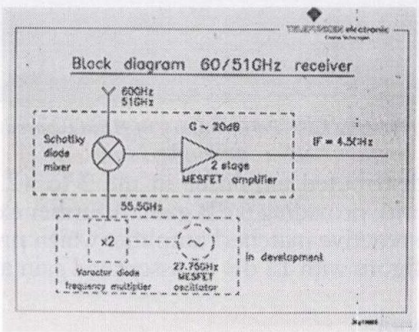

Fig. 19. TELEFUNKEN 60 GHz receiver

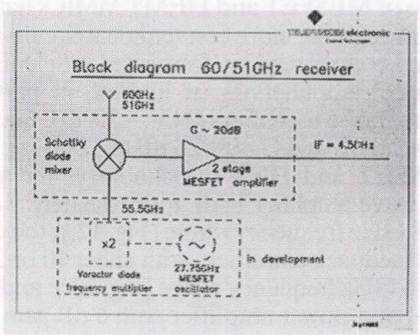

Fig. 20. TELEFUNKEN 4.5 GHz amplifier

A 60 GHz receiver has been developed (Fig. 19.) consisting of a single balanced mixer and a two-stage IF amplifier on a single chip. The 60 GHz input is detected by a diode with LO at 27.7 GHz multiplied by 2. The IF amplifier is at 4.5 GHz (chip size 4×4.5×0.15 mm, Fig. 20.).

Further components are under development at 30, 60 and 94 GHz in cooperation with Thomson-CSF.

4.8. Thomson

Starting from discrete microwave experience, GaAs integrated circuits were started at THOMSON COMPOSANT MICROONDES (TCM) in 1980. In mid 1984, the activity was merged with the corresponding teams

working at Central Research Laboratory of THOMSON CSF on monolithic and logic circuits.

Presently, two monolithic technologies based on ion implantation are available in a foundry: one for small signal and low noise applications, with an E-beam 0.5 μm gate length, and the other for power applications with a 0.7 μm gate length.

Further technologies based on molecular beam epitaxy layers are under development, one devoted to increase power capabilities to higher frequencies with a 0.5 μm gate length, the other to reach higher gain and lower noise figures at higher frequencies with a TEGFET (HEMT) technology, based on 0.3 μm gate length.

Using the same technology, discrete transistors are developed, delivering high power (1 W) up to 20 GHz, and satisfactory noise figure and gain at 40 GHz.

A library has also been developed, collecting models for passive and active components with linear and nonlinear characteristics. Part of the library is included in the Designer's Handbook which is supplied to designers using the foundry.

By utilizing either the presently available technologies or those under development, about a hundred MMICs have been realized in the TCM lines, covering all kind of circuits between 0.5 and 60 GHz.

Amplifiers (small signal, low noise, variable gain, medium power or high power), phase-shifters (analogue or digital), switches, oscillators, mixers are examples of the performed realizations.

These circuits are utilized in different types of subsystems like phased-array antenna modules, ECM equipments, front-end receivers or transmitters for terrestrial communication links, etc.

Among the developed MMIC's, the following are particularly interesting: a vectorial phase-shifter (Fig. 21.) providing continuous phase shift from 0° to 360° in X-band, with a bandwidth of 10% (chip size: 1 mm×2 mm); a power amplifier (Fig. 22.) delivering 1.5 W in X-band with 15 dB gain, 20% efficiency (chip size: 4 mm×2.8 mm); 7 chips for realizing a direct demodulation front-end receiver in the 5.9 to 8.5 GHz range (Fig. 23.): a low-noise amplifier, a 90° phase shift coupler, an in-phase coupler; 2 balanced mixers, a VCO and a buffer amplifier [40].

At the same location (Orsey), the Central Research Laboratory started in 1986 new activities in III—V components based on a long experience in material related topics.

These activities take place in the III—V Microwave Device Laboratory which claims a strong expertise in MBE and MOCVD epitaxial growth, characterization techniques and microwave advanced device processing, including fine-line electron beam litography, ohmic contact technology, dry etching and dielectric deposition techniques.

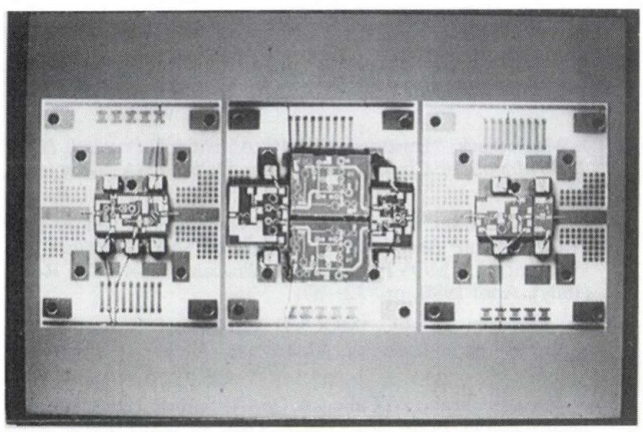

Fig. 21. THOMSON X-band vector phase shifter

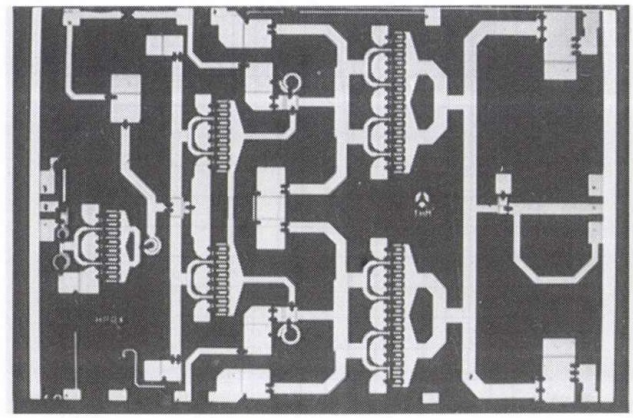

Fig. 22. THOMSON X-band power amplifier

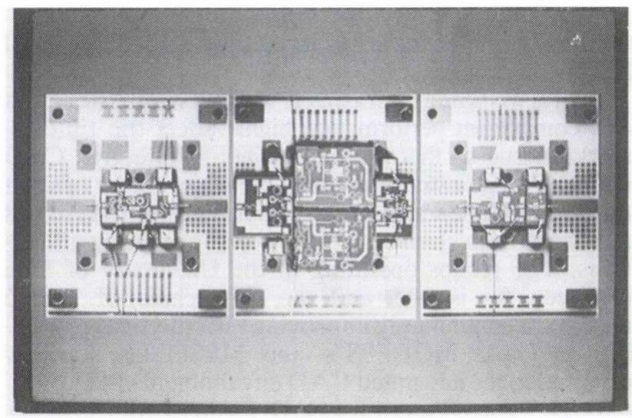

Fig. 23. THOMSON 5.9 to 8.5 GHz direct demodulation front-end receiver

5. CAD ACTIVITIES

Finally, a short survey is given of the CAD side of the MMIC field. The development of powerful and highly accurate models, based on physical and electromagnetic approach, for both active and passive devices, is un-

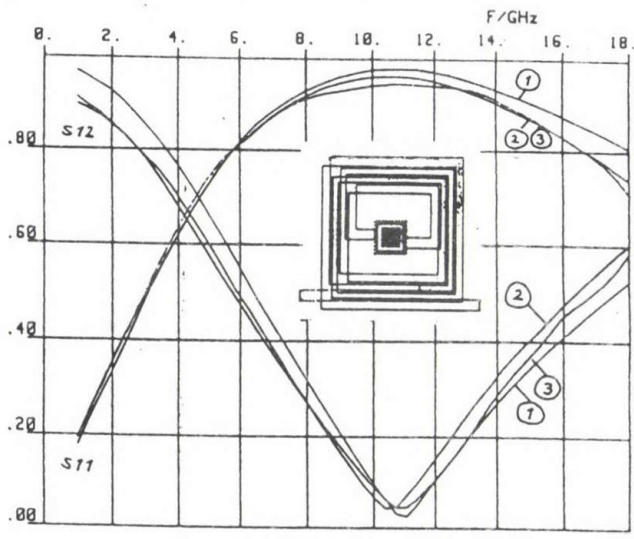

Fig. 24. Stacked offset spiral inductor
1. simple corner and loss description,
2. improved description,
3. RF on-wafer measurement

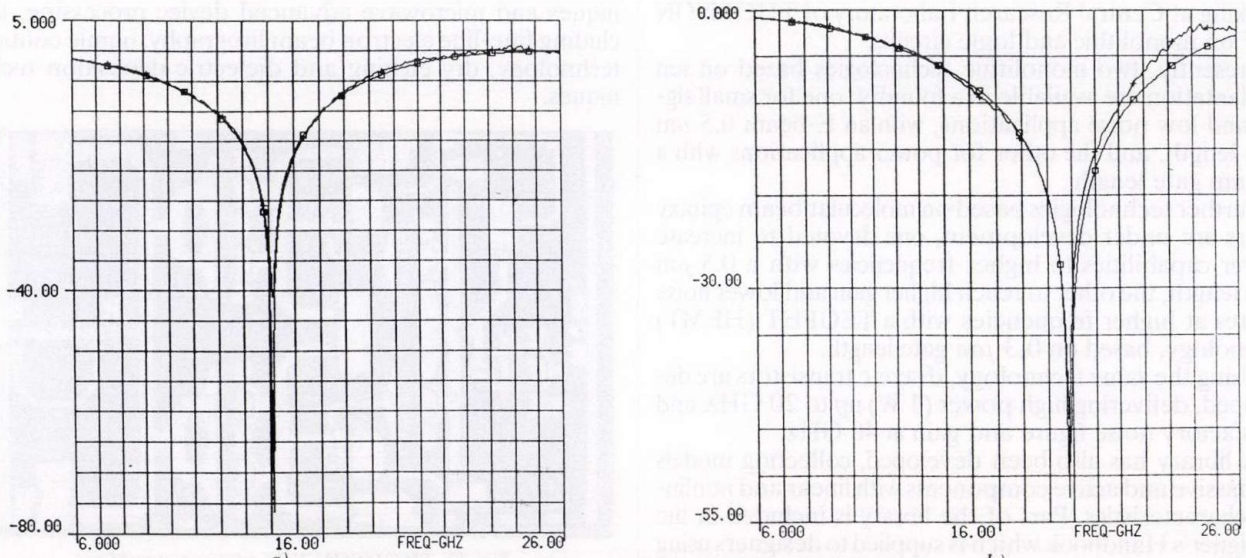

Fig. 25. Simulated and measured magnitude s21 for 10 Mil alumina. a) LS=80 mils; b) LS=60 mils

doubtedly one of the most interesting achievements of European researchers.

As it is well known, all aspects which concern the circuit and component performance highly affect the time-to-market issue so that the availability of effective CAD packages plays a strategic role in the achievement of short turnaround time frames. Significant contributions to this field have been given by groups working in many universities. The groups operating at the University of Lille (France), for istance, and the Polytechnic of Torino (Italy) are continuously improving their physical modelling of GaAs MODFET's and MESFET's specially oriented to the integrated CAD environments [41], [42].

R. H. Jansen (Plessey Research Caswell Ltd, England), has demonstrated the superiority of new geometry oriented MMIC design concepts, and developed very powerful CAD tools which perform the electromagnetic full wave simulation of complex MMIC conductor geometries, including parasitic coupling. As an example, Fig. 24. shows the experimental and theoretical behaviour of a stacked overlay spiral inductor in the 1 to 20 GHz range [24].

Another interesting and very recent example of a European contribution in the field of advanced CAD simulation tools is illustrated in Fig. 25. (a, b), showing the results of an improved simulation of a single stub configuration realized on a 10 mil alumina substrate. The experiments were provided by Essof, and the theory was obtained with an advanced simulation tool, developed at the University of Roma "Tor Vergata", based on the e.m. approach illustrated in [22].

6. CONCLUSIONS

The world-wide growing of interest and activities in the field of MMICs is now evident also in Europe. Some exciting opportunities in new civil markets like satellites, communications, transport and domestic applications, are strongly pushing on the establishment of an affordable technology and the contemporary assessment of powerful hardware and software tools for computer-aided engineering.

On the basis of similar American and Japanese experiences, many national and international programs have been started, giving a possibility to universities, industries and research labs to try new forms of collaboration and synergic cooperation. The first results are already demonstrating the validity of this kind of strategies and initiatives.

7. ACKNOWLEDGEMENTS

The realization of this review paper was made possible by the active contribution of a large number of colleagues who have been spending part of their valuable time in collecting and commenting the information here used by the author.

Thanking, all of them, a particular acknowledgement has to be paid to: J. Magarshack, G. Papageorgiou, G. Gatti, S. Iannazzo, A. Colqhoun, E. Pettenpaul, W. Menzel, I. Melhus, J. Perez Martinez, H. Meinel, C. Rumelhard, M. Van Rossum, J. L. Cazaux.

REFERENCES

[1] M. R. Stiglitz and L. D. Resnick, "The MIMIC Program: A Technology Impact Report", *Microwave Journal,* January 1989, pp. 30—36.

[2] M. Aikawa et alii, "MMIC Progress in Japan", *Proceed. IEEE 1989 Monolithic Circuits Symposium,* Long Beach (USA), June 1989, pp. 1—6.

[3] G. Papageorgiou, "III—V Activities in ESPRIT", *Proceed. of ESA/ESTEC Workshop on MMICs for Space Applications,* ESTEC, March 1990.

[4] F. Jean and W. Walker, "MMIC Reliability Issues and ESA Qualification Plan", *Proceed. of ESA/ESTEC Workshop on MMICs for Space Applications,* ESTEC, Noordwijk (The Netherlands), March 1990.

[5] J. Magarshack, "European MMIC Activities", *Proceed. IEEE 1990 Monolithic Circuits Symposium,* Dallas (USA), May 1990, pp. 85—90.

[6] D. Schnitz et alii, "The Application of GaAs Foil Rotation for Growth of InP Based III—V Compound Semiconductors in a Horizontal LP MOVPE Reactor", *Proceed. GAAS '90,* Roma (Italy), April 1990, pp. 32—37.

[7] M. Caldironi et alii, "MOCVD Growth of GaAs-Ga (1—x)Al(x)As structures for Microwave MESFETs", *Proceed. GAAS '90,* Roma (Italy), April 1990, pp. 43—48.

[8] A. Paccagnella and A. Callegari, "GaAs Surface Treatments and Device Applications", *Proceed. GAAS '90,* Roma (Italy), April 1990, pp. 49—54.

[8] A. Paccagnella and A. Callegari, "GaAs Surface Treatments and Device Applications", *Proceed. GAAS '90,* Roma (Italy), April 1990, pp. 49—54.
[9] B. Adelseck et alii, "A Monolithic 60 GHz Diode Mixer and IF Amplifier in Compatible Technology", *IEEE Trans. on MTT,* vol. 37, n. 12, December 1989, pp. 2142—2146.
[10] H. Kapusta et alii, "Design and Realization of 20 GHz Distributed Amplifier MMIC's", *Proceed. GAAS '90,* Roma (Italy), April 1990, pp. 62—67.
[11] J. M. Dieudonne, "A Simple Broadband DRO Design for Millimetre-Wave Applications", *Proceed. GAAS '90,* Roma (Italy), April 1990, pp. 81—86.
[12] P. Antolini et alii, "Design and Optimization for Industrial Production of a 4—8 GHz Monolithic Amplifier for High-Capacity Radio Links", *Proceed. GAAS '90,* Roma (Italy), April 1990, pp. 296—299.
[13] G. Montorial et alii, "Optimum Design and Realization of MMIC Power Amplifiers", *Proceed. 19th Eu.M. C.,* London (U.K.), Sept. 1989, pp. 451—455.
[14] D. Roques et alii, "A New Concept to Cancel Insertion Phase Variation in MMIC Amplitude Controller", *Proceed. IEEE 1990 Monolithic Circuits Symposium,* Dallas (USA), May 1990, pp. 59—62.
[15] B. Adelseck et alii, "A Monolithic 94 GHz Balanced Mixer", *Proceed. IEEE 1990 Monolithic Circuits Symposium,* Dallas (USA), May 1990, pp. 111—114.
[16] J. F. Vildalon et alii, "A Fully Automated On-Wafer Pulsed Measurement System, with Variable Pulse-Length and Duty Cycle, for Accurate Large Signal FET Modelling", *Proceed. 19th Eu.M.C.,* London (U.K.), Sept. 1989, pp. 569—575.
[17] G. Kompa and F. Lin, "New Algorithm Approach for Consistent Model Parameter Extraction of GaAs MESFET Equivalent Circuits", *Proceed. MIOP 1990,* Stuttgart (West Germany), April 1990, pp. 257—262.
[18] P. Donzelli et alii, "Thermal Model for Low and High Power GaAs MESFET Devices", *Proceed. GAAS '90,* Roma (Italy), April 1990, pp. 120—125.
[19] V. Rizzoli et alii, "A Fast and Accurate Microstrip Array Model for the Analysis of Integrated Passive Components of Complex Topology", *Proceed. GAAS '90,* Roma (Italy), April 1990, pp. 156—161.
[20] J. L. Caceres Armendariz and J. P. Martinez, "An Accurate Physical Simulator for the Extraction of MESFET Circuit Models", *Proceed. GAAS '90,* Roma (Italy), April 1990, pp. 108—113.
[21] G. Kompa and H. Schlechtweg, "Generalized Modelling of GaAs MESFETS and MODFETS Based on Highly Accurate Broadband Measurements", *Proceed. 19th Eu.M.C.,* London (U.K.), Sept. 1989, p. 179.
[22] F. Giannini et alii, "An Improved Equivalent Model for Microstrip Cross-Junction", *Proceed. 19th Eu.M.C.,* London (U.K.), September 1989, pp. 1226—1231.
[23] F. Giannini, "Advanced Applications of Radial Structures", *Proceed. of ESA/ESTEC Workshop on MMICs for Space Applications,* ESTEC, Noordwijk (The Netherlends), March 1990.
[24] R. H. Jansen, "Advanced CAD/CAM Software for Process-Related MMIC Design", *Proceed. of ESA/ESTEC Workshop on MMICs for Space Applications,* ESTEC, Noordwijk (The Netherlands), March 1990.
[25] F. J. Cotton et alii, "Uncommitted GaAs MMICs Assembled by Flip-chip Solder Bonding", *Proceed. GAAS '90,* Roma (Italy), April 1990, pp. 302—307.
[26] S. K. Altes et alii, "GaAs Phase-Coherent Microwave Multiple-Signal Generation Using All-Pass Networks", *Proceed. IEEE Monolithic Circuits Symposium,* Baltimore (USA), June 1986, pp. 71—74.
[27] P. Jean et alii, "Wide Band Monolithic GaAs Phase Detector for Homodyne Reception", *Proceed. IEEE Monolithic Circuits Symposium,* June 1987, pp. 123—125.
[28] A. Mauri et alii, "High Performance GaAs Monolithic Transimpedance Amplifiers for Multigigabit per Second Fiber Optic Links", *Proceed. GAAS '90,* Roma (Italy), April 1990, pp. 367—373.
[29] M. Lopriore and G. Gatti, "MMICs and Future ESA Programs", *Proceed. ESA/ESTEC Workshop on Monolithic Microwave Integrated Circuits for Space Applications,* STEC, Noordwijk (The Netherlend), March 1990.
[30] D. Roques et alii, "GaAs MMIC functions for C-band Receiver and T/R Module", *Proceed. ESA/ESTEC Workshop on MMICs for Space Applications,* ESTEC, Noordwijk (The Netherlands), March 1990.
[31] JL. Cazaux et alii, "Small size GaAs Monolithic Quadrature Coupler and Analog Phase-shifter using Lumped Elements", *2nd ISRAMT,* Beijing, China, Sept, 89.
[32] JL. Cazaux et alii, "A process Dependent Worst-Case Analysis for MMIC design based on a handy MESFET simulator", *IEEE-Trans on MTT,* Vol 37, n° 9, Sept. 89, pp. 1442/1451.
[33] A. Bensoussan et alii, "GaAs MMICs for Space Applications: a Product Assurance Policy", *Proceed. ESA/ESTEC Workshop on MMICs for Space Applications,* ESTEC, Noordwijk (the Netherlands), March 1990.
[34] G. Gregoris et alii, "Quality by design of MMIC — based systems", *Advanced Microelectronics Tech. Qualification,* Reliability and Logistic Workshop San Diego, California, August 90.
[35] M. Pouysegur et alii, "Fully or quasi-fully MMIC's equipment for space program" Proceed. *ASIA-PACIFIC Conference,* Tokyo, Japan, Sept. 90.
[36] JL. Cazaux et alii, "Ku-Band MMICs for Space-Born Active Antenna", *Proceed. 20th EuMC* — Budapest, Hungary, Sept. 90, pp. 287—292.
[37] A. Lane et alii, "S and C band GaAs Multifunction MMICs for Phased Array Radar", *Proceed. GaAs IC Symposium,* Oct. 1989, p. 259.
[38] F. L. M. Van den Bogaart et alii, A 10—14 GHz Linear MMIC Vector Modulator with less than 0.1 dB and 0.8° Amplitude and Phase Error", *IEEE Monolithic Circuits Symposium,* Dallas (USA), May1990, pp. 131—134.
[34] P. Gamand et alii, "2 to 42 GHz Flat Gain Monolithic HEMT Distributed Amplifiers", *Proceed. GaAs IC Symposium,* Nov. 1988.
[40] G. Pataut et alii, "A C-Band Direct Demodulation System", *Proceed. GAAS '90,* Rome, April 1990, pp. 184—189.
[41] T. Shawki and G. Salmer, "Computer Aided Analysis and Optimization of Subhalf-Micron-Gate MODFET Structures", *1990 IEEE MTT-S International Microwave Symposium,* Dallas (USA), May 1990.
[42] G. Ghione et alii, "Physical Modelling of GaAs Mesfets in an Integrated CAD Environment: from Device Technology to Microwave Circuit Performance", *IEEE Trans. on MTT,* vol. 37, n. 3, March 1989, pp. 457—468.

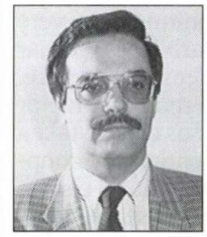

FRANCO GIANNINI received the degree in Electronics Engineering from the University of Roma "La Sapienza" in 1968, with a graduatin thesis on GaAs epitaxial growth and device fabrication techniques. In 1968 he joined the Institute of Electronics of "La Sapienza", where he was Assistant Professor until 1980. He was also Associate Professor of Microwaves at the University of Ancona, Italy (73—74), and of Solid-State Electronics (74—77) and Applied Electronics (77—80) at the University of Roma "La Sapienza". In 1980 he became Full Professor of Applied Electronics at "La Sapienza".

Since 1981 he has been with the University of Rome "Tor Vergata". He has been working on design methods of active and passive microwave components and circuits, including GaAs monolithic circuits. He is presently chairing the theme "MMICs in the 20 to 30 GHz range" of the CNR's National Project "Solid State Electronic Devices abd Materials", and he is active in the Esprit 5018 Cosmic Project. He is author and co-author of more than one hundred and twenty technical papers, and a consultant of several industrial and governmental organizations.

DISCONTINUITY PROBLEMS OF MMICS THREE-DIMENSIONAL ANALYSIS OF PLANAR CRICUIT DISCONTINUTIES

INGO WOLFF

DEPARTMENT OF ELECTRICAL ENGINEERING, 254 DUISBURG UNIVERSITY,
BISMARCKSTR. 69, D-4100 DUISBURG, GERMANY

A comparison of different methods for the characterization of planar and coplanar line discontinuities is given, thereby describing the present state of the art in this area of integrated microwave circuit CAD. Three-dimensional quasistatic capacitance circuit models and three-dimensional full wave analysis techniques like the spectral domain analysis technique using roof-top functions, and the finite-difference time-domain technique are described briefly and compared with respect to their numerical efficiency and capabilities.

1. INTRODUCTION

Microstrip and other planar line discontinuities have been the object of investigation for more than twenty years, because they have an essential influence on the computer aided design and the technical realization of integrated microwave circuits. With the introduction of monolithic integrated microwave circuits (MMICs) into microwave techniques, the requirements for good models which describe the discontinuities accurately over a large frequency range have become even more urgent. During the last two years, the development of coplanar circuits by monolithic integrated techniques required new models for the description of discontinuities. Moreover, real three-dimensional field-simulators are needed for the accurate description of multilayer microwave circuits including e.g. airbridge techniques and other three-dimensional techniques. In this paper, three different techniques which have been developed lately will be described, and their application to discontinuity problems in microwave integrated circuits will be discussed.

During the last three years, interesting new techniques based on the spectral domain analysis technique with a roof-top function current density description and, alternatively, based on the finite difference time domain technique have been developed. These techniques are very promising by offering the analysis of arbitrary planar structures and circuits in a three-dimensional space. Multi-layered structures can be considered, conductor losses, dielectric losses and radiation loesses can be taken into account, furthermore (this is very essential) the coupling of nearby discontinuities and line structures can be accurately calculated. The numerical expense of these techniques is still high, but there are techniques available to improve these analysis tools for future applications.

2. THREE-DIMENSIONAL QUASISTATIC ANALYSIS OF COPLANAR LINE DISCONTINUITIES

Line discontinuities appear in nearly every microwave circuit, and can be approximately described by lumped element equivalent circuits provided that their dimensions are small compared to the wavelength. For coplanar waveguides, this condition is fullfilled since the structure dimensions are almost independent of substrate thickness, and can therefore be chosen very small. Another interesting advantage of the coplanar waveguide is the small dispersion of its characteristic parameters due to the fact that the field is mainly concentrated in the spacings between the conductors, and does not change substantially with increasing frequency. This leads to the assumption that the frequency above which the static analysis of such structures is no longer valid is higher as in the case of a microstrip line. It is therefore of interest to test the validity of the static analysis results for coplanar waveguide discontinuities even at higher frequencies.

Several authors have reported on the calculation of equivalent capacitances for various discontinuities [1]—[5]. However, all these methods are applied to microstrip discontinuities only and cannot be implemented easily for other planar waveguides. Moreover, these methods do not consider the effect of metallization thickness of the conductors which, especially in the case of coplanar waveguide structures, can become comparable to the geometrical dimensions of the structure. The method presented in this paper is a general approach for finding the static capacitances of discontinuities as an abrupt change in conductor geometry. A three-dimensional finite difference method is applied to shielded coplanar structures, and the field distribution inside the shield is calculated using the successive relaxation method. The equivalent capacitances of the structure are then evaluated from the charge distribution on the conductors.

A program package has been developed which calculates the equivalent circuit capacitances of various ordinary discontinuities. The results for coplanar waveguide open-ends and gaps are presented in this paper. Since the equivalent parameters are calculated from the field distribution near the discontinuity, the method can be easily extended to any arbitary configuration of conductors on substrates with one or two layers. Further applications are demonstrated for coplanar interdigital capacitors on ceramic and gallium arsenide substrates. The effect of conductor metallization thickness as well as the influence of the shielding are also discussed. Measurements are performed in a broad frequency range to verify the accuracy of the applied method.

2.1. Numerical Calculation of the Field Distribution

The three-dimensional method presented here is a modified version of the well known finite difference method described in [6]—[9]. The planar structure containing the discontinuity and the semi-infinite trans-

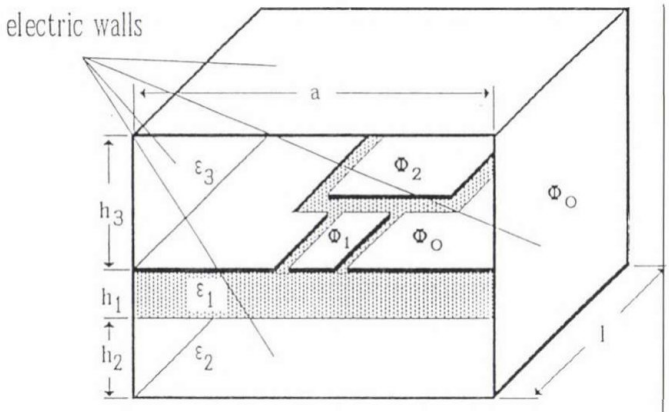

Fig. 1. Structure containing waveguide discontinuity

mission lines are surrounded by a shield of electric and magnetic walls. A magnetic wall is assumed where a transmission line intersects the shield (input and output ports). In Fig. 1. for example, the planar waveguide consisting of two semi-infinite coplanar lines and a junction region between them is shielded by two magnetic and four electric walls. The magnetic walls are defined at suitable distances from the discontinuity beyond which the infinite line conditions are fulfilled and the perturbations due to the discontinuity can be neglected. The bounded region is then divided into elementary boxes using a three-dimensional non equidistant cartesian grid. The electrical potential can be assumed to be constant inside the elementary boxes and confined at the middle of the box. Since the structure dimensions are small compared to the wavelength, the grid-points on the metallization are assumed to be at a constant potential (Fig. 2.).

Using Laplace's equation, the electrical potential at any point inside the shield can be written in finite difference form as a linear combination of potentials at neighbouring grid-points. The "relaxation method" is used for the solution of the resulting system of equations. The potential distribution inside the shield can be determined starting with assumed potential values at all the grid-points and modifying them as follows:

$$\Phi_{new} = \Phi_{old} - k \cdot R \qquad (1)$$

where R is the difference between Φ_{old} and the value given by (A10), and k is the relaxation constant which determines the speed of convergence. The optimal value of k is found here to be 1.8.

The accuracy of the calculated potentials depends on the number of iterations (n). This is demonstrated in Fig. 2. As shown in this Figure, 60 iterations are sufficient for

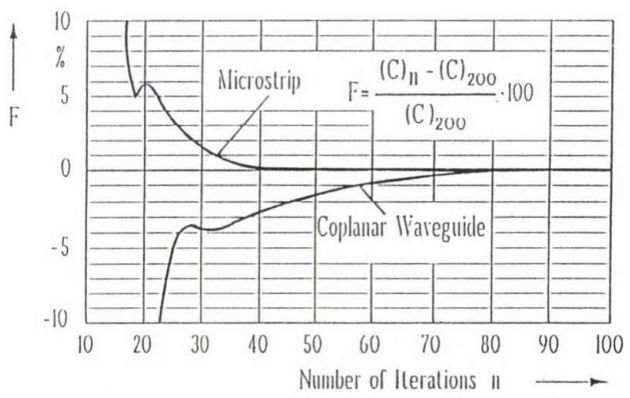

Fig. 2. Relative error of equivalent open-end capacitance as a function, of iteration number

an accuracy of better than 1% for the calculated equivalent capacitance of an open-ended line. The electircal field at any grid-point can then be calculated as

$$\vec{E} = -\vec{\nabla}\,\Phi. \qquad (2)$$

The field distribution obtained in this way is used in the next Section to calculate the charge distribution on the conductors.

2.2. Evaluation of Equivalent Capacitances

For the following descriptions, let us consider the configuration shown in Fig. 3. The field distribution calculated in (2) is used to find the total charge on the inner conductor (Q_{total}), as well as the charge per unit length on the connected transmission lines (Q'). Q' can be obtained from the relation

$$Q' = \varepsilon_0 \varepsilon_r \oint_C E_n \cdot ds \qquad (3)$$

where C is the contour of the integration region which covers the conductor cross section at the plane of the mag-

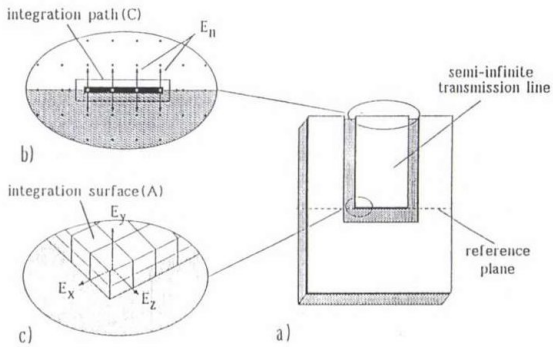

Fig. 3. Calculation of the charge per unit length (b) and the total charge (c) of an open ended coplanar line (a)

netic wall (Fig. 3b). The total charge can be calculated by integrating the normal component of the electric field over the inner conductor:

$$Q_{total} = \varepsilon_0 \varepsilon_r \oint_A \vec{E} \cdot \vec{n}\, dA \qquad (4)$$

The region of integration now covers the total conductor surface A (Fig. 3c). If the potential difference between the inner conductor and the ground planes is V, the capacitance associated with the discontinuity can be calculated from the difference between the total charge Q_{total} and the charge per unit length of the conected transmission line:

$$C_{eq} = (Q_{total} - 1Q')/V, \qquad (5)$$

where l/w is defined as the distance between the backtranformed reference plane of the discontinuity (e.g. Fig. 3a) and the magnetic wall. The effect of shielding on the equivalent capacitance is studied for a microstrip open-end (ε_r=9.8, h=0.635 mm) with the following dimensions:

width to height ratio ..... w/h=4,
distance to the lateral electrical walls .... $a/2$=10 h,
distance to the upper surface ..... b=10 h,
distance to the front electric wall ..... l_2=10 h,
distance to the magnetic wall ..... l_1=10 h.

Each of the last four parameters is changed separately while the others are held constant, and the equivalent capacitance of the open-end is computed each time. As shown in Fig.4., the distance to the magnetic wall l_1 is the

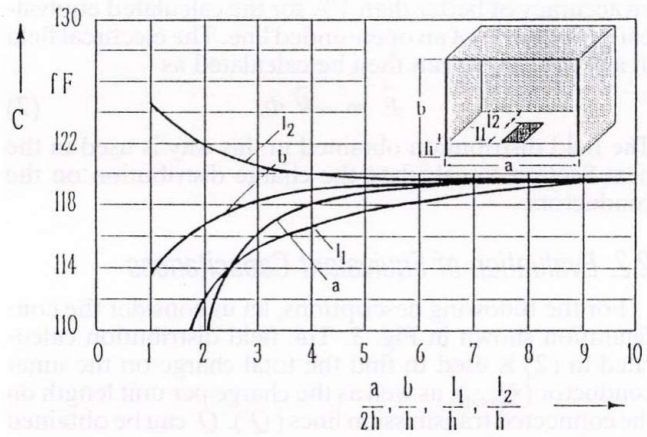

Fig. 4. Shielding effect on the equivalent capacitance of a microstrip open end

critical parameter and must be large enough. The distance to the front electric wall l_2 has a small influence on the calculated results.

2.3. Testing Structures

In this Section, several open-ends and gaps in various planar waveguides on ceramic and gallium arsenide substrates are treated. The effect of finite metallization thickness is discussed in more detail in the case of gaps. Moreover, coplanar interdigitated capacitors of various dimensions are investigated, and their scattering parameters are computed and compared with measured values.

A. Open-Ends

As is well known, the open-end of a transmission line stores electrical energy and can be simulated by an equivalent capacitance C (Fig. 5.e). An extended length Δl of the transmission line (Fig. 5.f) can also be used to model the open-end. The length Δl is defined as the ratio of the equivalent capacitance to the capacitance per unit length

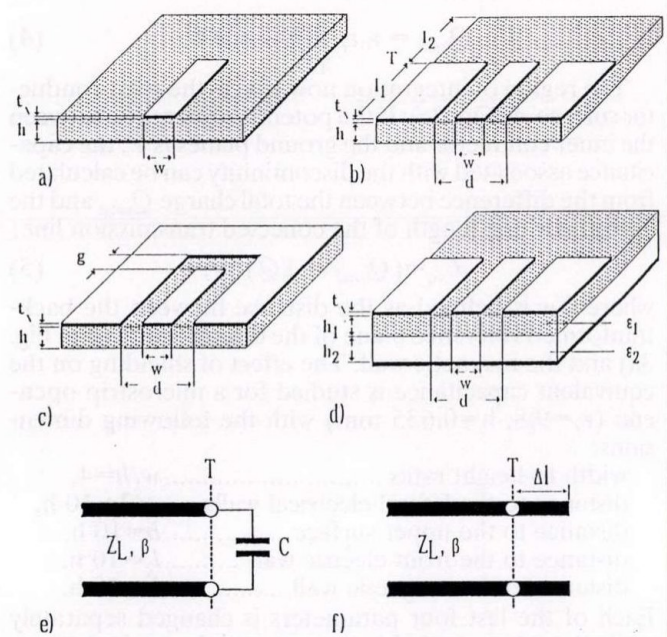

Fig. 5. Various open-ended planar waveguides and their equivalent circuit

of the line. In this paper, both C and Δl are calculated and used for the discussion of the result.

Figure 5. shows the various open-ended structures which are investigated. To indicate the accuracy of the chosen method, the extended lengths of microstrip open-ends of various dielectric constants as a function of width to height ratio have been compared with results from a spectral domain analysis presented in [10]. The data calculated with the presented method are in good agreement with the accurate values based on fullwave calculations.

The next test structure is the coplanar waveguide open-end of Fig. 5b. The field distribution of this structure in the conductor plane (Fig. 6.) indicates the scattering of the electric filed components of an assumed TEM wave at the end of the line. The calculated data of equivalent capacitances are plotted against the width to spacing ratio w/d for different substrate thicknesses (Fig. 7.). The equivalent capacitance increases steadily with the width of the

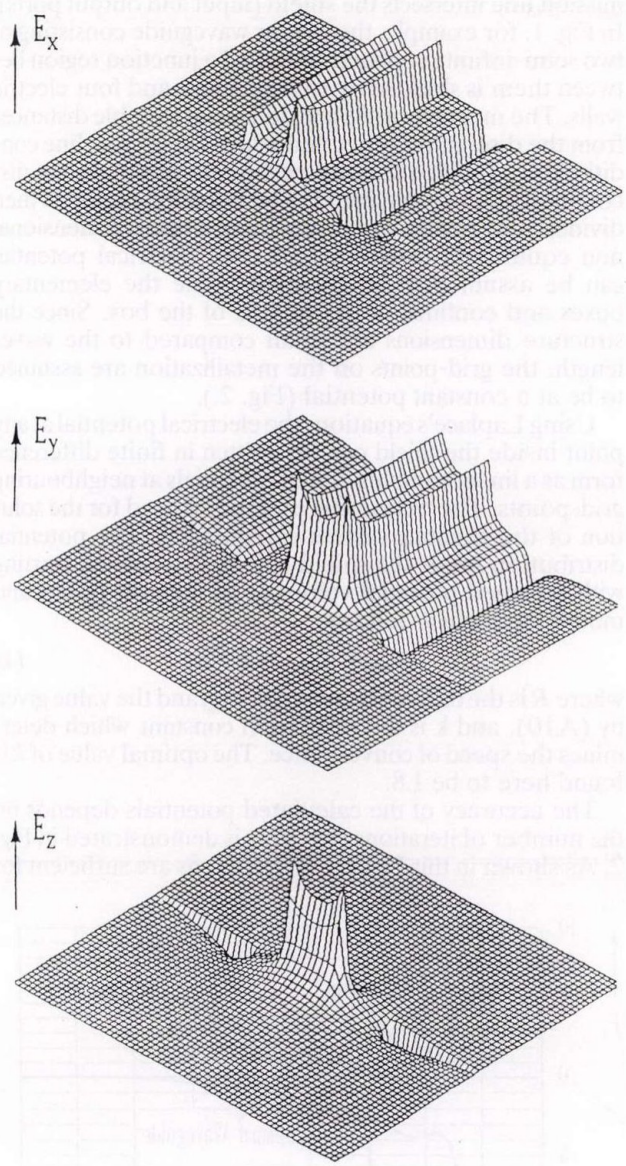

Fig. 6. Electric field components in the conductor plane of an open-ended coplanar waveguide supporting a TEM-wave

inner conductor. The calculated data are in good agreement with experimental values which are evaluated from the scattering parameter measurements in the frequency range from 45 MHz to 26.5 GHz.

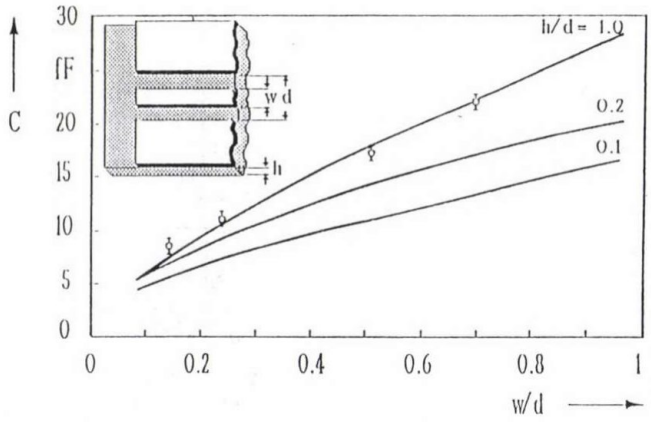

Fig. 7. Calculated equivalent capacitances of an open-ended coplanar waveguide ($\varepsilon_r = 9.8$, $h = 635\ \mu m$, $t = 0$) together with measured values for $h/d = 1.0$

B. Gaps and Impedance Steps

Based on the two-port pi-network model shown in Fig. 8e, the equivalent capacitances of gap and impedance step discontinuities (C_g, C_{p1} and C_{p2}) can be calculated in two steps. At first, the potentials on the inner conductors are assumed to be $\Phi_1 = \Phi_2 = 1$ V (see Fig. 1.) and at the ground plane $\Phi_0 = 0$ V (even mode). In this case, the capacitances C_{p1} and C_{p2} can be calculated as follows:

$$C_{p1} = (Q_{1_{\text{total}}} - l_1 Q'_1), \tag{6}$$

$$C_{p2} = (Q_{2_{\text{total}}} - l_2 Q'_2). \tag{7}$$

In the second step, the conductors are assumed to be at potentials $\Phi_1 = 1$ V, $\Phi_2 = -1$ V and $\Phi_0 = 0$ V (odd mode). Equations (6) and (7) are used again and the calculated

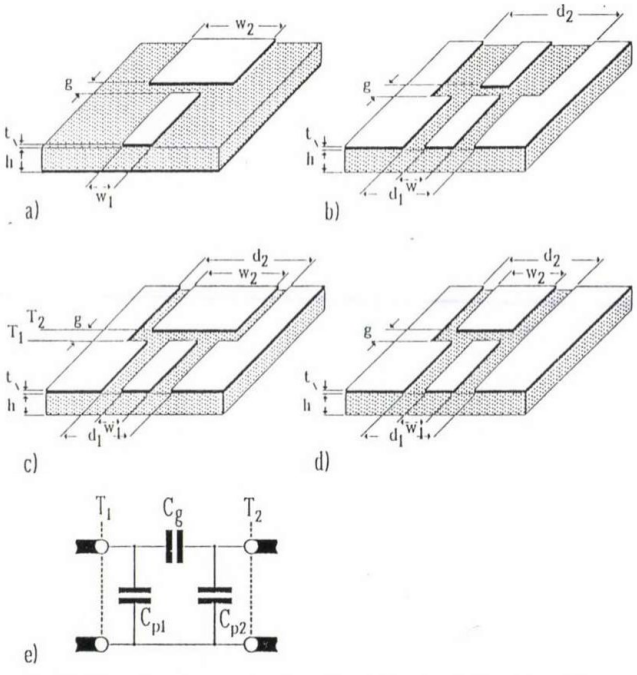

Fig. 8. Gaps in microstrip and coplanar lines and their capacitive pinetwork model

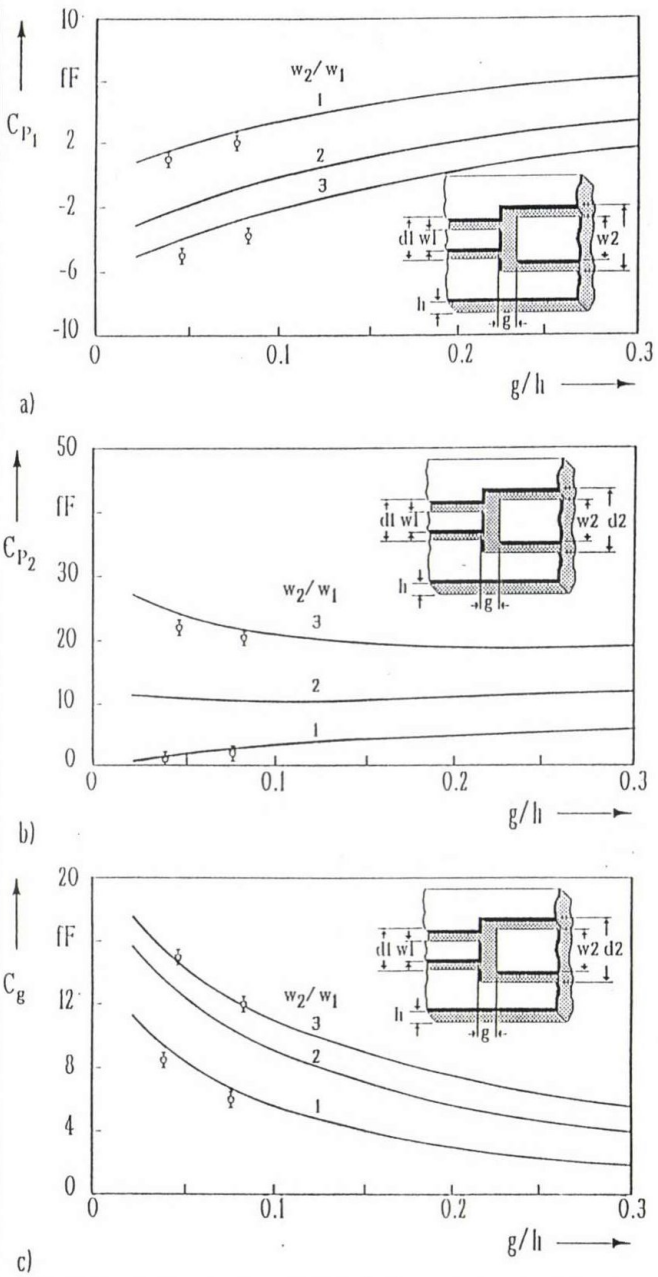

Fig. 9. Equivalent circuit capacitances of a symmetric gap between two 50Ω coplanar waveguides of different dimensions ($\varepsilon_r = 9.8$, $h = 635\ \mu m$, $w_1/h = 0.2$, $w_1/d_1 = d_2 = 0.56$, $t = 0$) together with measured values

capacitances in this case are called C_{11} and C_{22}. The series capacitance C_g can be determined as

$$C_g = 0.5(C_{11} - C_{p1}) = 0.5(C_{22} - C_{p2}). \tag{8}$$

In order to investigate the dependence of the equivalent network parameters on various geometrical dimensions, different types of gaps in coplanar waveguides (Fig. 8b—8d) are treated. Fig. 9. shows the calculated capacitances of a structure as shown in Fig 8c, where the lines have the same w/d-ratio but are of various dimensions, together with measured values. A negative value for the capacitance C_{p1} can be interpreted as an inductive effect of the discontinuity. The effect of metallization thickness on the equivalent capacitance C_g of the discontinuity is plotted in Fig. 10. As shown in this Figure, the metallization thickness cannot be neglected in the cases of very narrow gaps.

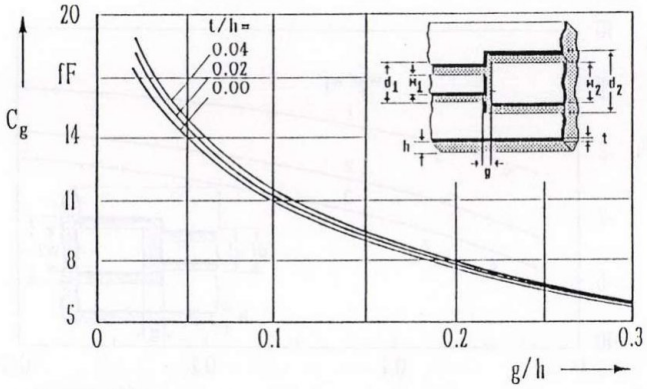

Fig. 10. The effect of conductor metallization thickness on the equivalent circuit capacitance ($\varepsilon_r = 9.8$, $h = 635\ \mu m$, $w_1/h = 0.2$, $d_1/h = 0.36$, $w_2/w_1 = 3$)

C. Interdigitated Capacitors

If the finger-lengths are small, interdigitated capacitors in principle can be considered as gaps between two transmission lines. In this case, the pure capacitive pi-network model shown in Fig. 8e can be used to describe such a structure. In order to check the validity limits of this model, coplanar interdigitated capacitors of various finger numbers and different geometrical sizes on ceramic and gallium arsenide substrates have been fabricated. The capacitances of the equivalent network are computed, and the calculated scattering parameters, together with results measured using an HP8510B Network Analyser (0.045—26.5 GHz), are plotted in Fig. 11. Although a

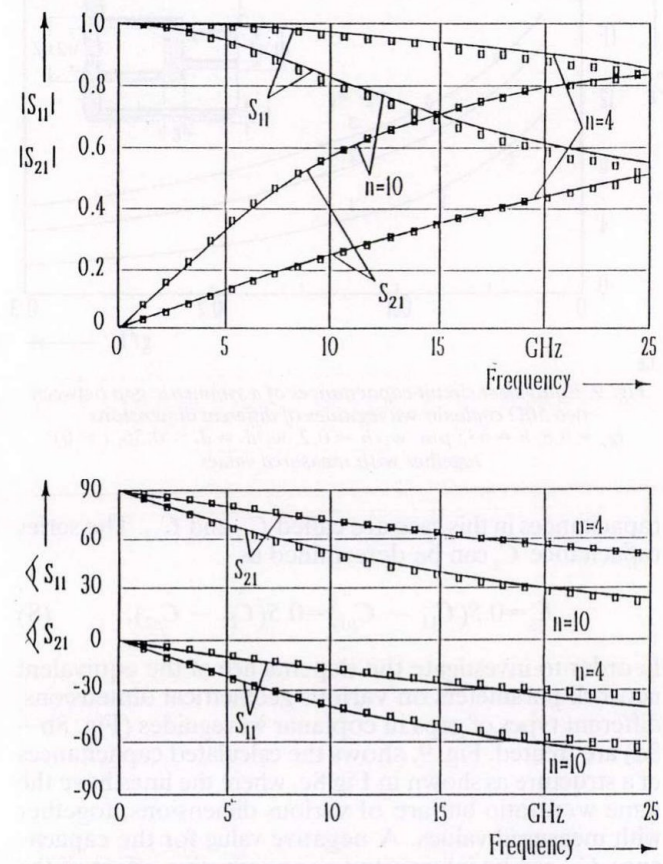

Fig. 11. The calculated (—) and measured (dots) scattering parameters of coplanar interdigital capacitors ($\varepsilon_r = 12.9$, $h = 400\ \mu m$, $1f = 100\ \mu m$ $n = 4$, $w_f = 17\ \mu m$, $s_f = 3\ \mu m$ (see Table 1, first line). $n = 10$, $w = 12\ \mu m$, $s_f = 2\ \mu m$ (see Table 1, second line)

Table 1.

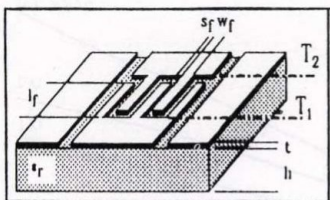

ε_r	nf	w_f	s_f	t	h	l_f	C_{p_1} in fF		C_{p_2} in fF		C_g in fF	
		µm	µm	µm	µm	µm	calc.	meas.	calc.	meas.	calc.	meas.
12.9	4	17	3	3	400	100	9.65	11	9.65	11	40.1	41
12.9	10	12	2	3	400	100	9.9	11	9.9	11	113.3	116
12.9	4	17	3	3	400	200	19.2	20	19.2	20	73	76
9.8	5	38	25	5	635	200	22.94	23	10.78	11	55	56
9.8	7	38	25	5	635	200	21.78	22	11.64	12	85	86

simplified circuit model is used, the agreement is very good up to 25 GHz. The small deviations of the reflection coeeficient at the highest frequencies are mainly caused by measurement difficulties at these frequencies due to the calibration.

In Table 1, the calculated and experimental data of the capacitors are listed. The experimental values are obtained from measured scattering parameters using optimization routines for the network fitting. In contrast to the microstrip case, the parasitic capacitances C_{p1} and C_{p2} of coplanar interdigitated capacitors do not depend on the size and number of fingers. This is due to the fact that the location of the ground planes can be varied conveniently in order to minimize the parasitic capacitances. As a result, it is possible to have a large value of C_g without increased parasitic effects. This can be done by using an increased number of fingers and a large spacing between the conductor and the ground planes.

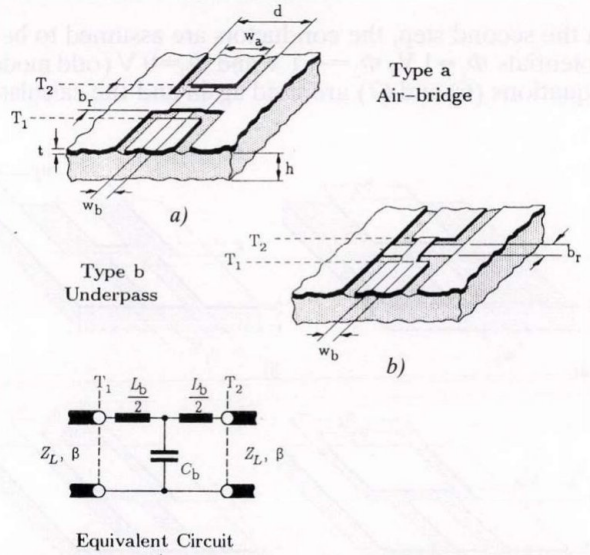

Fig. 12. The different types of airbridges: a) the conventional airbridge, b) the underpass and c) their equivalent circuit

D. Airbridges

A special discontinuity which is of high interest in coplanar circuits is the airbridge. Airbridges are insdispensable for the circuit design in coplanar waveguide technique because they have to ensure the biasing of active areas on the chip, and they must suppress multimode propagation along the RF signal paths. On the other hand they represent frequency dependent discontinuities causing losses and phase shifting.

There are at least two principle ways to build an airbridge in a MMIC fabrication process. Either the inner conductor remains a thin evaporated layer, and the strip, short circuiting the outer conductor of the CPW, is built by an electroplating process (type a, conventional airbidge, Fig. 12a.); or the inner conductor is galvanplastically built as a bridge across the deposited short circuiting strip in the ground metallization (type b, underpass, Fig. 12b.).

The elements of the equivalent circuit for describing the transmission properties of these airbridge constructions are calculated using the above described quasistatic finite difference technique. The distribution of the electrical field is calculated in the normal way and the capacitive elements of the equivalent circuit are derived from this electrical field distribution. The inductive elements of the circuit are also calculated using the finite difference technique, simulating the current distribution on the lines and near the discontinuity using the known charge distribution as a basis. From the current distribution, the magnetic field and the inductive elements can be derived.

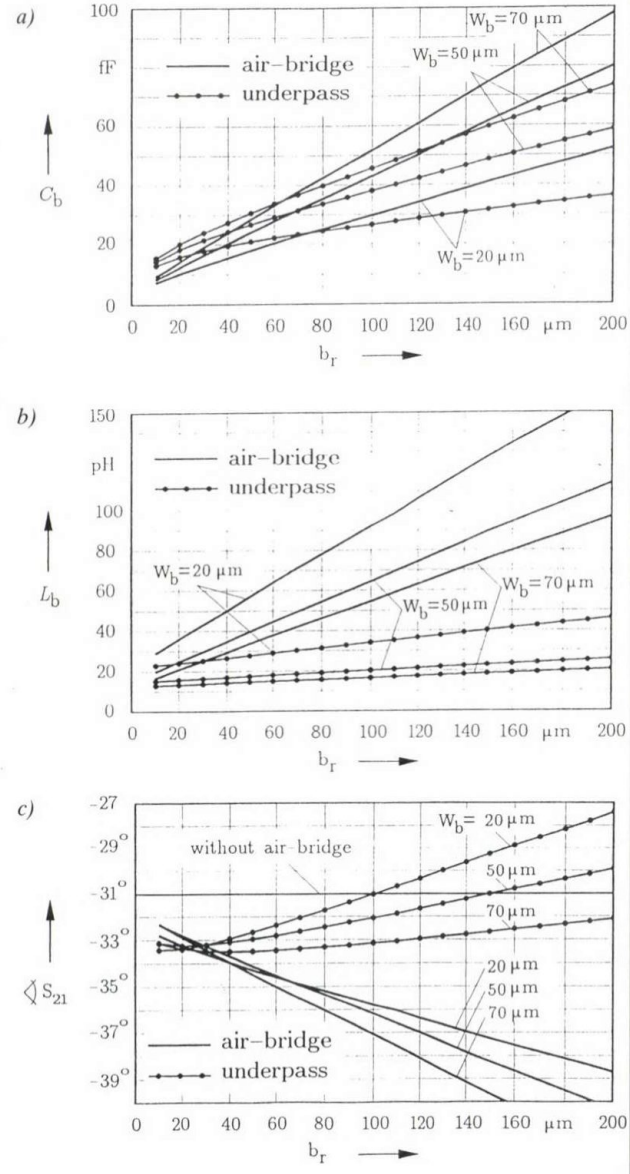

Fig. 13. a) capacitive and b) inductive elements of the equivalaent circuit for a conventional airbridge and an underpass, c) phase of the transmission coefficient. Outer line width w_a = 70 µm, line spacing d = 170 µm, bridge height t = 2.5 µm, bridge width b_r, inner line width w_b. Total line length l = 500 µm and frequency f = 20 GHz for Figure c)

Fig. 13a and 13b show the calculated result for the capacitive and inductive elements of the equivalent circuit as a function of the airbridge width b_r, with the width w_b of the inner conductor as a parameter. Big differences can be recognized in the dependences of the inductive elements on the airbridge width for the conventional airbridge (type a) and the underpass (type b). As a consequence, Fig. 13c shows the phase of the transmission coefficient S_{21} for the two airbridge constructions compared with a normal coplanar line of the same line width and spacing. As the Figure shows, above certain bridge widths, the underpass is electrically shorter than the undisturbed line. The conventional airbridge is always electrically longer than the undisturbed line.

This result is in a good agreement with the measurements as shown in Fig. 14. The change of the phase velocity in the airbridge region due to the additional capacitance is measured by means of slightly coupled CPW resonators. To gain significant frequency shifts, five to ten airbridges are involved in the corresponding line resonator. Additionally, each sample has a reference line in CPW technique without aribridges to normalize the network analyzer. The samples were tested using a microwave probe equipment.

There are two effects shifting the resonant frequency. On the one hand, the effective permittivity of the line may be reduced in the airbridge region. This effect gives a frequency shift to higher fequencies. On the other hand, there are additional capacitances to ground, loading the line resonator. This effect results in a frequency shift to wards lower frequencies. Also the measurement results indicate that the capacitive load effect is prevailing for airbridges of type A. For type B airbridges, the effect due to the reduced effective permittivity is the dominant one.

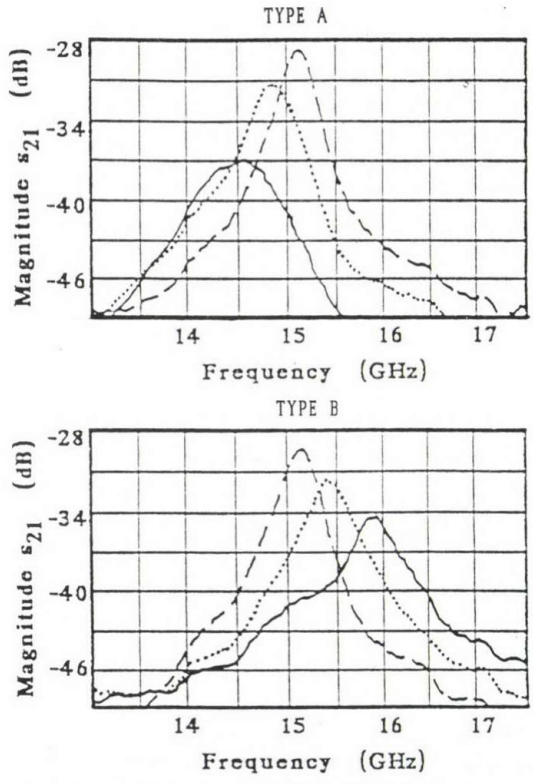

Fig. 14. Resonant frequency shift die to the total length of each air bridge of 10 µm (dotted line) and 50 µm (solid line) compared to a reference CPW resonator without air bridges (dashed line)

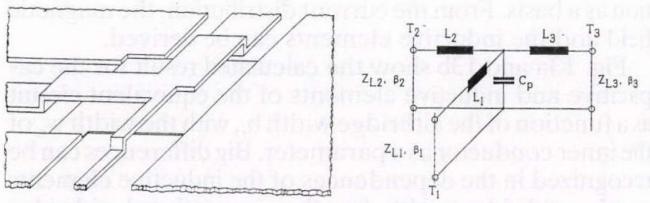

Fig. 15. The airbridge T-junction and its equivalent circuit

Besides the capacitive effects, also the ohmic losses of the different airbridge type must be taken into consideration.

Higher order modes on CPW are excited especially near asymetrical discontinuities. A T-junction in CPW technique, for instance, demands several airbridges to suppress higher order modes and to connect the RF grounds. It is very easy to avoid the excitation of higher order modes by applying an airbridge junction as it is shown in Fig. 15. An equivalent circuit of this airbridge T-junction can easily be found by using the above described finite difference method to calculate the additional capacitances and inductances in the discontinuity area.

3. SPECTRAL DOMAIN ANALYSIS USING ROOF-TOP FUNCTION FOR CURRENT DESCRIPTION

a) The Theoretical Method

Spectral domain analysis techniques have been used intensively for the analysis of single and coupled microstrip lines since they were introduced for the first time by Mittra and Itoh [11]. Only very simple discontinuities (open ends, gaps, impedance steps) have been analyzed using this technique. The numerical expense of this technique is high, and phenomena like surface wave excitation and radiation from the discontinuities cannot be described using this method because a metallic shielding is always needed.

Therefore it is not astonishing that methods which originally have been used for planar antenna analysis were applied in the analysis of simple microstrip discontinuities. Jackson and Pozar [13] and Katehi and Alexopoulos [14] described a solution for the open microstrip end and for a microstrip gap using a source formulation and Green's dyadic function in the spectral domain, thereby considering radiation and surface wave excitation at the discontinuities. They used halfperiod and piecewise sine-functions as expansion functions for the longitudinal currents, and the influence of the transversal currents was not considered.

All of the above techniques still have one essential disadvantage: for each microstrip discontinuity, a new field problem has to be solved. This can be overcome by using a treatment similar to Glisson [12] who, in a scattering problem, used simple current expansion functions which are defined piecewise over a rectangular surface which he called "roof-top-functions". This method has been used by Bailey and Deschpande [16] and Mosig [17] for the analysis of resonant frequency and input impedance of rectangular microstrip resonators. Rautio [18] for the first time used these expansion functions for the analysis of a simple microstrip discontinuity (open end), and Wertgen and Jansen [19], [20] developed it to a flexible design tool. Several improvements have been presented in [23].

Two different approaches are possible for the series expansion of the surface current density:

a) As much information on the geometrical sturcture and from known solutions for similar structures as possible is put into the functions describing the surface current density. For example, twice differentiable functions which satify the boundary conditions may be used as expansion functions to improve the convergence rate of the numerical method.
b) Simple expansion functions are used which approximate the surface current density only in a small area (subdomain), and which, by functional dependence and domain of existence, are not bound to a special geometrical structure.

The first approach has been used e.g. in [15] to analyze simple planar discontinuities. Using the approach b), however, enables any arbitrarily formed planar structure to be analyzed. New problems can directly be solved numerically, but with a reduced numerical efficiency. This reduced efficiency, however, can be overcome by the improved capabilities of modern computer systems.

To apply approach b) to a planar circuit problem, the metallized area in the x-y-plane is divided into e.g. rectangular cells. Curved boundaries can be approximated with sufficient accuracy by choosing a small cell size. Several basic functions can be used: a) piecewise sinusoidal basis functions; b) Unilinear roof-top functions as basis functions; c) Bilinear roof-top functions as basis-functions.

b) Theoretical and Experimental Results

As has been mentoned above, the classical way to solve the resulting system of equations for the current density expansion coefficients is the application of the moment method which leads to requirements of large computer storage. These requirements can be reduced by using iterative methods like the conjugate gradient method [21], [22] for solving the large systems of equations. Further improvements of the state of the art, as they have been described in [23], can be found as follows: a problem which leads to large computation time is the integration of the dyadic Green's function near the surface wave poles. New complex integration paths using linear curve sections can help reduce the computation time. Further improvements of the method with respect to computer time have been reached by separating an asymptotic part of the dyadic function which is characterized by a simple function and integrating it analytically. If losses of the material are additionally considered in the spectral domain calculation, the surface poles are shifted away from the real axis and the possibility exists to calculate the elements of the Z-matrix (which relates the electric field strength and the current density) with an efficient FFT-algorithm. The losses can be taken into account by considering the dielectric losses and the current losses in the ground plane metallization of the circuit (if it is available). The current losses of the metallic strip structure in the layered medium are incorporated into the boundary conditions. Surface waves and radiation losses can be accounted for by using a structure with an infinite shielding top plane or even an open space above the circuit.

One typical result from the spectral domain analysis using a roof-top function current density description is shown in Fig. 16. A radial stub with a closely coupled line and two closely coupled bend discontinuities has first been presented by Wertgen and Jansen [19], [20]. This structure has been produced and measured using the highly accurate measurement technique described in

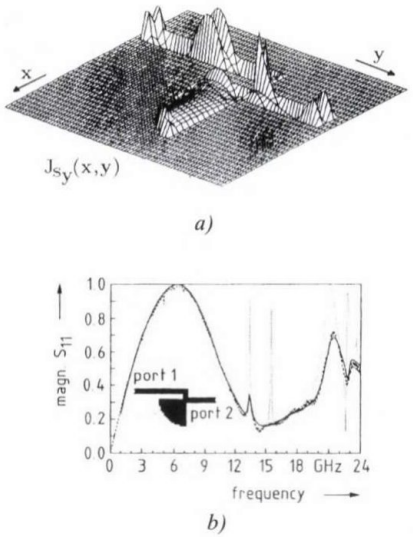

Fig. 16. Current distribution (a) and reflection coefficient (b) of a microstrip radial stub. (—) this method [23], (.....) Wertgen [19], (------) measured. Substrate and geometry: Al_2O_3, $\omega_r = 9.768$, tanδ = 0.0003, height = 0.635 mm, linewidth = .610 mm, gap = .61 mm, radius = 3.252 mm

[28], and the measurement results are compared to the theoretical results of Wertgen and Jansen and to the theoretical results using the improved method briefly described above.

Fig. 16a shows the current distribution on the radial stub as calculated using the roof-top functions. Figs. 16b and 16c show the magnitude and phase of the reflection coefficient. The improvements of the technique can clearly be recognized: Package resonances which occur in the calcualtion of Wertgen and which cannot be found in the measurements are no longer seen in the numerical results. Furthermore, the magnitude of the scattering parameters is much better (especially at resonant frequencies) if surface waves and radiation losses are taken into account (e.g. at 13.5 GHz and at frequencies higher than 18 GHz) (Fig. 16.). The good agreement between the measured and the calculated phases is also noted.

A second example given in Fig. 17. shows the calculated and measured scattering parameters S_{21} of a structure containing two coupled radial stubs which may be used to form a broadband dc-block as is shown in the Figure. Agreement between theory and experiment is very good over a large frequency range for the magnitude and the phase.

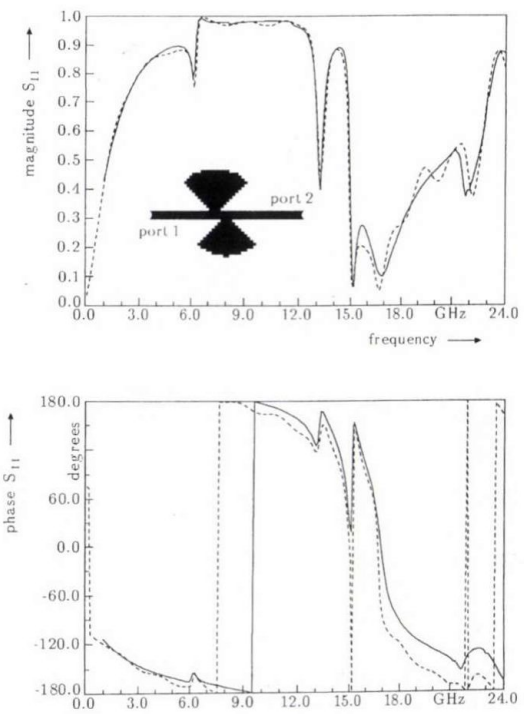

Fig. 17. Calculated (—) and measured (-------) reflection coefficient of a "shifted butterfly-structure". Substrate and geometry: Al_2O_3, $\varepsilon_r = 9.8$, tanδ = 0.003, height = 0.635 mm, linewidth = 0.16 mm, radius1 = 3.252 mm, radius2 = 2.847 mm, shift = 0.813 mm

4. THE FINITE DIFFERENCE TIME-DOMAIN APPROACH

a) The Theoretical Method

The Finite Difference-Time Domain method (FDTD-method) is a numerical technique for the analysis of electromagnetic field problems with a large numerical but low analytical expense. Despite the large numerical expense it is one of the most efficient techniques beacuse basically it only stores the field distribution at one time in memory instead of working with a large system matrix relating several unknowns. The field solution for every time is then determined by Maxwell's equations, and is calculated using a time-stepping procedure based on the finite difference method. The "leapfrog-algorithm" is used [24] which is determined by Maxwell's equations in four-dimensional finite difference form.

The electromagnetic field in the structure to be analyzed must be "excited", i.e. at the beginning of the calculation a certain field structure must be defined in the grid. Three possible methods will shortly be discussed:

a) At the time t_0 (starting time), the electromagnetic field is defined within the total space of the considered structure.
b) The second possibility is to define a harmonic field oscillation on a boundary of the structure.
c) The third form of excitation is to use an electromagnetic field pulse with a finite length in space and time. Using this kind of excitation, in principle arbitrary n-ports and their transmission properties can be analyzed if the incident, transmitted and reflected pulses can be separated. Because such a pulse contains a broad spectrum of frequencies, the transmission properties in a desired frequency range can be determined with only one analysis. The pulse length in time must be so short that the spectrum contains all the desired frequencies. The length in space must be so short that incident and reflected pulses can be exactly separated. On the other hand, the node distances of the grid which is used must be smaller than the space length of the pulse to guarantee an accurate calculation of the spatial field distribution.

Version c) of the discussed excitations is well suitable for the analysis of microstrip planar circuits. For the exciting pulse, a Gaussian pulse $f(t)=\exp[-(t-t_0)/T]$ may be used. The pulse width in time is determined by T. Because e.g. the microstrip line is dispersive, the pulse form is changed while propagating along the line. From the calculated electromagnetic field, time dependent voltages and currents can be calculated at the ports of the circuits. From the time dependent signals the equivalent values in the frequency domain can be determined using a Fourier-transformation, so that the scattering parameters at defined ports or reference planes can be calculated from these results.

b) Results and Discussion

An FDTD-program for analyzing planar microwave circuits of arbitrary metallization structure has been prepared in the author's research group. The metallization structure can be defined using a graphical editor. Input and output ports of the structures are uniform microstrip lines (e.g. 50 Ω lines for comparison with measurements). The structure is enclosed in a "shielding" of absorbing walls.

The total space is typically subdivided into 40 grid elements Δh parallel to the line length, 100 elements parallel to the width of the line and 20 elements perpendicular to the substrate material. The time length Δt typically is chosen so that the wave propagates along the grid length in five time steps. This time is calculated using a static approximation of the phase velocity. The spatial width of the exciting field pulse is about $40\Delta h$. From these data all other values are determined. If the pulse width is defined as the time or space where it has decreased to 0.05 of its maximum value, the maximum frequency which can be considered, using the mentioned pulse data, is about 50 GHz.

If t_0 is chosen to be $300\ \Delta t$, the pulse is "switched on" at a moment when its value is still very small ($2 \cdot 10^{-12}$ of the maximum value). The fields are evaluated at the absorbing boundaries for the electric fields and at $0.5\ \Delta h$ in front of the boundaries for the magnetic fields. About 1000 time steps are used for the analysis, and 2^{13} time ponts are used for the Fourier transformation to get accurate results in the frequency domain. The values for time steps higher than 1000 are filled with zero.

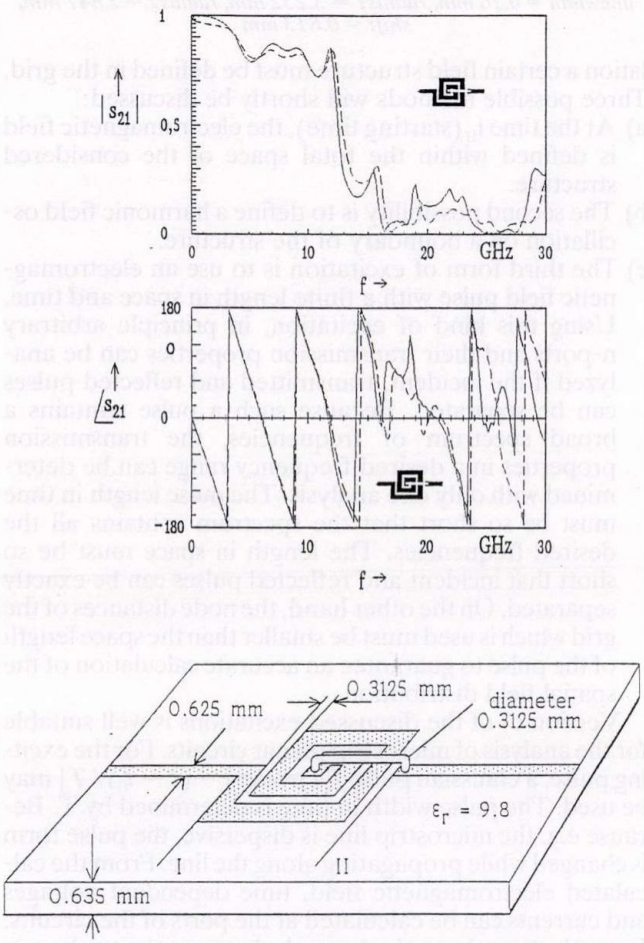

Fig. 18. The spiral inductor and the calculated (—) and measured (- - - - -) transmission coefficient of the spiral inductor. The dimensions of the inductor have been chosen to be very large so that resonance effects could be measured in the frequency range up to 30 GHz

The application of the method to only two different discontinuities shall now be discussed. More detailed information may be found in [25]. It will be shown that the finite difference time domain analysis technique can be used to analyze three dimensional structures. In a first example, a spiral inductor shown in Fig. 18. includes an airbridge above the surface of the substrate material. The structure is analyzed using the FDTD method. As the calculated and measured s-parameters of this complicated planar component show, the agreement between theory and measurement is excellent even for frequencies above the first resonant frequency for the inductor, for the magnitudes as well as for the phases.

Finally, a coplanar airbridge problem shall again be analyzed using this full-wave three-dimensional analysis technique. Fig. 19. shows a coplanar band reject filter with the dimensions given in (Fig. 19a). This filter has been analyzed once (Fig. 19b), and secondly without (Fig. 19c) the aribridges near the T-junction discontinuity shown in (Fig. 19a).

The filter has been designed for application in a frequency multiplier operating from 18 to 36 GHz. It therefore should have no transmission at 18 GHz and good transmission at 36 GHz. The stub length was selected to be 1.780 mm. As Fig. 19b shows, the analysis including the (three-dimensional) airbridge is in quite good agreement with the measurements. Fig. 19c shows how the filter transmission properties are changed if the airbridge is not taken into account.

From this application it follows that e.g. for the design of millimeter-wave coplanar circuits, a full-wave three-dimensional field simulation technique must be available to receive relevant results from the computer aided design methods.

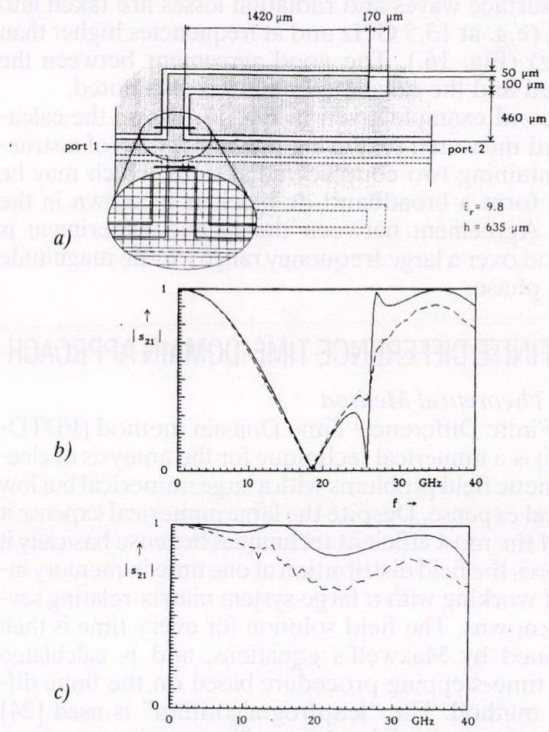

Fig. 19. A coplanar band reject/band pass filter for 18/26 GHz (a), calculated (—) and measured (- - - - -) considering airbridges (b) and without airbridges (c)

5. FINAL DISCUSSION

For modern MMIC design, analysis programs which are able to analyze multilayer and three-dimensional structures must be available. For coplanar circuits which will be of high interest for the future, in many cases three-dimensional static analyses can be used with advantage. In the case of microstrip circuits, discontinuities in multilayered circuits, closely coupled discontinuities and arbitrary planar structures can be characterized using spectral domain techniques and roof-top description of the current density. In cases where real three dimensional full-wave analysis is needed, the finite-difference time domain technique is a very flexible tool.

All mentioned techniques are able to consider conduction losses. The spectral domain analysis and the finite difference time domain technique additionally consider radiation losses and excited surface waves. If a closed package is considered, the spectral domain techniques can be used to analyze possible package resonances and coupling phenomena excited by these package resonances.

REFERENCES

[1] P. Silvester and P. Benedek, "Equivalent capacitances of microstrip open circuits", *IEEE Trans. Microwave Theory Tech.*, vol. MTT-20, pp. 511—516, Aug. 1972.

[2] P. Benedek and P. Silvester, "Equivalent capacitances of mcirostrip gaps and steps", *IEEE Trans. Microwave Theory Tech.*, vol. MTT-20, pp. 729—733, Nov. 1972.

[3] M. Maeda, "An analysis of gap in microstrip transmission lines", *IEEE Trans. Microwave Theory Tech.*, vol. MTT-20, pp. 390—396, 1972.

[4] C. Gupta and A. Gopinath, "Equivalent circuit capacitance of microstrip step change in width", *IEEE Trans. Microwave Theory Tech.*, vol. MTT-25, pp. 819—822, Oct. 1977.

[5] P. Silvester and P. Benedek, "Microstrip discontinuity capacitances for right-angle bends, T-junctions, and crossings", *IEEE Trans. Microwave Theory Tech.*, vol. MMT—21, pp. 341—346, May 1973.

[6] H. G. Green, "The numerical solution of some important transmission-line problems", *IEEE Trans. Microwave Theory Tech.*, vol. MTT-13, pp. 676—692, Sept. 1965.

[7] M. V. Schneider, "Computation of impedance and attenuation of TEM-lines by finite difference methods", *IEEE Trans. Microwave Theory Tech.*, vol. MTT-13, pp. 793—800, Nov. 1965.

[8] H. E. Stinehelfer, "An accurate calculation of uniform microstrip transmission lines", *IEEE Trans. Microwave Theory Tech.*, vol. MTT—16, pp. 439—444, July 1968.

[9] T. Hatsuda, "Computation of coplanar-type strip-line characteristics by relaxation method and its application to microwave circuits", *IEEE Trans. Microwave Theory Tech.*, vol. MTT-23, pp. 795—802, Oct. 1975.

[10] M. Kirschning, R. H. Jansen and N. H. L. Koster, "Accurate model for open end effect of microstrip lines", *Electron. Lett.*, vol. 17, pp. 123—124, 1981.

[11] R. Mittra and T. Itoh, "A new technique for the analysis of the dispersion characteristics of microstrip lines", *IEEE Trans. Microwave Theory Tech.*, vol. MTT-19, pp. 47—56, 1971.

[12] A. W. Glisson, *On the development of numerical techniques for treating arbitrarily- shaped surfaces.* Ph. D. Thesis, Unviersity of Mississippi, USA, 1978.

[13] R. W. Jackson and D. M. Pzar, "Full-wave analysis of mcirostrip open-end and gap discontinuities", *IEEE Trans. Microwave Theory Tech.*, vol. MTT-33, pp. 1036—1042, 1985.

[14] P. B. Katehi and N. G. Alexopoulos, "Frequency-dependent characteristics of microstrip discontinuities in millimeter-wave integrated circuits", *IEEE Trans. Microwave Theory Tech.*, vol. MTT-33, pp. 1029—1035, 1985.

[15] N. H. L. Koster and R. H. Jansen, "The microstrip step discontinuity: A revised description", *IEEE Trans. Microwave Theory Tech.*, vol. MTT-34, pp. 213—222, 1986.

[16] M. C. Bailey and M. D. Deshpande, "Integral equation formualtion of microstrip antennas" *IEEE Trans. Antennas Propagat.*, vol. AP-30, pp. 651—656, 1982.

[17] J. R. Mosig, "Integral equation models, Sommerfeld integrals, method of moments", *Workshop on Microstrip Antennas,* Montreux, 1988.

[18] J. C. Rautio, *A time-harmonic electromagnetic analysis of shielded microstrip circuits.* Ph. D. Thesis, Syracuse Unviersity, 1986.

[19] W. Wertgen, *Electrodynamische Analyse geometrisch komplexer (M)MIC-Strukturen mit effizienten numerischen Strategien (Electrodynamic analysis of geometrically complex (M)MIC structures with efficient numerical strategies.* Doctoral Thesis. Duisburg University, FRG, 1989.

[20] W. Wertgen and R. H. Jansen, "A 3d fieldtheoretical simualtion tool for the CAD of mm-wave MMICs", *Alta Frequenza* (Italy), vol. LVII-N.5, pp. 203—216, 1988.

[21] R. Chandra, *Conjugate gradient methods for partial differential equations.* Ph. D. Thesis, Yale University, USA, 1978.

[22] A. F. Peterson, *On the implementation and performance of iterative methods for computational electromagnetics.* Ph. D. Thesis, University of Illinois at Urbana-Champaign, USA, 1986.

[23] T. Becks and I. Wolff, "Improvements of spectral domain analysis techniques for arbitrary planar circuits", submitted to 20th European Microwave Conf., Budapest, 1990.

[24] K. S. Yee, "Numerical solution of initial boundary value problems involving Maxwell's equations in isotropic media", *IEEE Trans. Antennas Propagat.*, vol. AP-14, pp. 302—307, 1966.

[25] M. Rittweger and I. Wolff, "Analysis of complex passive (M)MIC components using the finite difference time-domain approach", *1990 IEEE MTT-S Internat. Microwave Symp. Digest,* Dallas, pp. 162—167, 1990.

[26] D. H. Choi and W. J. R. Hoefer, "The finite-difference-time-domain method and its application to eigenvalue problems", *IEEE Trans. Microwave Theory Tech.*, vol. MTT-34, pp. 1464—1470, 1986.

[27] N. H. L. Koster, *Zur Charakterisierung der frequenzabhängigen Eigenschaften von Diskontinuiäten in planaren Wellenleitern. (The frequency dependent characterization of discontinuities in planar waveguides).* Doctoral Thesis, Duisburg, University, FRG, 1984.

[28] G. Gronau and I. Wolff, "A simple broad-band device deembedding method using an automatic network analyzer with time-domain option", *IEEE Trans. Microwave Theory Tech.*, vol. MTT-37, pp. 479—483, 1989.

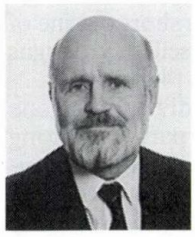

Ingo Wolff was born in Köslin, Germany in 1938. He studied electrical engineering at the Technical University of Aachen and received the dipl. ing. degree in 1964. In 1967 he received the doctoral in 1970 the habilitation degree again frm the Technical University of Aachen, West Germany. From 1970 and 1974 he was a Lecturer and Associate Professor for high-frequency techniques in Aachen. Since 1974 he has been a Full Professor of electromagnetic field theory at the University of Duisburg. His main research interests are electromagnetic field theory applied to the CAD of MICs and MMICs. milimneter wave componenets and circuits, and field theory of anisotropic materials. He is a Fellow of the IEEE.

COMPUTER AIDED DESIGN TECHIQUES FOR INTEGRATED MICROWAVE OSCILLATORS

BERND ROTH, ADALBERT BEYER

DUISBURG UNIVERSITY, DEPARTMENT OF ELECTRICAL ENGINEERING AND SFB 254, BISMARCKSTRAßE 69, D-4100 DUISBURG 1, FEDERAL REPUBLIC OF GERMANY.

In this paper a procedure is described allowing to predict the operating frequency, the power of the harmonics and the noise behaviour for integrated microwave oscillators. In addition, study results are presented showing the performance capability of this CAD-tool for the design of such oscillators. The approach uses methods of field theory as well as linear and non-linear network analysis, technological aspects also being taken into account. Interrelations between these areas are shown and discussed by means of numerical and experimental results.

1. INTRODUCTION

The design of oscillators requires a profound knowledge in several quite different areas of electrical engineering, this being especially true for microwave and millimeterwave oscillators.

Oscillators of high quality will be mainly designed by means of a large-signal analysis. Additionally, a small-signal and quasi-large-signal analysis is necessary because this yields the starting values for a large-signal analysis [6], [8], [10], [17], [20], [24].

The design of the oscillator itself as well as the optimization of the various components requires the simulation and the modeling of semiconductor elements such as FETs, GUNN elements and varactor diodes. Various kinds of simulators correspond to the specific requirements. On the one hand it may be useful to obtain minimum calculating times and thus fast circuit simulations, on the other hand it can be necessary to include many different physical effects to optimize the technology of the components [4], [9], [28], [29], [32], [46], [48], [51], [57], [58]. Advances regarding the integration of microwave and millimeter wave components demand an extension of two-dimensional simulations and the development of truly three-dimensional simulations.

The numerical calulation of electromagnetic fields represents a very important basis for the computer aided design (CAD) of integrated micro- and millimeter wave circuits, since such methods can give exact informations about the transmission properties of complex components. Of special interest for the design of oscillators is the numerical analysis of resonator structures to obtain useful equivalent circuits [1], [2], [42], these circuits preferably being described by analytic expressions to guarantee fast models suitable for CAD applications [15], [16], [39], [40], [45], [49].

Furthermore, the simulation of oscillator noise behaviour is of great importance. An efficient noise model describes the influence of several different physical parameters on the performance of the component provided. The program is able to reproduce the exact geometrical structure of the single component in the simulation [19], [21], [25], [30], [33,], [35], [38].

Other aspects are the optimizations regarding optimum yield and fabrication tolerances [3], [47]. Furthermore, problems of tuning, stability and measurement technique have to be considered during the design phases [22], [36], [43], [50], [52], [54], [56].

In the following some of the topics mentioned above are discussed.

2. DESCRIPTION OF ACTIVE ELEMENTS

2.1. Theoretical Background

Several different procedures for the modeling of microwave transistors have already been published [3], [9], [16], [17], [28], [32], [48], [49], [57]. In many cases, the models are matched to measured scattering parameters, and mostly numerical optimization procedures are employed for the calculation of the model parameters. This is problematic as ambiguous solutions can be found if a network containing more than sixteen elements is analyzed. Furthermore, optimizers are time-consuming, especially for the evaluation of the FET-model for a wide range of bias conditions.

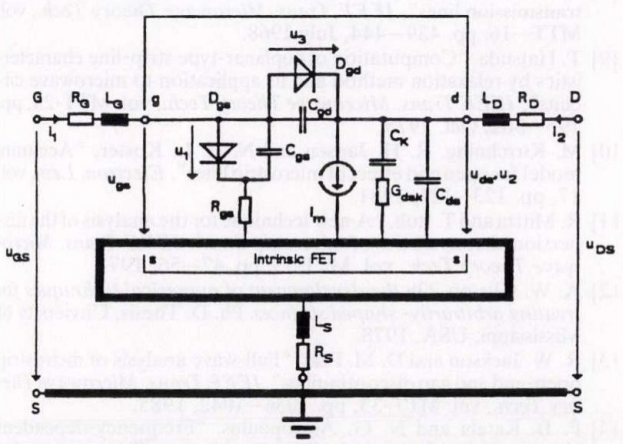

Fig. 1. Equivalent circuit of a Metal-Semiconductor (Shottky-Gate) Field-Effect Transistor (MESFET) or High Electron Mobility Field-Effect Transistor (HEMT).

The model chosen uses the well-known equivalent circuit diagram shown in Fig. 1. Because of the detailed description of the procedure in [46], only a short outline of the method is given here. Results of oscillator designs based on this method were published in [43], [44].

At the beginning, the transistor is subdivided into one inner part and one outer part, the inner part comprising the nonlinear characteristics. The calculation of the equivalent circuit components is carried out exclusively by means of measured scattering parameters and avoids any time-consuming optimization algorithms. By subdividing the equivalent circuit, the measurements at different bias conditions render possible a unique analytical calculation.

The components C_{in}, C_{out} and C_f describing the influence of the connection metallization are measured directly by means of an undopped transistor structure. It is worth to mention, however, that this method can also be used for transistors with packaging, where a "passive housing" has to be measured at first.

At the "pinch-of" bias ($U_{GS}=U_P$, $U_{DS}=OV$) at which the equivalent circuit of the inner transistor is reduced to the components C_{gs}, C_{dg} and C_{ds}, the determination of the remaining parasitic components of the transistor can be treated as the measurement of passive components. For all frequencies, this capacitive Π structure can be converted into an equivalent T-structure. The parasitical resistors and the inductance can be added to the particular branches of the T-structure. With regard to the parasitic capacitances C_{in}, C_{out} and C_f, the measured scattering parameters can be converted into impedance parameters. By a comparison of the calculated and measured impedance parameters, the wanted outer components can be determined.

Taking into account these outer network components, the measured scattering parameters yield the inner admittances. Because of the subdivision, it is possible to calculate the network components of the inner transistor for arbitrary bias points analytically without approximations. For lower frequencies the transconductance (g_m) and the output admittance (G_{ds}) can be determined directly from the scattering parameters. It was shown in [46] that the resulting values for g_m and G_{ds} are at least valid up to a frequency of 26.5 GHZ, the the calculation being possible for arbitrary bias points even outside saturation. The remaining inner network can be described by average values in the frequency range between 3 GHz and 10 GHz. This method describes the small-signal equivalent circuit diagram of the transistor (Fig. 1.) depending on the respective bias. With regard to an evaluation of the nonlinear relations in a large-signal model, the network components are described as functions of the inner voltages (u_1, u_2). For the static case, simple mesh equations can be found for the measurable outer voltages (U_{GS}, U_{DS}), the gate current I_G as well as the drain current I_D being functions of the bias point. If the nonlinear network components are characterized by outer voltages, the outer voltages can be replaced by the inner voltages. The scattering parameters and the DC-characteristics can be directly determined with a measurement program.

With a suitable computing program, the modeling can be carried out efficiently for a great number of bias points. The results for the network components show a relatively smooth characteristic over the range of bias points, allowing an interpolation of the intermediate values. For this reason further optimization is no longer necessary. The interpolation is based on bi-cubic spline functions.

In the next step the relations between the small-signal and the large-signal values are considered. In the equivalent circuit diagram of the inner transistor, the capacitances are now assumed to be voltage-controlled, while the remaining components are voltage-controlled current sources. The time-dependence of the voltages and currents can be described as the superposition of a static part and an AC-term. It can be demonstrated that the small-signal and the large-signal capacitances are identical, while the static voltages can only be replaced by the DC-characteristics up to approximately 100 kHz, because of the time delay resulting from the elctron transit time. For the small-signal operation above 100 kHz, the small-signal values calculated from the DC-output characteristics are only approximately valid and have to be modified by correction terms being slightly nonlinear regarding the bias point. Experimental results show that the slightly non-linear equivalent components R_{gd}, C_{ds} and τ_0 can be replaced by their corresponding small-signal values as a first approximation in the dynamic analysis. Furthermore, for positive gate-source voltages, the current of the sheet-diodes has to be added to the gate current.

The nonlinear analysis of the transistor is implemented employing the "Harmonic Balance" procedure explained further below. The solution of the network problem yields the inner voltages u_1 and u_2, respectively their complex phasors. Experimental investigations demonstrate that the problem is sufficiently described by a certain number of complex phasors, this number depending on the degree of the nonlinearity and the magnitude of the signal voltages.

2.2. Numerical and Experimental Results of FET-Modeling

The transistors modeled will be measured by means of a commercial on-wafer measurement set-up. A special DC source, allowing an automatic DC- and AC-scattering parameter measurement, makes possible a variation of the bias point; the measurement data can be obtained as a function of both the outer and the inner operating voltages. In Fig. 2., some results, extracted from the procedure explained above, are plotted.

3. A SHORT DESCRIPTION OF THE HARMONIC BALANCE METHOD

3.1. The Harmonic Balance Method for Oscillator Development

This part describes the application of a nonlinear device modeling to the design of microwave and millimeterwave oscillators. Transient processes are not considered since only the harmonic steady state is of interest. Under such conditions a very powerful method, namely the Harmonic Balance approach, is used which is based on some modifications in comparison with the classical approach [28]. In order to reduce CPU-time, some justified restrictions are introduced:

- In microwave networks inductances are mostly given by structures of metallization which are always linear: the network does not include any nonlinear inductance.
- It is assumed that voltage-controlled sources are included in equivalent circuits of transistors.
- Furthermore, state variables will be defined as voltages at the ports between the linear and the nonlinear subnetwork.

If autonomous networks should be calculated, it must be taken into account that the frequency is determined by the system itself and may change during the calculation process. Thus, the frequency is an additional state variable. It can be computed by the use of the rule that in an autonomous system, the phase of one harmonic of one state voltage can be fixed arbitrarily, for example set to zero.

Considering all these assumptions, the well known subdivision of the network in a nonlinear part to be calculated in time domain and a linear part to be calculated in frequency domain can be carried out as shown in Fig. 3.

The scheme of calculation is organized in four steps. At

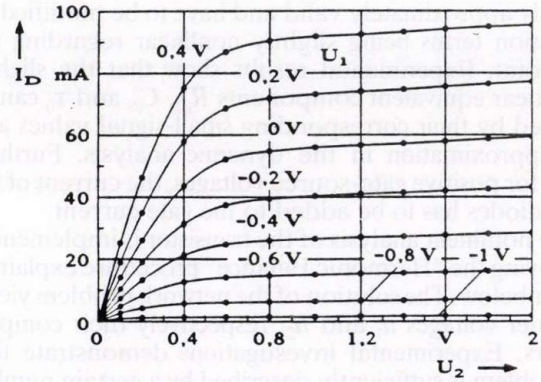

a)

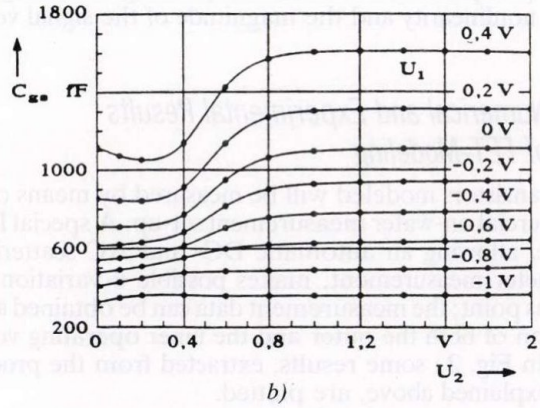

b)

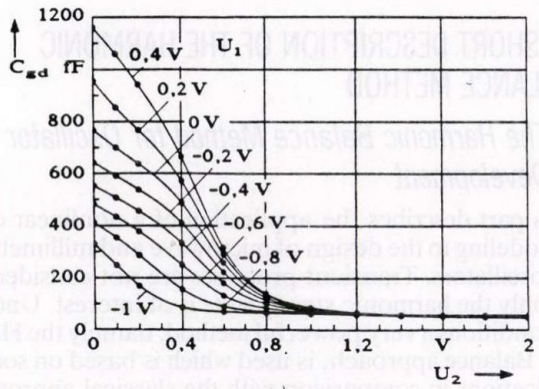

c)

Fig. 2. Results regarding the large signal behaviour of a GaAs-MESFET
a) I_D-U_{DS} characteristics,
b) The gate-source capacitance C_{gs},
c) The gate-source capacitance C_{dg} as a function of the drain-source voltage U_{DS}.

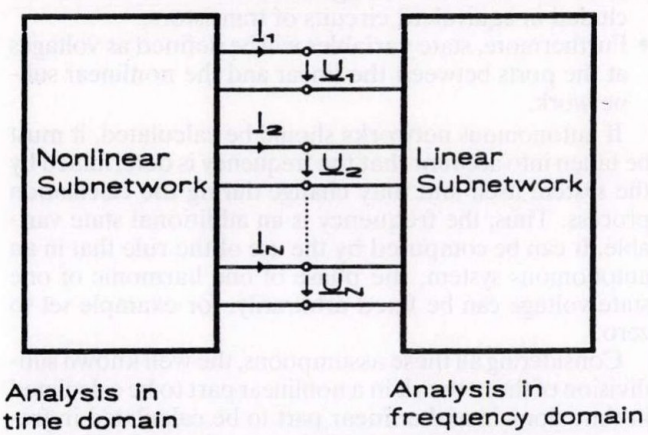

Fig. 3. Subdivision of a network into a nonlinear and a linear subnetwork.

first, the condition of oscillation is checked and if the circuit oscillates at all, the frequency of fundamental oscillation is computed by linear calculations. Next, a vector of state variables consisting of the port voltages is defined:

$$U = [U_1, U_2, \ldots, U_N]^T$$
$$U_k = [U_{k0}, U_{k1}, \ldots, U_{kM}], \quad k = 1, 2, \ldots N \tag{1}$$

The first index marks the number of intrinsic (or state) voltages, the second the harmonics, zero means DC. In the third step, this vector is transformed into the time domain. The resulting time-vector leads to the currents at the ports applying the elements of nonlinear network ($f_{nl}(u)$).

$$U \rightarrow u, \quad i = f_{nl}(u) \tag{2}$$

If the currents are transformed back into the frequency domain, it is possible to determine a new vector of state voltages by use of the linear network. Herein complex AC-analysis is applied.

$$i \rightarrow I, \quad U = f_l(I) \tag{3}$$

Going back to equation (2) closes the loop and yields a fixpoint problem depending on the vector of state voltages U:

$$U = f(U) \tag{4}$$

with:

$$f(U) = [f_1(U), f_2(U), \ldots, f_N(U)]^T$$
$$f_k(U) = [f_{k0}(U), f_{k1}(U), \ldots, f_{kM}(U)] \tag{5}$$

Expression (5) defines a system of nonlinear equations allowing to determine the complex amplitudes of the state voltages. For the frequency of fundamental oscillation ω_0, an additional equation is needed:

$$\mathrm{Im}(U_{11}) = 0 \tag{6}$$

There are several ways to solve such a problem. The simplest one is the usage of regula falsi method, proposed by Camacho-Penalosa for mixer and upconverter applications [7]. This method has been successfully transferred to oscillator calculations. Its main advantage is the very easy numerical handling of the correction term K:

$$U^{[n+1]} = f(U^{[n]}) + K(U^{[n]}) + K(U^{[n]}, U^{[n-1]}) \tag{7}$$

with:

$$K(U^{[n]}, U^{[n-1]}) = \frac{[f(U^{[n]}) - f(U^{[n-1]})][U^{[n]} - f(U^{[n]})}{[f(U^{[n]}) - U^{[n]}] - [f(U^{[n-1]}) - U^{[n-1]}]} \tag{8}$$

The multiplications and divisions in equation (8) have to be carried out element by element. The term K can be derived from the Jacobian of Newton's method if only the main diagonal of this matrix is taken into account [28]. Next, the derivatives are replaced by the difference quotients between the $(n-1)$-th and the n-th step of interation. This guarantees short CPU-times for a large class of microwave oscillators.

Figure 4. shows an overview of the complete computation process for the oscillator simulation. In that process, the computation of the complex amplitudes and the frequency of fundamental oscillation are located in separate loops. Similar approaches are shown in [48].

As mentioned, the computation starts with a linear analysis, which evaluates the frequency of fundamental oscillation. Furthermore, the intrinsic voltage U_{11} is set to U_S, for example 300 mV without an imaginary part, because there the phase of U_{11} is set to zero.

The network function includes the description of the linear and nonlinear network as explained before. Then, the convergence of the resulting fix-point problem will be

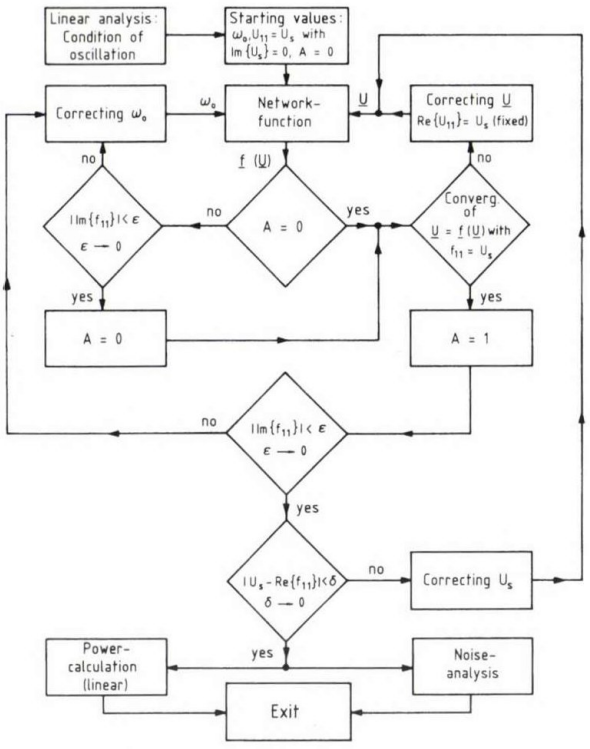

Fig. 4. Block diagram of the numerical computation process

During this correction, the real part of U_{11} is set first to U_S to prevent numerical instability. After this correction is completed, the program changes to the frequency-correcting cycle. Here the frequency of oscillation is calculated by a one dimensional regula-falsi iteration under the assumption that the imagniary part of f_{11}, respectively U_{11} is set to zero in this autonomous system.

The program iterates between the two loops and if convergence can be obtained in both cases, the up to now fixed voltage U_S is corrected in the outermost loop by a further one dimensional regulafalsi iteration as mentioned for the frequency correction. The result of all these iterations is the determination of the vector of state voltages U. By the knowledge of this, it is possible to calculate each voltage and each current inside the linear subnetwork and thus the output power of the oscillator can be expressed by elementary network analysis.

Furthermore, the time dependencies of the nonlinear elements are known. This allows to calculate the conversion matrices which are necessary to establish a large-signal — small-signal noise analysis.

3.2. Numerical Results

Figure 5. shows the layout of an oscillator in coplanar line technique, while in Figure 6. its corresponding equivalent circuit is shown. It should be mentioned, however, that the field theory applied as well as the operating principles of this oscillator will be explained later on.

The source of the FET is connected to the ground via capacitors or varactors which serve as a serial feedback. The FET, the varactor and the output load present at the reference plane P—P' a reflection coefficient r greater than unity. This oscillator is simulated by means of the harmonic balance method described above.

In Figure 7. a diagram of the simulated power of a one-varactor tunable oscillator with a 0.3 μm gate FET is depicted. The fundamental oscillation as well as the second

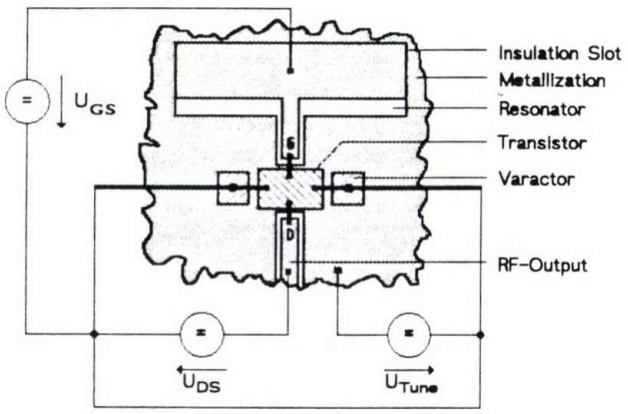

Fig. 5. Structure of an oscillator with a slot line resonator

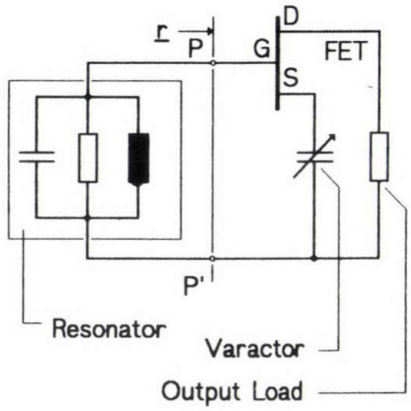

Fig. 6. Equivalent circuit of the oscillator shown in Fig. 5.

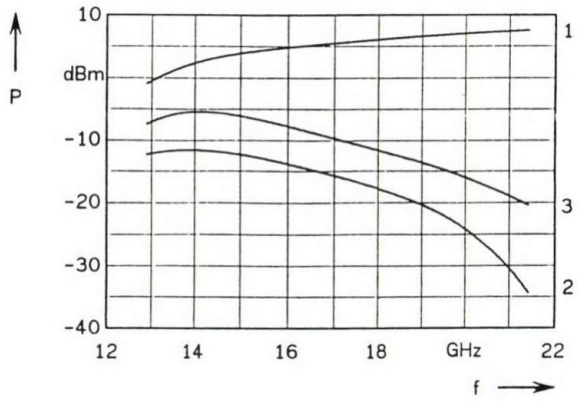

Fig. 7. Simulated output power of a one varactor tunable oscillator

and third harmonics are calculated. It can be recognized that this oscillator delivers an output power of about 5 dBm at the operating frequency of 17 GHz. In this case the powers of the second and the third harmonics are — 16 dBm and — 10 dBm, respectively.

4. FIELD THEORY FOR THE DESCRIPTION OF OSCILLATOR CIRCUITS

4.1. A Generalized Method for the Calculation of Rectangular Subsectional Microwave and Millimeterwave Structures

The design of oscillators in the microwave or millimeterwave range requires the rigorous theoretical field description of the passive part of such circuits [1], [2],

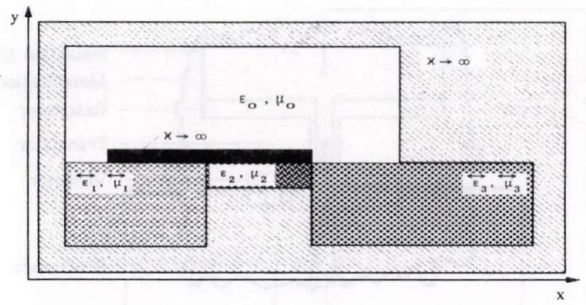

Fig. 8. A transverse structure with isotropic and anisotropic subsections

[42]. This allows an efficient CAD procedure to be used for oscillator design. In the following, a generalized method, based on the mode-matching technique, will be presented.

An assumption to treat generalized uniform transmission lines (see Fig. 1.) with a computer is useful. It is supposed, however, that only those arrangements should investigated which can be subdivided into homogeneous rectangular subregions. The procedure will be explained for the transverse structure plotted in Fig. 8.

Let N be the number of these rectangular subregions. The description of the whole waveguide according to Fig. 8. is given by

$$P_0 = [P_{0i};\ i = 1N] \tag{9}$$

with:

$$P_{0i} = [G_i, M_i] \tag{10}$$

In this formulation G_i means the geometrical and M_i the material property for the respective subregion i. Analyzing P_o with a computer automatically leads to a more detailed description for P and A with:

$$P = [P_{0i}, S_i;\ i = 1 \ldots N] \tag{11}$$

and

$$A = [A_m;\ m = 1 \ldots M] \tag{12}$$

with

$$A_m = [i_m, s_m, k_m] \tag{13}$$

and

$$K_m = [k_l;\ l = 1 \ldots L_m] \tag{14}$$

S_i describes the boundary at the rectangular subregion i and A contains the continuity conditions of the tangential field components at the surfaces between the subregion i_m and the subregions $k_i(l=1(1)L_m)$. The eigenfunctions which develop the tangential electric field components are those from the subregion i_m. The boundary description S_i of the subregion i in this formulation is too complicated to be analysed because it contains one, two, three, or four boundary numbers (see Fig. 9.). It is advantageous to use the well-known superposition principle which leads to elementary subregions shown in Fig. 10.

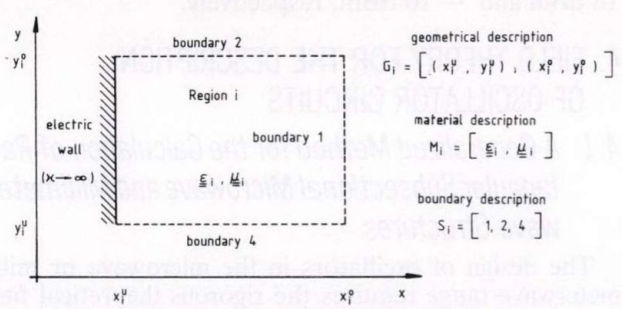

Fig. 9. A homogeneous filled rectangular subregion

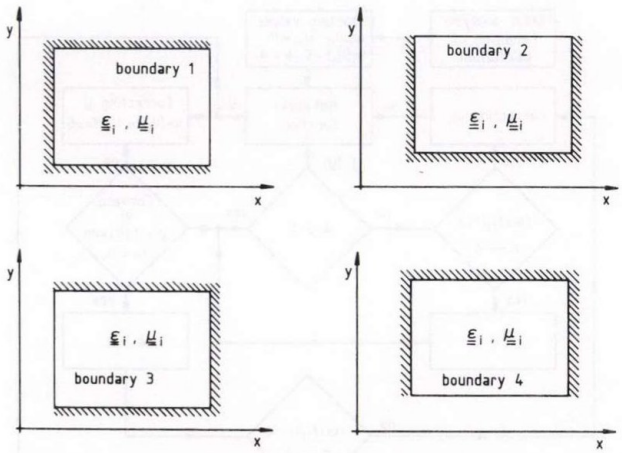

Fig 10. Elementary homogeneously filled rectangular subregions used in this theory

For these subregions one can use field solutions like TE_z waves and TM_z — waves for isotropic material properties and modified field solutions for anisotropic media, with diagonal permeability and permitivity tensors.

The continuity condition of the tangential electric and magnetic field components at a surface between two or more subregions can be satisfied by applying mode matching techniques for one of the descriptions A_m, to

$$\mathbf{D} e_{ii}^{ss} C_i^s = \sum_{l=1}^{L_m} \mathbf{D} E_{ik_l}^{st} C_{k_l}^t \tag{15}$$

$$\sum_{r \in S_{k_l}} \mathbf{D} h_{k_l k_l}^{tr} C_{k_l} = \sum_{r \in S_i} \mathbf{D} h_{k_l i}^{tr} C_i \quad l = 1 \ldots L_m \tag{16}$$

If one assumes m=1 (1) M for all these equations, a homogeneous, nonlinear matrix equation

$$\mathbf{S}(k_z) C = 0 \tag{17}$$

for the propagation constant k_{zi} is obtained. Solving this equation leads to the propagation modes k and the electromagnetic fields (with its amplitudes C_i) of the waveguide.

Let N_{oo} be the truncation index of the smallest B_{min} for all subregions in the transverse structure. The truncation index of an elementary subregion i with boundary s is given by the ratio B^s/B_{min}, $N_i^s = [B^s/B_{min}] N_{oo}$. Using this formulation for the truncation index N, the system matrix size N becomes

$$N_0 = \sum_{i=1}^{N} \sum_{s \in S_i} (2N_i^s - 1) \tag{18}$$

By inserting the equations for the electric field adaption (see Eq. (15)) the rank of the system matrix can be reduced to

$$N_r = N_0 - \sum_{m=1}^{M} (2N_{i_m}^{s_m} - 1) \tag{19}$$

For the calcualtion of three-dimensional structures it is also possible to extend this method like mentioned at the beginning of this part. From practical points of view it should be noted, however, that only a few of such structures were implemented. All these arrangements can be used for oscillator developments in which the transmission properties of these structures will be determined or field distributions have to be calculated.

4.2. Experimental and Numerical Results of Investigations on a Resonator in Coplanar Technique

The applicability of the method described above is shown for the example of a planar millimeterwave resonator (see Fig. 11.) which is used for the oscillator structure shown in Fig. 5.

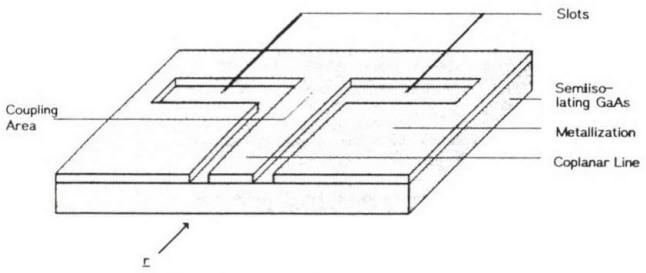

Fig. 11. View of a planar resonator

The resonator shown in Figure 11. consists of two resonator slots, a coplanar feeding line and a coupling area between coplanar and slot line. On both sides of the plane is air, the resonator substrate has no backside metallization. Good Q-factors can be expected because there is only low field concentration inside the lossy dielectric substrate of slot lines and coplanar lines.

a) At first, the electromagnetic behaviour of the slot resonators and the coplanar line is calculated with the help of the generalized method discussed above.

b) In the second step, the coupling area has been considered as an inner discontinuity. The boundary conditions inside this inner discontinuity are to satisfy a two-dimensional orthogonal expansion.

c) The third step leads to the scattering parameters of the coupling area and thus to the reflection coefficient **r** of the complete circuit. In order to obtain it, the boundary condition in the matching planes between the inner discontinuity and the connected lines must be satisfied.

From the reflextion coefficient **r** calculated above, it is possible to derive the frequencies of resonance, Q-factors and equivalent circuits of each resonance-mode within the considered frequency range.

It is often advantageous to introduce an equivalent circuit showing the transmission behaviour of the resonator in the operating frequency range (see Fig. 12.). Furthermore, the results of this description can be easily included in the oscillator development procedure. The equivalent circuit given by Fig. 12. is based on a modified theory of homogeneous lines. This means that the discontinuities and end-effects are described by inductances. By using the scattering parameters, the input impedance of the resonator can also be determined. As a comparison of calculated and measured results, magnitude and phase of the input impedance of one resonator as a function of the frequency are depicted in Fig. 13.

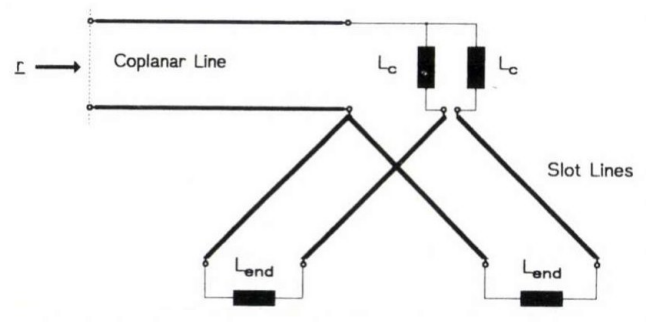

Fig. 12. Equivalent circuit of the resonator shown in Figure 11.

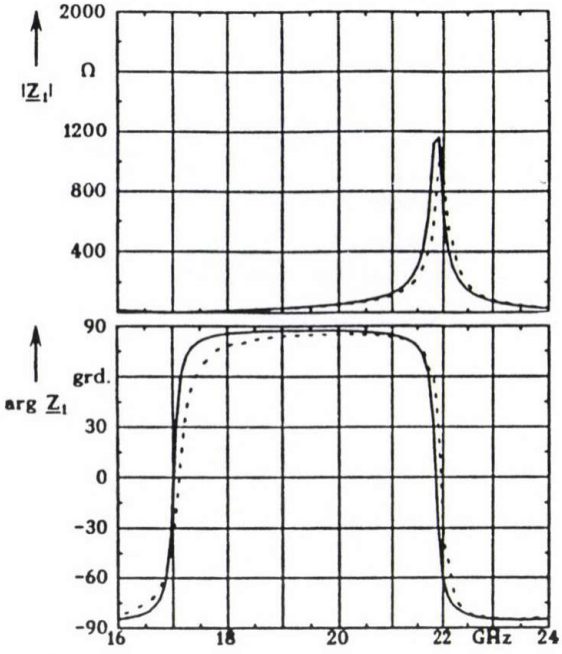

Fig. 13. Magnitude and phase of the impedance of a slot line resonator versus frequency (the third parallel resonance is visible in the upper part). w_{slot}=100 μm, l_{slot}=8711 μm, thickness of dielectric: 250 μm, ε=9.8 (solid line-calculated, dotted line-measured)

5. OSCILLATOR DESIGN

5.1. Oscillator Structures

Some examples of oscillators which have been designed by the modelling and the simulation techniques and the field theory explained in the foregoing Chapters are discussed in the following.

5.1.1. Oscillators in Coplanar Line Technique

Figure 5. shows a view on the first structure, while in Figure 6. the corresponding equivalent circuit is depicted. The construction of the oscillator is based on the coplanar line technique. The passive structure is etched on an alumina substrate with no backside metalization. As mentioned already, the source of the FET is connected to the ground by means of capacitors or varactors. This serial feedback renders possible — along with the output load at the drain — to obtain a reflection coefficient **r** at the gate greater than unity. By connecting a resonator structure to the gate, the circuit becomes an oscillator. In this example, a slot line resonator with coplanar coupling is used, as discussed above. The very narrow DC-insulation slot is necessary for the gate biasing of the FET, bridged by capacitors. The semiconductor elements are sticked on the structure and connected by bondwires.

Another similar oscillator structure is shown in Figure 14.; its equivalent circuit is given by Figure 15. The resonant circuit at the gate comprises a capacitor and a bondwire as inductance. The capacitive serial feedback in this case is represented by a fixed capacitor. The drain is connected directly to the output line.

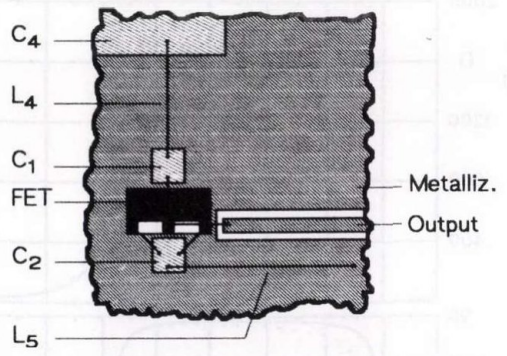

Fig. 14. Top view of a lumped element oscillator

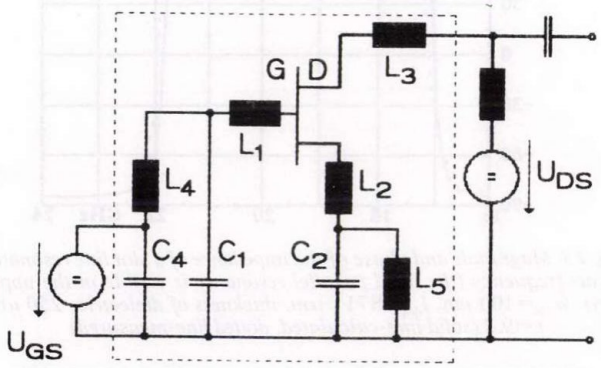

Fig. 15. Equivalent circuit of the oscillator shown in Fig. 14.

Using this oscillator with fixed capacitors only, the tuning range is very small due to the shift of the bias voltages. If a tunable oscillator is required, the mentioned principle can be enhanced by replacing the capacitors by varactors. The Figure 16. shows the structure of the tunable oscillator, and the corresponding equivalent circuit is plotted in Figure 17. It can be recognized that this oscillator is only little more complicated than the previous one.

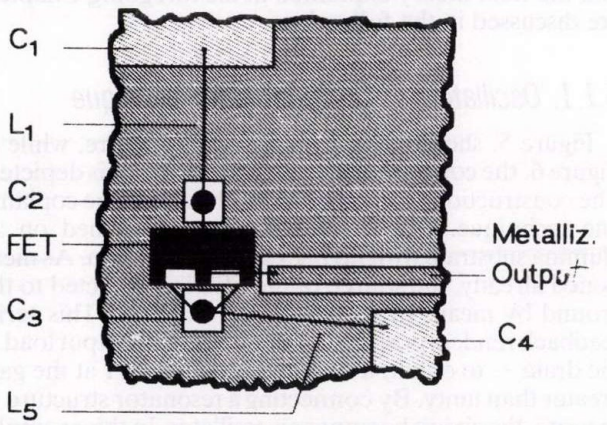

Fig. 16. Top view of a varactor tuned oscillator

A varactor tuned oscillator with two varactors can be built up as shown in Figure 16. By means of this network, a tuning bandwidth somewhat more than one octave can be obtained. The other way is to use only one varactor in the resonant circuit at the gate of the FET, and to implement the capacitive serial feedback by a fixed capacitor. Such a circuit is easier to produce but it shows a tuning range smaller than one octave.

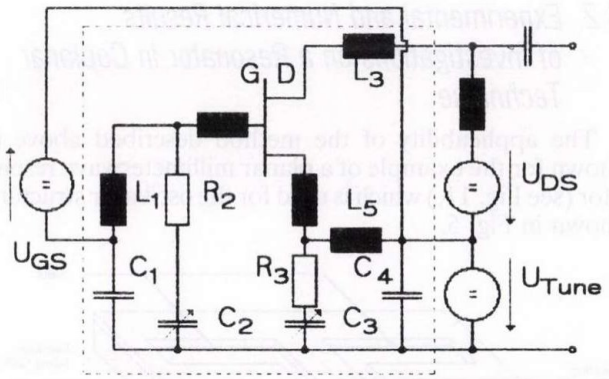

Fig. 17. Equivalent circuit of the oscillator shown in Fig. 16.

5.1.2. Oscillators in Slot Line Technique

A completly different type of oscillator is feasible by using a slot line resonator and its coupling (see Fig. 18.). The resonator is excited by a feedback FET. This coupling is formed by the electromagnetic field between the two slots. This slot line oscillator has two output ports.

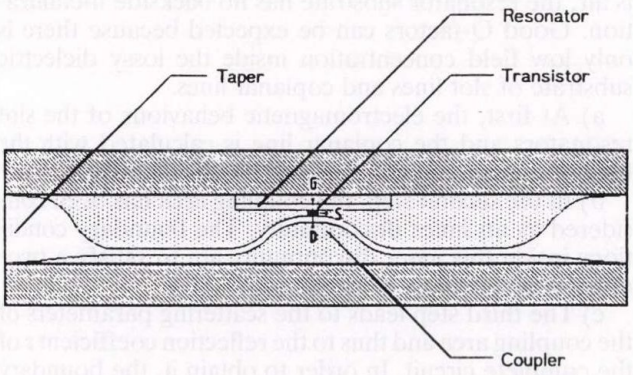

Fig. 18. Layout of an oscillator in slot line technique

For the oscillator represented in Figure 18, an equivalent circuit was developed as shown in Figure 19.

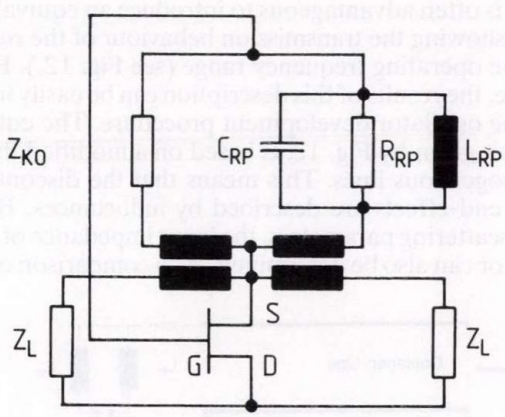

Fig. 19. Equivalent circuit of the slot line oscillator

The first version of the oscillator described above has been built up on RT/Duroid 5880-substrate as a hybrid integrated chip. The attachment of the transistor has been sticked on a galvanical gilded slot line structure by a low-loss adhesive. The electrical contacts were made by bond-wires.

5.2. Numerical and Experimental Results in Oscillator Design

Next, a calculation example of an oscillator with device parameters of the passive environment as shown in Fig. 5 will be presented. Actually, a part of these investigations was already presented in Chapter 3.2 in which the simulated power of such an oscillator is discussed. The CPU-time for the calculations of frequency and power of eight harmonics was 38 seconds on a 25 MHz-PC. The fundamental oscillation delivers about 5 dBm power at a frequency of 17 GHz, while at 19 GHz a power of about 7.3 dBm is available. In this context, the time dependence of the equivalent circuit nonlinear elements is of interest. The first example C_{gs} is given by Figure 20.

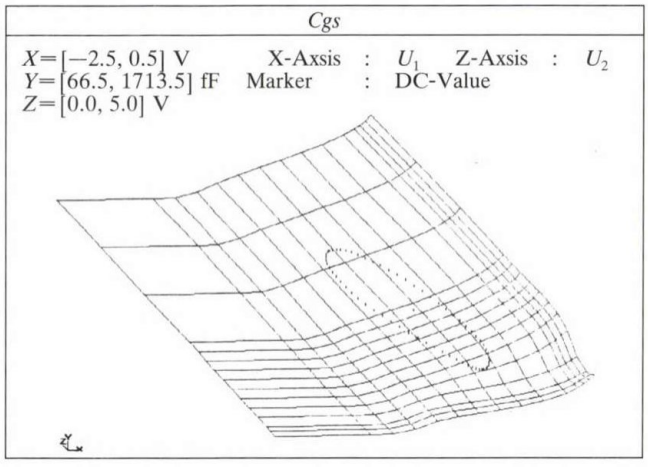

Fig. 20. Nonlineár behaviour of C_{gs} of a FET in an oscillator circuit

The field of surface lines shows the nonlinear element (Y-axis) as a function of the state voltages u_1 (X-axis) and u_2 (Z-axis). The values of the nonlinear element during oscillation are marked by the elliptic curve. A similar behaviour of the drain current is shown in Figure 21.

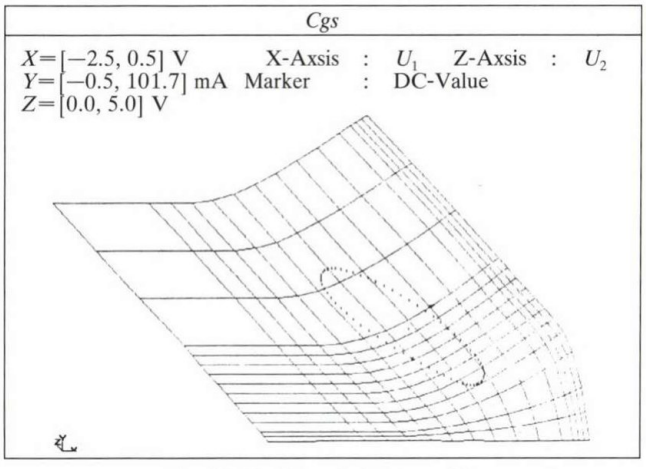

Fig. 21. Nonlinear behaviour of I_d

In both cases (Figures 20. and 21.) it can be recognized that an extremely nonlinear range is covered.

Figs. 22. and 23. show the drain capacitance C_{ds} and the time constant τ dependence. For these elements, the strong nonlinear region will not be reached. This confirmes that they can be handled as quasi linear.

Finally, the measured spectrum of an investigated fixed frequency oscillator (see Fig. 5.) with a 1.3 μm gate FET is shown in Figure 24. The difference between simulation

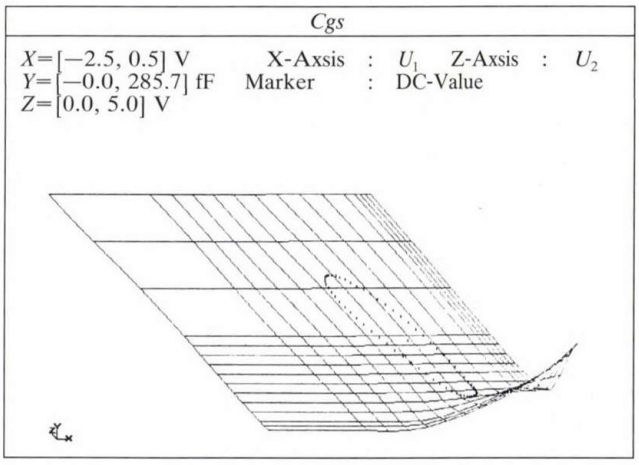

Fig. 22. Nonlinear behaviour of G_{ds}

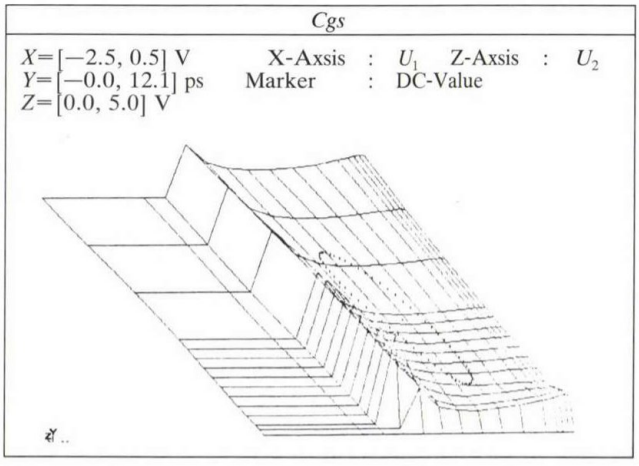

Fig. 23. Nonlinear behaviour of time constant τ

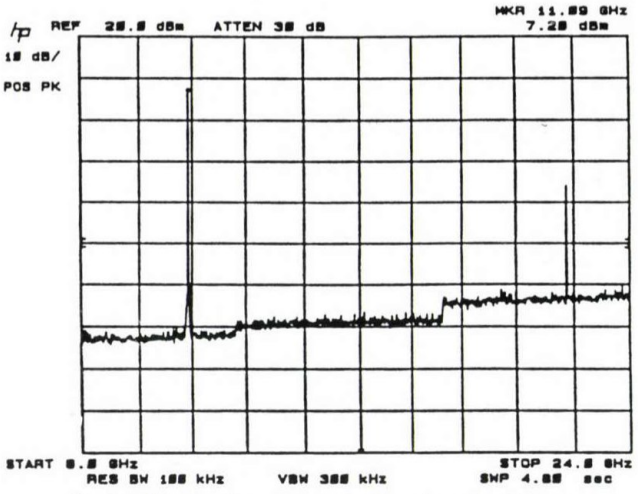

Fig. 24. Measured spectrum of an investigated oscillator

and measurement was within 5% in frequency and 10—15% in power, if the modelling of active and passive devices are carried out carefully. The spectrum of fundamental and second harmonic oscillation is depicted.

6. SOME ASPECTS ON NOISE SIMULATION

6.1. Theoretical Considerations

As well known, the spectrum of a real oscillator is not a pure delta function, because of the presence of noise. Especially the near carrier noise is an important technical

parameter of an oscillator. Figure 25. shows the schematic spectrum of such a circuit, consisting of a carrier and two noise sidebands.

In order to get an insight into the effects which introduce the spectrum spread in the vicinity of a carrier, let us consider the output signal $x(t)$ of an oscillator as an infinite sum of cosine functions perturbed by phase and amplitude modulation:

$$x(t) = \sum_{h=0}^{\infty} X_0^{(n)} \left(1 + \frac{\Delta x^{(n)}(t)}{|X_0^{(n)}|}\right) \cos|n\Omega_0 t + \Phi_0^{(n)} + \Delta\varphi^{(n)}(t)| \tag{20}$$

Using the initial asumption that the modulation index is small:

$$\frac{\Delta x^{(n)}(t)}{|X_0^{(n)}|} \ll 1 \tag{21}$$

and

$$\Delta\varphi^{(n)}(t) \ll 1\text{rad} \tag{22}$$

only one upper sideband (USB) and one lower sideband (LSB) oppears. Hence,

$$x(t) = \mathrm{Rm}\left[\sum_{h=0}^{\infty} X_0^{(n)} e^{jn\Omega_0 t} + \right.$$
$$\left. + X_{USB}^{(n)} e^{j(n-l_0+\omega_0)t} + X_{LSB}^{(n)} e^{j(n\Omega_0-\omega_0)}\right] \tag{23}$$

In case of phase modulation (PM),

$$X_{USB}^{(n)} = j\frac{|X_0^{(n)}|\Delta\Phi^{(n)}}{2} e^{j\Phi_0^{(n)}} \tag{24}$$

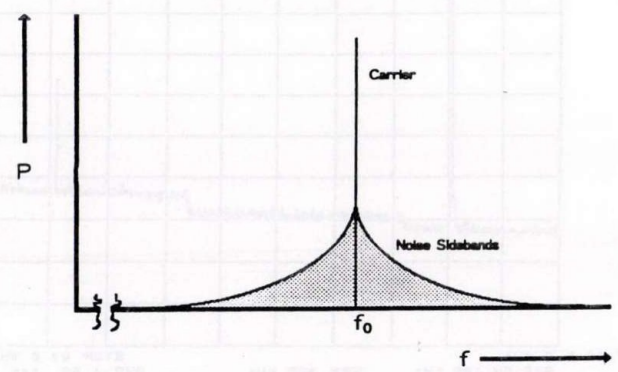

Fig. 25. Spectrum of an oscillator near carrier

$$X_{LSB}^{(n)} = j\frac{|X_0^{(n)}|\Delta\Phi^{*(n)}}{2} e^{j\Phi_0^{(n)}} \tag{25}$$

In case amplitude modulation (AM),

$$X_{USB}^{(n)} = \frac{\Delta X^{(n)}}{2} e^{j\Phi_0^{(n)}} \tag{26}$$

$$X_{LSB}^{(n)} = \frac{\Delta X^{*(n)}}{2} e^{j\Phi_0^{(n)}} \tag{27}$$

Under the mentioned assumption of small modulation, the sidebands of PM and AM can be superpositioned on the complete sideband phasors depending on the phasors of the PM ($\Delta\phi$ and AM-process ($\Delta X^{(n)} / |X_0^{(n)}|$):

$$X^{(n)} = X_{PM}^{(n)} + X_{AM}^{(n)} \tag{28}$$

If more harmonics must be taken into account, a vector of sidebands should be introduced.

$$X_{SSB} = \begin{bmatrix} X_{LSB}^{*(N)} \\ \vdots \\ X_{LSB}^{*(1)} \\ X_0^0 \\ X_{USB}^{(1)} \\ \vdots \\ X_{LSB}^{(N)} \end{bmatrix} = \begin{bmatrix} X_{-N} \\ \vdots \\ X_{-1} \\ X^0 \\ X_1 \\ \vdots \\ X_N \end{bmatrix} \tag{29}$$

Furthermore, a modulation phasor is defined by equation (30) which contains the AM components above and the PM components below.

$$X_{MOD} = \begin{bmatrix} \Delta X^{(N)}/|X_0^{(N)}| \\ \Delta X^{(1)}/|X_0^{(1)}| \\ X^0 \\ \Delta\Phi^{(1)} \\ \vdots \\ \Delta\Phi^{(N)} \end{bmatrix} \tag{30}$$

Applying the modulation theory of equations (20) to (29) to these vectors, a matrix decribing the relation between X_{mod} and X_{SSB} can be derived. Inverting this matrix delivers another one which is useful to calculate the modulation vector if the sideband vector is available as shown in expressions (31) and (32).

$$X_{MOD} = \mathrm{M}_{PMAM} \cdot X_{SSB} \tag{31}$$

$$\mathbf{M}_{PMAM} = \begin{bmatrix} e^{j\Phi_0^{(N)}}/|X_0^{(N)}| & \dots & 0 & 0 & 0 & \dots & e^{-j\Phi_0^{(N)}}/|X_0^{(N)}| \\ \vdots & \ddots & \vdots & \vdots & \vdots & & \vdots \\ 0 & \dots & e^{j\Phi_0^{(1)}}/|X_0^{(1)}| & 0 & e^{-j\Phi_0^{(1)}}/|X_0^{(1)}| & \dots & 0 \\ 0 & \dots & 0 & 1 & 0 & \dots & 0 \\ 0 & \dots & e^{j\Phi_0^{(1)}}/|X_0^{(1)}| & 0 & -je^{-j\Phi_0^{(1)}}/|X_0^{(1)}| & \dots & 0 \\ \vdots & & \vdots & \vdots & \vdots & \ddots & \vdots \\ je^{j\Phi_0^{(N)}}/|X_0^{(N)}| & \dots & 0 & 0 & 0 & & -je^{-j\Phi_0^{(N)}}/|X_0^{(N)}| \end{bmatrix} \tag{32}$$

In case of noise, the complex phasors are not directly available as numerical values. Therefore, spectral densities $S_{PM}(\omega)$, $S_{AM}(\omega)$ must be used. What the engineer is mostly interested in is the value of the sideband power P_{SSB} divided by the power of the carrier P_O. For the PM-process, we have

$$\left|\frac{X_{USB}}{X_0}\right|^2 = \frac{1}{4}|\Delta\Phi|^2 = \frac{1}{4}|\sqrt{2}\Delta\Phi_{rms}|^2 = \frac{S_{PM}(f)}{2} \quad (33)$$

$$\left.\frac{P_{SSB}}{P_0}\right|_{dBc} = 10\log\frac{S_{PM}(f)}{2} \quad (34)$$

The calculations on the AM-sidebands can be carried out in a similar way:

$$\left|\frac{X^{(n)}_{USB}}{X_0}\right|^2 = \frac{1}{4}\left|\frac{\Delta X}{X_0}\right|^2 = \frac{S_{AM}(f)}{2} \quad (35)$$

$$\left.\frac{P_{SSB}}{P_0}\right|_{dBc} = 10\log\frac{S_{AM}(f)}{2} \quad (36)$$

Equations (33) to (36) describe the dependence of the noise sidebands on the spectral densities of the noise process. The question is then, how to determine the spectral densities of the complete noise process and how to apply equation (31) to separate PM and AM components.

In order to answer this question, one has to analyze the reasons why near carrier noise appears in the spectrum of an oscillator. In the channel of a MESFET, statistical changes of the number and mobility of the charge carriers takes place at low frequencies. These changes in channel conductivity can be interpreted as an additional noise current between drain and source of the FET, which has a spectral density proportional to the reciprocal of frequency. The constant K_N is a function of both state variables u_1 and u_2.

6.2. Discussion of Some Results

The physically correct location of the noise source in the equivalent circuit of the FET is very important because the nonlinear conversion of the noise to the output terminals of the active device can only be taken into account if nonlinear behaviour (steady state) of the transistor is known. Thus one has no chance to calculate equivalent external noise sources, before nonlinear analysis of the circuit has been carried out. This means that the noise source must be located at a position in the equivalent circuit of the FET which is equivalent to the locus of physical origin of this noise, namely the channel of the FET (see Fig. 26.).

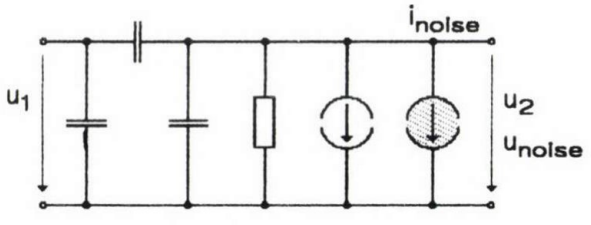

Fig. 26. Intrinsic FET and noise source to describe low frequency noise

$$S_{LFN} = \frac{K_N}{f} \quad (37)$$

$$K_N(t) = f(u_1(t), u_2(t)) \quad (38)$$

The constant K_N can be determinded by connecting a voltage source to the gate, a current source to the drain of the FET and measuring the RMS value of the drain source voltage. The diagram in Fig. 27. shows an example of the measured so called 1/f-noise of a 1.3 μm gate FET.

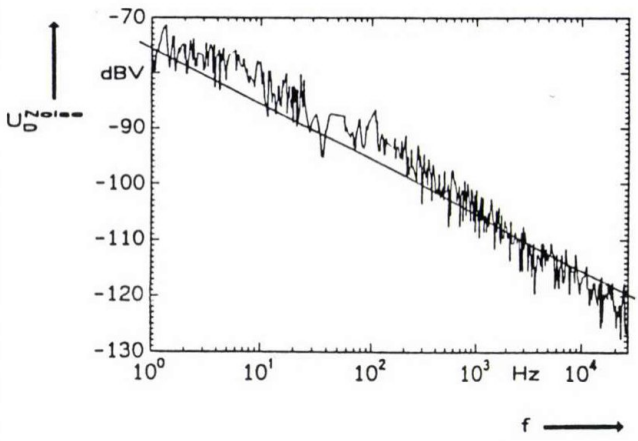

Fig. 27. Example of the measured output-noise of a 1.3 μm gate-length FET, U_{GSDC}= O V, U_{DSDC}= 2 V

It is seen that the 1/f dependence is not exactly valid but it is a good approximation. From the measured values, the spectral density of the noise source as well as $K_N(z_1, u_2)$ can be calculated.

6.3. The Method of the Conversion Matrix

In practically used oscillators, the noise is much below signal level, so one can use large signal—small signal analysis to determine how low-frequency noise is converted to the particular carrier. In [19] the method of nodal noise analysis is described, which is very useful and easily applicable to this particular oscillator-noise problem.

In case of deterministic signals as shown in [28], it is possible to define complex vectors for the small signal sidebands and a conversion matrix including the Fourier coefficients of the large signal time dependence of a nonlinear device. An example of the conversion via a nonlinear conductance is shown by equations (39) and (40):

$$\mathbf{M}_G : \; m_{Gij} = G_{i-j} \quad i,j = -N \ldots N \quad (39)$$

$$I = \mathbf{M}_G U \quad (40)$$

The matrix M_G describes the conversion from one sideband vector to the other. The vectors and matrices of a linear element include values different from zero only in the main diagonal. If the computation of the conversion through a two-port should be carried out, the elements e.g. of the admittance matrix are conversion matrices themselves and those of the vectors vectors themselves.

It is well known that for analyzing the conversion of a small signal noise via a deterministic large signal pumped network, a correlation matrix can be defined (see e.g. [19] which includes the spectral densities of the noise sidebands in the main diagonal, and their correlation spectra in the other elements: (41)

$$\mathbf{C}^u = \begin{bmatrix} S_{-N,-N} & \cdots & & & S_{-N,N} \\ \vdots & \ddots & & & \vdots \\ \vdots & & S_{-1,-1} \; S_{-1,0} \; S_{-1,1} & & \vdots \\ \vdots & & S_{0,-1} \; S_{0,0} \; S_{0,1} & & \vdots \\ \vdots & & S_{1,-1} \; S_{1,0} \; S_{1,1} & & \vdots \\ \vdots & & & \ddots & \vdots \\ S_{N,-N} & \cdots & & & S_{N,N} \end{bmatrix}$$

For the conversion this yields:

$$\mathbf{C}' = \mathbf{Y} C^{u} \mathbf{Y}^{*T} \tag{42}$$

This latter equation can be handled relatively easy.

In application of the explained principles, the first step in the noise calculation is the computation of the correlation matrix of the pumped noise source with the help of a basic 1/f-noise matrix.

$$\mathbf{C}^{NF}(f_{\nu}) = \begin{bmatrix} 0 & & & 0 \\ & 0 & 0 & 0 \\ & 0 & 1/f_{\nu} & 0 \\ & 0 & 0 & 0 \\ 0 & & & 0 \end{bmatrix} \tag{43}$$

Next, a conversion matrix M_K is derived from the time dependence of the noise factor K_N. This dependence is known after nonlinear analysis is carried out and u_1 and u_2 are calculated.

$$K_N(t) \rightarrow \sum_{i=1}^{\infty} K_{N_i} \quad \mathbf{M}_K : m_{kij} = K_{N(i-j)} \tag{44}$$

The correlation matrix of the pumped noise source can be determined with the help of equation (5.23).

$$\mathbf{C}^{ig2} = \mathbf{M}_K \mathbf{C}^{NF} \mathbf{M}_k^{*T} \tag{45}$$

The following step is the conversion due to the nonlinearities of the oscillator network. Therefore, the oscillator-noise model shown in Figure 28 is used. For near carrier noise only, the source I_{q2} is taken into account.

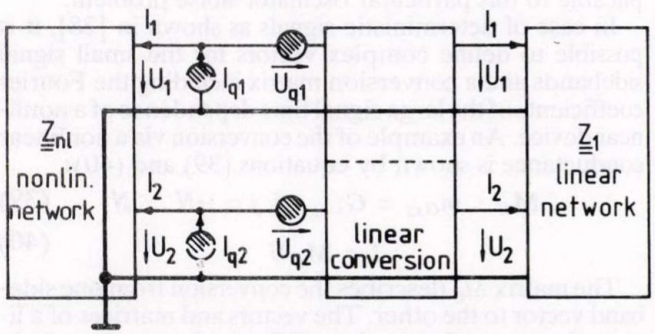

Fig. 28. Oscillator noise model

By the knowledge of the linear and nonlinear network, two martices can be defined which describe the conversion from the noise sources to the voltages at the ports of the linear network.

$$\mathbf{M}_1 = [\mathbf{E} + \mathbf{Z}_l \mathbf{Z}_{nl}^{-1} (\mathbf{E} - \mathbf{M}_{LT} \mathbf{Z}_l)]^{-1} \mathbf{Z}_l \tag{46}$$

$$\mathbf{M}_2 = \mathbf{M}_1 \mathbf{Z}_{nl}^{-1} \tag{47}$$

with

$$\mathbf{M}_{LT} = \begin{bmatrix} \mathbf{Z}_1 & \mathbf{Z}_F \\ \mathbf{Z}_F & \mathbf{Z}_2 \end{bmatrix} \tag{48}$$

In case of deterministic signals, the conversion could be described as follows:

$$U = \mathbf{M}_1 \cdot I_g + \mathbf{M}_2 U_g \tag{49}$$

This leads to the corresponding equation for noise conversion:

$$\mathbf{C}^{n} = [\mathbf{M}_1, \mathbf{M}_2] \cdot \begin{bmatrix} \mathbf{C}^{Ig} & \mathbf{C}^{I_g U_g} \\ \mathbf{C}^{I_g U_g} & \mathbf{C}^{U_g} \end{bmatrix} \cdot [\mathbf{M}_1, \mathbf{M}_2]^{*T} \tag{50}$$

Using the transfer functions H_1 and H_2 which describe the signal transfer from the harmonic balance ports of the linear network to the output of the circuit, the conversion via the linear network to the output can be calculated.

$$\mathbf{C}^{U_{out}} = [\mathbf{H}_1, \mathbf{H}_2] \cdot \mathbf{C}^{u} \cdot [\mathbf{H}_1, \mathbf{H}_2]^{*T} \tag{51}$$

Finally the spectral densities must be separated into PM- and AM noise components. For deterministic signals, this is expressed by equations (31) and (32), but equation (42) can also be applied.

7. CONCLUSION

A generalized oscillator CAD procedure has been presented for the simulation by harmonic balance. Based on the results of nonlinear calculation, a large signal—small signal analysis has been established in order to calculate the noise behaviour of the circuit. Some examples of realized oscillators have been investigated. In future a systematical CAD-optimizer for microwave oscillators has to be applied. Furthermore, the improvement of technological parameters in hybrid and monolithical integration is an important task.

8. ACKNOWLEDGEMENTS

The authors would like to thank Dipl.-Ing. Johannes Borkes, Dipl.-Ing. Axel Heitbrink, Dipl.-Ing. Stefan Heinen and Dipl.-Ing. Jürgen Kunisch for many interesting and helpful discussions.

REFERENCES

[1] A. K. Agrawal and B. Bhat, "Resonant characteristics and end effects of a slot resonator in unilateral fin-line." *Proceedings of the IEEE,* Vol. 72, No. 7, 1984, pp. 1416—1418.

[2] I. Bahl and P. Bhartia, *Microwave solid state cuircuits design.* John Wiley and Sons. New York, 1988.

[3] J. W. Bandler, S. H. Chen and S. Daijavand, "Microwave device modeling using efficient 1^1 optimization: A novel approach." *IEEE Transactions on Microwave Theory and Techniques,* Vol. MTT-34, No. 12, 1986, pp. 1282—1293.

[4] A. Beyer, G. Richard and D. Köther, "Determination of the equivalent circuit of gunn-elements for X-band oscillator applications." *International Journal of Infrared and Millimeter Waves,* Vol, 7. No. 10, October 1986, pp. 83—98.

[5] J. W. Boyles, "The oscillator as a reflection amplifier: An initiative approach to oscillator design." *Microwave Journal,* Vol, 11, June 1986, pp. 83—98.

[6] T. J. Brazil and J. O. Scanlan, "A non-linear design and optimization procedure for GaAs MESFET oscillators." *1987 IEEE International Microwave Symposium Digest,* Vol, 2, Las Vegas (USA), 1987, pp. 907—910.

[7] P. Camacho, "Numerical steady-state analysis of nonlinear microwave circuits with periodic excitation." *IEEE Transactions on Microwave Theory and Techniques,* Vol. MTT-31, No. 9, 1983, pp. 724—730.

[8] L. D. Cohen and E. Sard, "Recent advances in the modelling performances of millimeterwave InP and GaAs VCO's and oscillators." *1987 IEEE International Microwave Symposium Digest,* Vol. 1, Las Vegas (USA), 1987, pp. 429—432.

[9] W. R. Curtice, "A MESFET model for use in the design of GaAs integrated circuits." *IEEE Transactions on Microwave Theory and Techniques,* Vol. MTT-28, No. 5, May 1980, pp. 448—456.

[10] W. R. Curtice and M. Ettenberg, "N-FET a new software tool for large-signal GaAs FET circuit desing." *RCA Review,* Vol. 46, September 1985, pp. 321—339.

[11] R. J. Gilmore and F. J. Rosenbaum, "An analytic approach to optimum oscillator design using s-parameters." *IEEE Transactions on Microwave Theory and Techniques,* Vol. MTT-31, No. 1983, pp. 633—639.

[12] R. J. Gilmore, "Design of a novel FET frequency doubler using a harmonic balance algorithm." *1986 IEEE MTT-S International Microwave Symposium Digest,* Baltimore, pp. 585—588.

[13] R. Goldwasser, D. Donoghue, G. Dawe, S. Nath, C. Fingermann, I. Crossley, C. Mason, L. Raffaelli and R. Tayrani, "Monolithic Ka-band VCO's." *1988 IEEE Microwave and Millimeter-Wave Monolithic Circuits Symposium, Digest of Papers,* New York (USA), 1988, pp. 55—58.

[14] J. M. Golio and C. M. Keowne, "New approach for FET oscillator design." *Microwave Journal,* Vol, 21, October 1978, pp. 59—61.

[15] J. M. Golio, P. A. Blakey and R. O. Grondin, "A general CAD tool for large-signal GaAs MESFET circuit design." *1985 IEEE MTT-S International Microwave Symposium Diges,* St. Louis pp. 417—420.

[16] J. M. Golio and P. A. Blakey, "A large signal GaAs MESFET model implemented on SPICE." *IEEE Circuits and Devices Magazine,* Vol. 1, September 1985, pp. 21—30.

[17] R. Goyal (Editor): *Monolithic microwave integrated circuits: technology anddesign.* Artech House, Norwood, MA, 1989.

[18] S. Hamilton, "Microwave oscillator circuits." *Microwave Journal,* April 1978, pp. 63—84.

[19] S. Heinen, J. Kunisch and I. Wolff, "Considerations on the analysis of mixers with arbitrary topology including signal and noise properties." *1990 First International Workshop of the West German IEEE MTT/AP Joint Chapter on Integrated Nonlinear Microwave and Millimeterwave Circuits (INMMC' 90) Digest,* Duisburg, October 1990, pp. 63—77.

[20] M. M. Johnson, "Large signal GaAs MESFET oscillator design." *IEEE Transactions on Microwave Theory and Techniques,* Vol. MTT-27, No. 3, March 1979, pp. 217—227.

[21] L. Kreischer, "Noise tuning of GaAs-MESFET oscillators." *Electronics Letters,* 1 st March 1990, Vol. 26, No. 5, pp. 315—316.

[22] A. P. S. Khanna and J. Obregon, "Direct measurement of the non-linear MIC oscillator characteristics using injection loking polar diagram." *1983 IEEE International Microwave Sympolium Digest,* Boston (USA), 1983, pp. 501—503.

[23] K. Kurokawa, "Some basic characteristics of broadband negative resistance oscillator circuits." *The Bell System Technical Journal,* July—August, 1969, pp. 1937—1955.

[24] K. S. Kundert and A. Sangiovanni-Vincentelli, "Simulation on nonlinear circuits in the frequency domain." *IEEE Transactions on Computer-aided Design,* Vol, CAD-5, No. 10, October 1986, pp. 521—534.

[25] G. Lan, D. Kalokitis, E. Mykietyn, E. Hoffman and F. Sechi, "Highly stabilized, ultra-low noise FET-oscillator with dielectric resonator." *1987 IEEE International Microwave Symposium Digest,* Las Vegas (USA), Vol. 1, pp. 83—86.

[26] S. A. Maas, *Microwave Mixers.* Artech House, Detham, MA, 1984.

[27] S. A. Maas, *Nonlinear microwave circuits.* Artech House, London, 1988.

[28] A. Madjar and F. J. Rosenbaum, "A large-signal model for the GaAs MESFET." *IEEE Transactions on Microwave Theory and Techniques,* Vol, MTT-29, No. 8, August 1981, pp. 781—788.

[29] A. Materka and T. Kacprzak, "Computer calculation of large-signal GaAs FET amplifier characteristics." *IEEE Transactions on Microwave Theory and Techniques,* Vol. MTT-33, No. 2, February 1985, pp. 129—135.

[30] E. Niehenke and R. Hess, "A microstrip low noise X-band voltage controlled oscillator." *IEEE Transactions on Microwave Theory and Techniques,* Vol. MTT-28, No. 12, December 1979, pp. 1075—1079.

[31] J. Obregon and A. P. S. Khanna, "Exact derivation of the non-linear negative resistance oscillator pulling figure." *IEEE Transactions on Microwave Theory and Techniques,* Vol. MTT-30, No. 7, July 1982, pp. 1109—1111.

[32] R. S. Pengelly, *Microwave field-effect transistor theory design and applications.* (Second Edition), Research Studies Press Ltd., Letchworth, Herfrodschire (England), 1986.

[33] A. F. Podell, "A functional GaAs FET noise model." *IEEE Transactions on Electron Devices,* Vol. ED-28, Vol. 5, May 1981, pp. 511—517.

[34] R. A. Pucel, R. Bera and D. Masse, "Experiments on integrated gallium arsenid FET oscillators at X-band." *Electronics Letters,* Vol. 11, No. 15, May 1975, pp. 219—220.

[35] R. A. Pucel, H. Statz and H. A. Haus, "Signal and noise properties of gallium arsenid microwave field-effect transistors." *Advances in Electronics and Electron Physiscs,* Vol. 38, 1975, pp. 195—265.

[36] R. A. Pucel, "Design consideration for monolithic microwave circuits." *IEEE Transactions on Microwave Theory and Techniques,* Vol. MTT-29, No. 6, June 1981, pp. 513—534.

[37] G. W. Rhyne and M. B. Steer, "A new frequency domain approach to the analysis of nonlinear microwave circuits." *IEEE MTT-S International Microwave Symposium Digest,* St. Louis pp. 401—404.

[38] A. N. Riddle and R. H. Trew, "A new measurement system for oscillator noise characterization." *IEEE International Microwave Symposium Digest,* Vol. 1, Las Vegas (USA), 1987, pp. 509—512.

[39] V. Rizzoli, A. Lipparini and E. Marazzi, "A general-purpose program for nonlinear microwave circuit design." *IEEE Transactions on Microwave Theory and Techniques,* Vol, MTT-31, No. 9, September 1983, pp. 762—770.

[40] V. Rizzoli and A. Neri, "State of the art and present trends in nonlinear microwave CAD techniques." *IEEE Transactions on Microwave Theory and Techniques,* Vol. MTT-3, No. 2, February 1988, pp. 343—365.

[41] V. Rizzoli and A. Neri, "A fast newton algotithm for the analysis and design of microwave oscillators and VCO's." *19th European Microwave Conference,* London, September 1989, pp. 386—391.

[42] B. Roth and A. Beyer, "Planar slotline millimeterwave resonators with coplanar coupling." *19th European Microwave Conference,* London (England), 4—7 September 1989, pp. 507—512.

[43] B. Roth, H. Sledzik, M. Joseph and A. Beyer, "An advanced method for the design and simulation of integrated microwave oscillators." *14th International Conference on Infrared an Millimeter Waves,* Würzburg (Germany), October 2—6, 1989, pp. 342—343.

[44] B. Roth, H. Sledzik and A. Beyer, "Recent developments for the design and simulation of integrated microwave oscillators." *MIOP'90,* Stuttgart (Germany), 24. 04—26. 04. 1990, pp. 103—110.

[45] B. Roth and A. Beyer, "An advanced CAD-procedure for the design and simulation of autonomic systems applicated to an integrated microwave oscillator (Invited paper)." *20th European Mierowave Conference,* Budapest (Hungary), 10—13, September 1990, pp. 45—56.

[46] H. Sledzik and I. Wolff, "Analytical derivation of a nonlinear FET-equivalentcircuit for MMIC applications." *International Journal of Infrared and Millimeter Waves,* Vol. 10, No. 3, March, 1989, pp. 310—319.

[47] M. A. Smith, T. S. Howard, K. J. Andersom and A. M. Pavio, "RF nonlinear device characterization yields improved modeling accuracy." *1986 IEEE MTT-S International Microwave Symposium Digest,* Baltimore pp. 381—385.

[48] H. Statz, P. Newman, I. W. Smith, R. A. Pucel and H. A. Haus, "GaAs FET device and circuit simulation in SPICE." *IEEE Transactions on Electron Devices,* Vol. ED-34, No. 2, February 1987, pp. 160—169.

[49] S. E. Sussman-Fort, S. Narasimhan and K. Mayaram, "A complete GaAs MESFET computer model for SPICE." *IEEE Transactions on Microwave Theory and Techniques,* Vol. MTT-32, No. 4, April 1984, pp. 471—473.

[50] A. A. Sweet, *MIC & MMIC amplifier and oscillator circuit design.* Artech House, London (England), 1990.

[51] Y. Tajima, B. Wrona and K. Mishima, "GaAs FET large-signal model and its application to circuit design." *IEE Transactions on Electron Devices,* Vol. ED-28, No. 2, February 1981, pp. 171—175.

[52] R. J. Trew, "Design theory for broadband YIG-tuned FET oscillators." *III Transactions on Microwave Theory and Techniques,* Vol, MTT-27, No. 1, January 1979, pp. 8—12.

[53] H. Q. Tserng and B. Kim, "110 GHz GaAs FET oscillator." *Electronics Letters,* Vol. 21, 1985, pp. 178—179.

[54] C. Tsironis and P. Lesartre, "Temperature stabilization of GaAs FET oscillators with dielectric resonators." *Proceedings of the 12th European Microwave Conference,* Helsinki (Finland), 1982, pp. 181—186.

[55] D. A. Warren, J. M. Golio and W. L. Seely, "Large and small signal oscillator analysis." *Microwave Journal,* May 1989, pp. 229—246.

[56] W. Wagner, "Oscillator design by device line measurement." *Microwave Journal,* Vol. 22, Februar 1979, pp. 43—48.

[57] M. Weiss and D. Pavlidis, "Power optimization of GaAs implanted FET's based on large-signal modeling." *IEEE Transactions on Microwave Theory and Techniques,* Vol. MTT-35, No. 2, February 1987, pp. 175—188.

[58] H. A. Willing, C. Rauscher and P. deSantis, "A technique for predicting large signal performance of a GaAs MESFET." *IEEE Transactions on Microwave Theory and Techniques,* Vol. MTT-26, No. 12. December 1978, pp. 1017—1023.

[59] R. G. Winch, "K-band FET doubling oscillator." *Electronics Letters,* Vol. 18, October 1982, pp. 946—947.

[60] Y. Xuan and C. M. Snowden, "A new generalized approach to the design of microwave oscillators." *IEEE International Microwave Symposium Disegt,* Vol. 2, Las Vegas (USA), 1987, pp. 661—664.

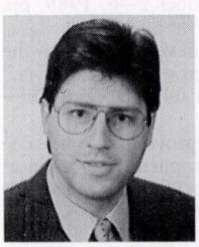

Bern Roth received the diploma in electrical engineering in 1988. From 1988 he is employed as an Assistant at the Department of Electrical Engineering of the Duisburg University. He is currently pursuing the Dr.-Ing. (Ph.D.) degree in electrical engineering. His research focuses on integrated microwave and millimeter wave nonlinear circuits and measurement techniques.

Adalbert Beyer received the diploma in 1964 and the Dr.-Ing. (Ph.D) degree in 1969, both in electrical engineering. 1976 he joined the Duisburg University, where he is currently a Professor of electrical engineering and field theory and Foundation Member of the "Sonderforschungsbereich 254". His areas of research interest are in the field theory, microwave- and millimeter wave techniques, in the CAD- and FET-applications, and especially in the theory and in the measurement of integrated circuits and in remote sensing. In 1987 he was a Visiting Professor at The University of Ottawa/Canada. Also in 1990 he spent a period as a Visiting Professor at The University of Texas at Austin/TX/USA. He is author and coauthor of several books, patents and more than 100 technical papers. Professor Beyer is Member of VDE/ITG, Senior Member of IEEE and Member of the MTT-13, The Committee on Microwave Ferrites.

GaAs PRODUCTS FROM HUNGARY

INTRODUCTION

From the beginning of its foundation in 1958, the Research Institute for Technical Physics of the Hungarian Academy of Sciences has been considering that one of its most important task was the study of semiconductor materials and devices. Based on the results in the technology of GaAs epitaxy, in 1972 it started to develop microwave active devices. The first one was the Gunn diode, it was followed by the low-noise GaAs Schottky diode and later the family of Schottky tuning varactors were developed, utilising the further progress reached in the technology of the epitaxy. The pilot line production of the developed diodes was solved also in the Institute, in this manner it is the supplier of the professional telecommunication factories for more than ten years.

Due to their advantageous propagation properties the microwaves can be used not only in dedicated telecommunication and radar systems, but in many other fields, e.g. space guarding, vehicle indentification, distance-, moisture- and temperature measurement, heat treatment in the industry and in the medicine, etc. Faithfully to the traditions of the Institute the applications of the devices were also investigated in these areas. At first general purpose waveguide transmitter and receiver modules were developed for the X band. Further on they were furnished with coding circuits for vehicle identification purposes. A dedicated VCO and a front end were also developed for a microwave distance mesasuring apparatus, but they can be applied also for other tasks. All of these modular products are based on own GaAs active devices; they are produced and supplied in cooperation with different industrial firms. The simultaneous development of the active devices and modules resulted in mutual benefits in both branch of activities.

In the followings the products are reviewed and finally the present development work is outlined.

GaAs ACTIVE DEVICES

Gunn-diodes

The different types of these GaAs bulk effect devices can be used in fixed frequency and electrically or mechanically tuned oscillators typical in the X band, some special types are applicable for lower (7 GHz), or higher (up to 18 GHz) frequencies. The output power of the different types varies between 5...200 mW in continuous regime, or up to 300 mW under pulsed conditions. The minimum efficiency is 1% of the low power diodes and about 3% of the high power devices. The optimum bias varies between 5...15 V for the different types used in continuous regime. In the case of pulsed operation the best performance can be reached by using about 1.6 times higher biasing pulses than the optimum value of the DC bias of the same diode. The pulse widths can be decreased down to several microseconds. The operating temperature range extends from −40 C to +70 C.

The diodes are encapsulated into metal-ceramic cases type AV-120, having a thread (# 3—48 UNC-2A, or M 2.5) for the improving the heat contact with the environment. The diodes having output power greater than 20 mW are mounted in face-down position into the package.

Schottky-diodes

The small area Schottky diodes are fabricated on thin (< 1 μm) n-type GaAs epitaxial layers, grown onto high conductivity n^+—GaAs substrate. The epitaxial layer is covered by CVD SiO_2 film in which windows are opened by photolithography for the active junction areas. Each diode chip contains 9 different windows with diameters ranging from 5 μm to 25 μm. For applications at different frequencies different diode areas and layer doping is proposed [1]. The typical parameters of the standard catalogue types are: breakdown voltage measured at 100 μA reverse current: minimum 3 V (typical 20 V); series resistance: 5 Ohms; junction capacitance 0.08 pF; total (encapsulated) capacitance 0.25 pF. The maximum value of forward current is 5 mA DC, or 60 mA pulse (pulse length max. 1 ms.). The mixer diodes are categorized by their noise figures measured in a mixer unit. (RF: 7500 MHz, IF: 70 MHz, IF amplifier noise figure: 1.5 dB.) The maximum noise figure values of the standard types are: 5 dB, 5.5 dB and 6.5 dB. Similarly the detector diode types are selected according the tangential sensitivity [1], the limiting values of the different types are: 60 dBm, 55 dBm and 50 dBm. (The values are measured in a tuned cavity at 10 GHz by a video amplifier having the 3 dB suppression at 20 Hz and 20 kHz.)

Two kinds of encapsulation are available, the S-4 type metal-ceramic housing and the LID ceramic package. The first one is applicable in coaxial and waveguide circuits, it allows an operating temperature range between −55...+70 C. The LID package is ideal for microstrip and stripline circuits, in this case the operating temperatures range from −40 C to +70 C.

GaAs Schottky Tuning Varactors

These types of varactors are used in general for voltage controled tuning of oscillators, amplifiers, filters and phase-shifters and for modulation purposes. The capacitance-voltage (C—V) characteristics of varactors may be given as

$$C = C_0 \left(1 + \frac{V}{\emptyset}\right)^{-\gamma} \qquad (1)$$

where C_0 is the capacitance at zero bias $\emptyset$ is a coefficient and γ (gamma) is the power of the exponent.

Expression (1) may be rewritten in a form more convenient for application:

$$C = C_0 \left\{1 + \frac{V}{V_{max}} \left[\left(\frac{C_0}{C_{min}}\right)^{\frac{1}{\gamma}} - 1\right]\right\}^{-\gamma} \qquad (2)$$

Here V_{max} is the maximum control voltage and C_{min} is the corresponding minimum capacitance. Over V_{max} the capacitance either does not change any more or does not satisfy Expession (2) with the given gamma value. If the value of gamma is about 0.5, the varactor is called abrupt, if gamma is higher, it is called hyperabrupt.

Three subfamilies — an abrupt, a hyperabrupt with constant gamma of 1.0—1.2 and a hyperabrupt with variable gamma — are offered.

The tuning varactors are mounted either in LID or hermetic coaxial metal-ceramic parkages. Vactor chips also are available.

Transmitter and Receiver Modules

The general purpose microwave transmitter and receiver modules are half wavelength waveguide cavities containing a Gunn, or a Schottky diode. The mechanical dimensions are shown in Fig. 1.

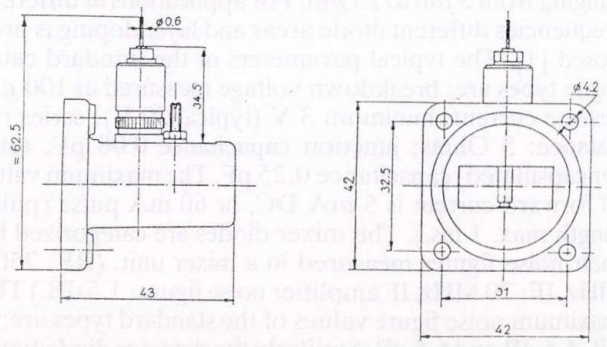

Fig. 1. The outlines of the transmitter and receiver modules

The body is made of Al based light metal alloy by casting. The flange is the standard R-100, its connecting surface is achieved by milling, the notch for the O-ring (watertight option) is turned. Holes and threads for the diode mount and for the single tuning screw are drilled into positions depending on the operating frequency specified. The outer conductors of the diode mounts are made of nickel silver by turnery. The inner conductor in the coaxial diode mount acts as a first order low pass filter with cut-off frequency of 1 GHz. The top of the inner conductor at the diode is the impedance transofmer to match the diode to the waveguide. As the impedances of the Gunn and Schottky diodes are different and depend on the frequency and the power specified, the shapes of these tops are different, while the remaining parts of the mount are uniform. The insulators in the diode mounts are made of plastics. The inner conductors are pressed to the diodes by springs with stainless steel plates for improving the resistance against mechanicsl shocks and vibration.

The typical characteristics of the AM-2 transmitter and VM-2 receiver modules are:

AM-2 Typical characteristics (25 °C)

Efficiency	1% min
Operating Temperature	−40...+70 °C
Storage Temperature	−40...+70 °C
Operating Mode	CW or pulse
Operating Voltage	6...12 V DC
Output Power	min. 10 mW, max. 40 mW
Operating Frequency	8.2...12.4 GHz

Maximum ratings

Operating Voltage	max. 12 V DC, max. 24 V pulse
Current	max. 250 mA
Pulse Length	min. 5 μs

VM-2 Typical characteristics (25 °C)

Centre frequency	8.2...12.4 GHz
Bandwidth (3 dB7)	100...300 MHz (200...500 MHz at higher bias)
Bias	20...100 μA
Sensitivity	1...5 mV/μW (0.5...3 mV/μW at higher bias) (with microwave power less then 1 μW)
Minimal signal detected	1...10 pW (−60...−50 dBm)
Maximal frequency at the output	20...200 MHz (increasing with bias)

Maximum ratings

Temperature	−50...+70 °C
Incident microwave power	max. 100 mW
Bias current	max. 10 mA (1 s pulse) max. 1 mA (continuous)
Reverse voltage	max. 5 V

A twin version of the modules exist also for Doppler-reflexion intruder alarms. Fig. 2. shows the outline of it. The other mechanical and electrical parameters are equivalent with the parameters of the single modules.

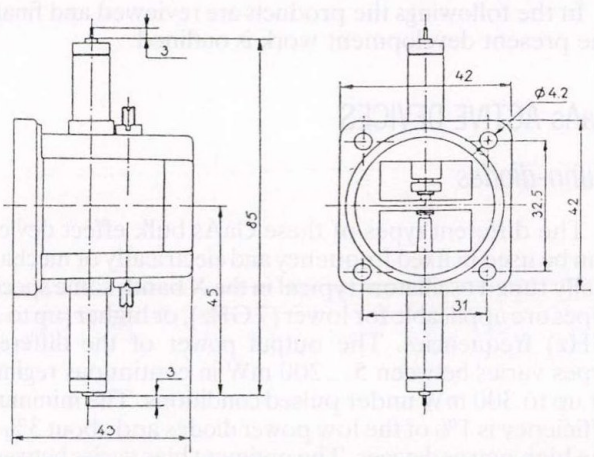

Fig. 2. The outline of the DP-2 module containing the transmitter and receiver parts in combined mount

For applications in microwave vehicle identification and control systems [2] hybrid IC's were developed for pulse coding and decoding of the transmitted and received signals. These circuits have the standard RS-232 interface. The coding means a full on/off modulation of the microwave signal due to the pulse modulation of the supply voltage. The data speed is 60 kbit/s. The total system has a modular construction allowing the possibility of building configurations with different complexity.

Microwave Front End

The type MK-2 microwave front end was developed for microwave distance measurement purposes. Because of its large bandwith and high output power it can also be applied for data transmission.

The X-band microwave front end contains a varactor tuned Gunn oscillator mounted on the rear side of a parabolic dish producing a beam angle of max 6 °. The receiver and the single ended mixer are placed in the focus of the dish. The intermediate frequency signal is amplified by a hybrid preamplifier. The oscillator and the mixer is controlled by a monitor. All microwave active semiconductor devices are in-house made GaAs ones. The complete front end is a factory repairable sub-assembly.

RESEACH AND DEVELOPMENT

The present R & D activities in the Microwave Department of the Institute are focused on new GaAs active devices. Considering the demands of the high-speed sampling circuits the development of monolithic Schottky diode Quad circuit is in progress. In this case the diodes have a planar construction, they are fabricated on the top of the n-type GaAs epitaxy grown onto semi-insulating substrate. Both the Schottky and ohmic metalization takes place on the top of the wafer. The monolithic construction gives hope of the considerably uniformity of the diodes, which is necessary in the Quad bridge.

The other essential circuit used in the sampling circuits is the high speed switching pulse generator. For these purposes the GaAs optical switches were studied. An apparatus for laboratory investigations was constructed [3] and a new, simple device principle was proposed [4]. The technology of the proposed device is compatible with the technology of MESFET's and therefore further integration will be possible.

The detailed study of the relation between the microwave parameters and the inner structure of diodes is a permanent problem in this laboratory. The improvement of the accuracies of microwave measurements and evaluations make possible the calculations of the true doping densities and mobilities in varactor diodes from the measured S parameters [5].

Bearing the detectors the properties on planar doped barrier diodes (PDBD's) are examined [6], [7], [8]. The investigated devices have a n^+—n—p^{++}—n—n^+ layer structure, where the p^{++} layer is thinner than the Debey length. The structure is similar to two p—n junctions in back-to-back configuration, but the total amount of the acceptors built into the p^{++} layer are small for forming the p—n barriers having a height about Eg, the formed barrier height can be influenced by the total amount of dopants in the p^{++} layer and by the thicknesses of the n layers. The most attractive feature of these devices is the technologically controllable barrier height. Therefore the limitations associated with the fixed surface barrier in GaAs Schottky diodes can be overcome. The multilayer semiconductor structures can be built only by the up-to-date epitaxial tehnologies as MBE or equivalent. The work is going on in cooperation with the Technical University of Tampere (Finnland), where the GaAs MBE layer structures are grown. Utilizing the low barrier of the PDBD's a simple zero bias detector was constructed for the 2.45 GHz frequency. The radiation detector works without battery, the minimum detectable intensity is 10 $\mu W/cm^2$ fulfilling the requirements of the rigourous Hungarian health protection standard.

REFERENCES

[1] B. Szentpáli and A. A. Papp, "Optimum design of GaAs Schottky diodes" *Proc. Conf. Microwaves and Optoelectronics MIOP '88,* March 2—"4, 1988, Wiesbaden, Germany, 8B4.

[2] Z. Mirk, K. Kazi, B. B. Szendrényi, I. Mojzes and A. Tichy-Rács, "Microwave Vehicle Identification and Control system." *Proc. of MIOP '90.* pp. 475—"480. 1990.

[3] G. Reisinger, M. Serényi, B. Szentpáli and P. Tütő, "Optical Modulation of Microwave Devices (in German)." *Proc. of MIOP '89.* Sindelfingen 28, Febr—"2, March 1989, P5 B.

[4] B. Szentpáli, F. Riesz, P. Gottwald and G. Reisinger, "GaAs Optical Switch Prepared by MESFET Technology." *Microwellen & HF Magazin.* Vol. 16, No. 7, pp. 483—"484, 1990.

[5] K. Kazi, B. B. Szendrényi, B. Szentpáli and I. Mojzes, "Characterisation of Microwave Diode Chips Using Measured S-Parameters." *Digest of the First International Wirkshop of the West German IEEE MTT/AP Joint Chapter on Integrated Nonlinear Microwave and Millimeterwave Circuits. (INMMC '90).* pp. 229—"242.

[6] B. Szentpáli, Zs. J. Horváth, I. Mojzes, H. Asonen, A. Salokatve and M. Pessa, "GaAs Triangular Barrier Diodes for Microwave Purposes." *Proc. of MIOP '89.* Sindelfingen, 28, Febr—"2, March 1989, P33.

[7] V. V. Tuyen and B. Szentpáli, "Tunnelling in planar doped barrier diodes." *J. Appl. Phys.* 68, No. 6, pp. 2824—"2828, 25, Sept, 1990.

[8] B. Szentpáli, V. V. Tuyen, M. Németh-Sallay, A. Salokatve, H. Asonen and M. Pessa, "The planar doped barrier diodes." *Proc. of First International Conf. on Epitaxial Crystal Growth,* Budapest, Hungary, 1—"7, April, 1990. *Crystal Properties and Preparation.* Vol. 32—"34, (1191), Pt. II, pp. 718—"722, Trans. Tech. Publ. ISSN 0252-1067.

B. SZENTPÁLI

■ US SEMINAR ON TELECOMMUNICATIONS

A seminar concerning policy and regulatory frameworks that enhance the development of telecommunications has taken place on July 22nd and 23nd in Budapest. This seminar was a part of the Eastern European Telecommunication Development Support Seminar series, sponsored by the US Department of States Bureau of Communications and Information Policy and the U.S. Embassies in the countries in question.
The seminar presented in Hungary comprised three modules as detailed in the following.

MODULE I — ELEMENTS OF A MODERN TELECOMMUNICATIONS INFRASTRUCTURE

OUTLINE: A) Elements of Tecelommunications Facilities
B) Elements of Telecommunications Services
C) Enhanced Services
D) Interfaces between Network Elements
E) Technology Choices
F) Implications for the Regulatory Framework and Rules

The purpose of this module was to provide the technological foundations of the course. The four fundamental parts of a telecommunication network (long distance network, local network, inside wiring, and customer premises equipment) were briefly discussed, and the basic and enhanced services offered on the public network were reviewed. Finally, the technological choices available for the various network elements were discussed.

MODULE II — ECONOMIC POLICY AND REGULATORY FRAMEWORK

OUTLINE: A
Basic Economic and Policy Principles

1. Competitive Markets
2. Special Cases Involving Legal and Natural Monopolies Providing Essential Services
3. Prospects for Competition in Terms of Facility and Service Elements
4. U.S. Experience with Market Structure and Competition

OUTLINE: B
Regulatory Frameowrk

1. Goals of Economic Regulation in a Market Oriented Economy
2. Traditional Regulation of Public Utilities
3. Special Issues Surrounding Mixed Monopoly/Competition
4. Alternatives to Traditional Regulation
5. Review of U.S. Experience with Alternative Forms of Regulation and the Evolution Toward a Competitive Telecommunications Marketplace

The purpose of this module was to provide the basic economic rationale for regulation as it has evolved in the U.S., and to present a framework for the regulation in an environment where there is a mixture of monopoly and competitive elements. The first part of the module dealt with a brief review of market oriented economic theory and the advantages of private enterprise and competitive markets. The special problems associated with firms with monopoly power over essential services as a result of natural monopoly or franchised monopoly conditions were reviewed, together with economic rationale for regulation under these conditions. Major categories of networks and services descirbed in Module I were examined in terms of whether they exhibit strong natural monopoly characteristics that would warrant economic regulation.

In the second part of this module, the goals of economic regulation in a market oriented economy were outlined, with a discussion of the economic rationale for traditional public utility regulation and alternative forms of regulation. Traditional forms of rate-of-return regulation utilizing a government regulatory body (a commission) were also described, and the advantages/disadvantages reviewed.

Next, the special issues of cross-subsidization and discrimination that arise when a firm with monopoly power also praticipates in adjacent competitive markets were treated. Finally the recent U.S. experience with these alternative forms of regulation and the use of competition to spur innovation and reduce costs were assessed and discussed.

MODULE III — LEGAL FRAMEWORK AND RULES

OUTLINE: A) Distribution of Functions — Government, Providers, End Users
B) Franchising/Entry, Expansion, Exit Approval
C) Pricing/Tariffing
D) Policing Discrimination/ Anticompletitive Activities
E) Making the Transition from Monopoly Competition/Deregulation
F) Spectrum Management/Radio Licensing
G) General Administrative Process

In this module, a possible legal framework for creating a market oriented telecommunications industry in the Host Country has been presented. Main topics included a basic legal structure looking toward the separation of the provision of telecommunications services from governmental policy and regulatory functions, and relying upon competition rather than regulation to the maximum extent possible. The roles to be played by the three sets of stakeholders, the government, the service providers and the end users have been discussed, together with laws/rules dealing with the awarding of franchises and the issuance of permits or other authority for the construction, expansion of withdrawal of telecommunications facilities/services. Another topic covered the laws/rules dealing with carrier pricing and tariffing.

Following the treatment of dicrimination and other forms of anticompetitive behaviour, laws/rules dealing with the transition from monopoly provision of services to a more competitive environment have been treated. For example, as certain portions of the market become more competitive (and eventually fully competitive), regulatory burdens should be lightened and, when appropriate, lifted altogether. The laws/rules necessary to assure appropriate deregulation during the transition from a mon-

opoly to a competitive environment have also been reviewed.

In the next portion of the module, laws/rules governing the allocation and assignment of the radio spectrum have been presented. The focus in this module was on the relationship of spectrum allocation policies to telecommunications policy, and laws/rules for actually implementing spectrum management as a governmental function. As the final topic, laws/rules dealing with administrative procedures to be used in the regulation of telecommunications have been described.

All modules were presented by highly experienced experts. Dale N. Hatfield, formerly holding high level government positions concerning telecommunications policy, is presently involved in directing telecommunications programs at various universities. Robert R. Bruce, a partner in a major law firm in Washington, D.C., focused on telecommunications policy and regulations, further on international trading problems of telecommunication services. Dr. James H. Alleman, formerly with GTE and ITU, is presently working at the Unviersity of Nebraska.

Information from the US Embassy

■ BOOK REVIEWS

MICROWAVE INTEGRATED CIRCUITS by I. Kása

The book presents fundamental and up-to-date information on hybrid microwave integrated circuits (MICs) and beyond the description and analysis, it provides basic design methods for specific problems.

The book is written primarily for electronic engineers, interested in the field of MIC design or application. By giving an overview of the possibilities and limitations of the MIC applications, it is intended also for engineers active in equipment and system design. The book may be used advantageously by university and college students striving for a deeper understanding of this important topic.

The book starts with a brief introduction to the technological aspects, then a survey of the applied transmission line types is given. This is followed by chapters giving a detailed discussion of passive linear integrated circuit elements such as integrated directional couplers, hybrids, filters and some types of nonreciprocal circuits, YIG and ferrite devices. As the advantages and benefits of the microwave integrated circuits can be fully exploited only by the extensive use of semiconductor devices, several chapters are devoted to active and nonlinear solid state circuits, including fundamental types of integrated oscillators, amplifiers and mixers.

Each chapter is completed with an extensive bibliography including references to basic results as well as recent significant papers, so these can give directions in further study and research.

The main value of the book is the profound and consistent discussion which helps the reader gain a comprehensive and balanced view on hybrid microwave integrated circuits.

(The monograph was published in 1991 as a joint edition by Akadémiai Kiadó, Budapest, Hungary and Elsevier Science Publishers, Amsterdam, The Netherlands, the latter as vol. 24. in the Series *Studies in Electrical and Electronic Engineering)*

GaAs MONOLITHIC INTEGRATED CIRCUITS by I. Mojzes

This book is one of the first attempts to treat the vast and extremely complex field of compound semiconductor integrated circuits construction and technology as deeply as possible, while at the same time treating the many practical aspects of this subject.

The treatment of the material presented is essentially selfcontained. Starting at a basic level, the author leads the reader gradually to the more advanced and complicated topics. In the first Chapter, a history of semiconductor devices is presented. Based on the short summary of the physical properties of GaAs the main steps of the compound semiconductor device technology is described. Specific methods such as lift-off are analysed in detail.

Using fundamentals the active devices used in monolithic microwave integrated circuits (MMIC) are described. Passive components are very important constituent parts of these devices. The construction and technological realisation of specific parts of these circuits such as interconnection and air-bridges are presented in detail. For realization of MMICs specific circuits are required having low losses and high speed. In Chapter 6 these realizations are summarized and compared. The description of the application of these devices is started with application specific GaAs integrated circuits: memories, frequency dividers, amplifiers, mixers, delay line oscillators are the most important fields of application of MMICs. Measuring methods, reliability aspects, radiation hardness are also treated in the present book.

It is a useful reference for student and researchers as well as for users of the field. A glossary of the most important terms used in MMICs is presented in English, German, Russian and Hungarian.

In conclusion, it can be said that this book gives an excellent review of the state-of-the-art in this field.

(Műszaki Könyvkiadó, Budapest 1988. in Hungarian p. 235., with 178 Figures.)

CENTENNIAL SCIENTIFIC DAYS OF PKI
20—22 November, 1991 — Budapest, Hungary

Organized by PKI Telecommunication Institute

in association with the Hungarian Telecommunications Company and the Scientific Society for Telecommunications

Under the auspices of the International Telecommunication Union and the Universal Postal Union

Venue: Hotel Agro, Budapest XII., Normafa út 42.

Programme

Wednesdy, 20 November	• Opening session • International relations • Switching • Telecommunications regulations
Thursday, 21 November	• Postal services • Telephony • Optical communications • Advanced telecom services
Friday, 22 Nobember	• Networking • Radiocommunications • Telecommunications economy • closing session

Information for authors

JOURNAL ON COMMUNICATIONS is published monthly, alternately in English and Hungarian. In each issue a significant topic is covered by selected comprehensive papers.

Other contributions may be included in the following sections:

- INDIVIDUAL PAPERS for contributions outside the focus of the issue,
- PRODUCTS-SERVICES for papers on manufactured devices, equipments and software products,
- BUSINESS-RESEARCH-EDUCATION for contributions dealing with economic relations, research and development trends and engineering education,
- NEWS-EVENTS for reports on events related to electronics and communications,
- VIEWS-OPINIONS for comments expressed by readers of the journal.

Manuscripts should be submitted in two copies to the Editor (see inside front cover). Papers should have a length of up to 30 double-spaced typewritten pages (counting each figure as one page). Each paper must include a 100—200 word abstract at the head of the manuscript. Papers should be accompanied by brief biographies and clear, glossy photographs of the authors.

Contributions for the PRODUCTS-SERVICES and BUSINESS-RESEARCH-EDUCATION sections should be limited to 16 doublespaced typewritten pages.

Original illustrations should be submitted along the manuscript. All line drawings should be prepared on a white background in black ink. Lettering on drawings should be large enough to be readily legible when the drawing is reduced to one- or two-column width. On figures capital lettering should be used. Photographs should be used sparingly. All photographs must be glossy prints. Figure captions should be typed on a separate sheet.

For contributions in the PRODUCTS-SERVICES section, a USD 110 page charge will be requested from the author's company or institution.

TINA

Toolkit for Interactive Network Analysis

This comprehensive software package allows the user to sketch analog circuit diagrams of arbitrary complexity and simulate their operations on IBM PC XT/AT/PS2 or compatibles. Formation and testing of either linear or non-linear circuits may be accomplished in a matter of minutes with the effective CAE tools provided. *TINA*'s "electronic breadboard" cuts design cost and reduces the number of necessary experiments. The unique features of TINA are the **optimization** and the **measurement interface**. Electronic circuits can be designed, analysed, troubleshooted and tuned in the same integrated environment. Both TINA's own measurement add-ons and a wide range of IEEE bus controlled instruments are supported.

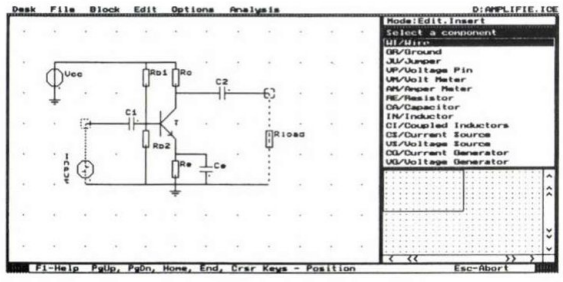

Circuit diagrams are designed in an easy-to-handle schematic editor. Element symbols chosen from a component catalog are positioned by the cursor keys or a mouse .Tolerances can be assigned to the circuit elements, **Monte-Carlo** and **worst-case analysis** are available to statistically test circuit performance. An **extensive semiconductor catalog** is provided which allows the user to select the required semiconductor components from a user-extendable library. Standard file formats and export transactions allow access to well known other packages like PSpice, WordPerfect, AutoCAD, and Ventura.

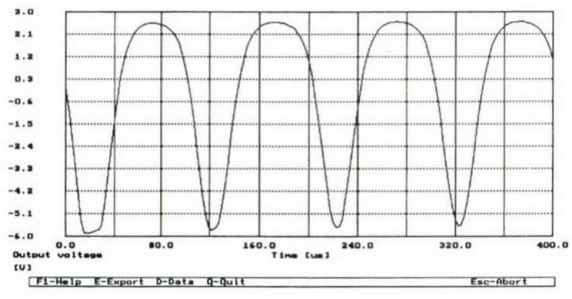

DC, transient and Fourier-analysis can handle linear and non-linear components. Electrical input can be selected from several wave-form options (pulse, unit step, sinusoidal and general trapezoidal wave etc.) and parameterized as required.

AC analysis can handle linear resistive and dynamic elements, and is also capable of displaying the Bode diagram.

TINA allows **stepping of component values**, of model parameters, and of temperatures. The results may be plotted as a family of curves. In addition, during the DC analysis, component values and model parameters can be swept (i.e. altered continuously) thus displaying the response.

A special feature of *TINA* is the **optimization**. Specifying a desired quantity (voltage, current, frequency, etc.) in the circuit, prompts the program to find the value of a selected component (if it exists) that meets this specification.

The **TINA-LAB measurement card** turns your PC into a powerful engineering workstation. The built in function generator provides input for the analyzed circuit, while the output signals can be measured in multimeter or oscilloscope mode. Frequency response (Bode diagram) can also be measured by combining a wobbulated sinusoidal test signal with peak detection. High frequency measurements can be carried out by using the IEEE 488 interface.

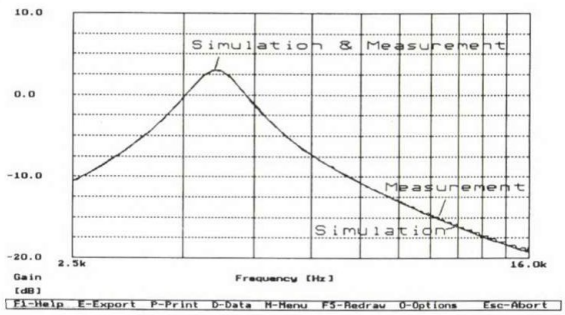

Educational applications are facilitated through **voltage, ampere and power meters**, complete demo facilities and a **built-in word processor.**

Professional version for designers, special **NOVELL network version** for schools, student version for home usage are available

Developed by: **RAIR Computer Ltd.**

H-1145,Budapest Gyarmat u. 45/c

Tel.: (361) 1699-915, (361) 2524-390

Fax: (361) 2524-506

HELLO...
SIEMENS SPEAKING...
HERE WE ARE...

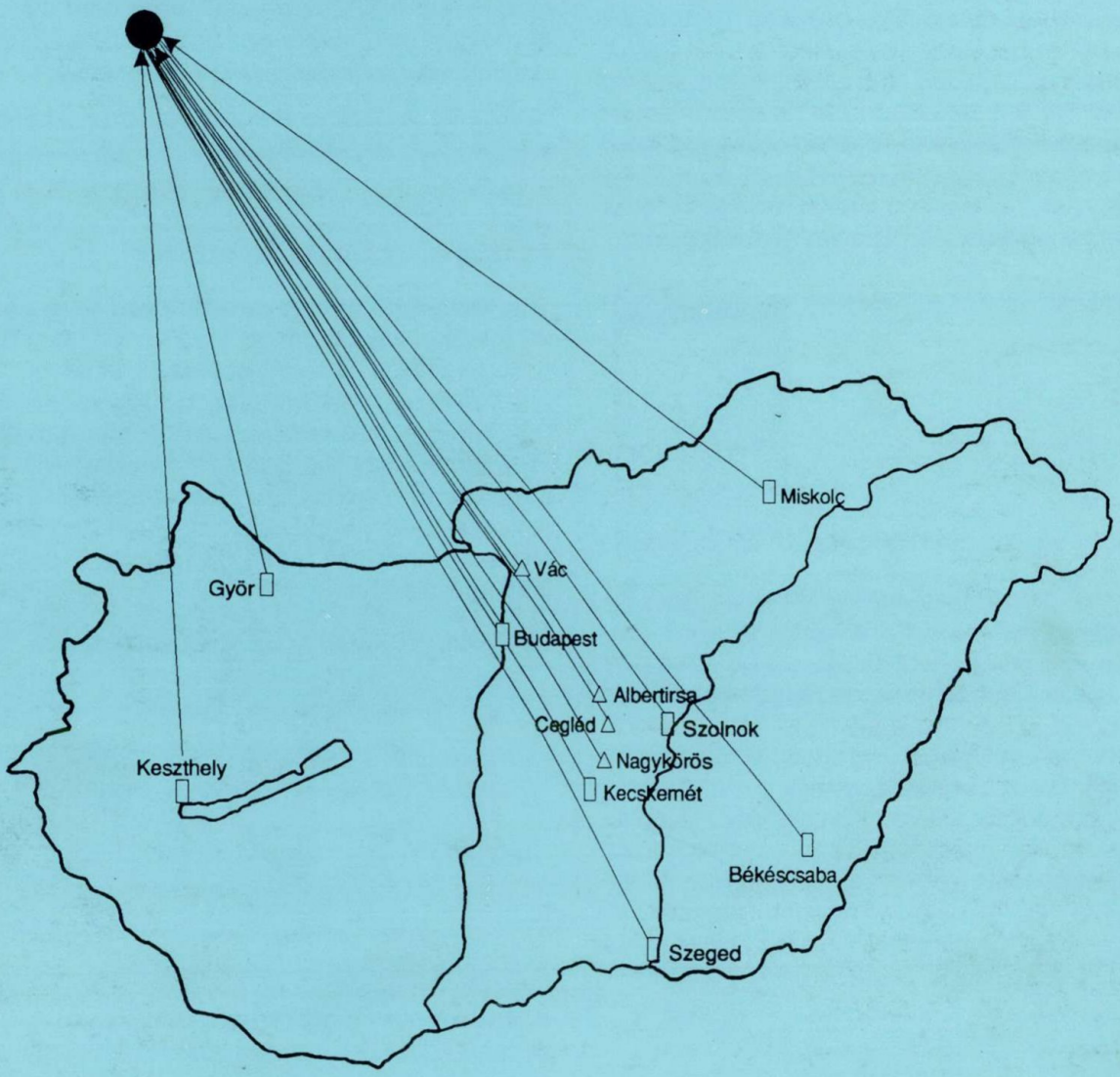

△ EWSD Public Exchanges 1991
▯ EWSD Public Exchanges 1992

Siemens Telefongyár Kft

1143 Budapest XIV. Gizella út 51-57. Hungary
H-1956 Budapest 70. P.O.B. 16.

Telefon: (36-1) 252-0222 Fax: (36-1) 252-2749
Telex: 22-4087